2011

Electrophysiological characterization of enteric neurons isolated from the immortomouse

Edward G. Hawkins
Virginia Commonwealth University

ELECTROPHYSIOLOGICAL CHARACTERIZATION OF ENTERIC NEURONS ISOLATED FROM THE IMMORTOMOUSE

A dissertation submitted in partial fulfillment of the requirements for the degree of Doctor of Philosophy at Virginia Commonwealth University.

by

Edward Gregory Hawkins

Bachelor of Science, Animal Physiology and Neuroscience,
University of California at San Diego, 2000

Director: Hamid I. Akbarali, Ph.D.
Professor, Department of Pharmacology & Toxicology

Virginia Commonwealth University
Medical College of Virginia Campus
Richmond, Virginia
May, 2011

Acknowledgments

It has been a long road and there are many individuals who deserve recognition and my thanks for their mentorship, support, friendship, and patience. Starting from the beginning of my scientific career, Dr. Ben Cravatt and Dr. Aron Lichtman always supported me and gave me the opportunities I needed to begin my graduate career. It is as a result of what I learned from them that I was accepted to Virginia Commonwealth University and began the next stage of my career development. Many thanks must go to Dr. Billy Martin and Dr. William Dewey who were very supportive of my graduate training. I also cannot emphasize how grateful I am to Dr. Hamid I. Akbarali for being an incredible mentor. His timeless patience, teaching and guidance, and input were paramount to the completion of this thesis. I have learned many things from him and now feel comfortable to take on the challenges of conducting my own research as a result of his training. I would also like to express my gratitude to my graduate committee members, Drs. Clive Baumgarten, John Grider, Laura Sim-Selley, and William Dewey. Their insight has been indispensible and they helped visualize this project from several different angles. I would also like thank the current members of the Akbarali lab; Dr. Gracious Ross for his patience and being someone to always inspire me to do more and Dr. Minho Kang, our resident expert in molecular biology has been so helpful in so many ways. To the new members of the lab (Drs. Tricia Hardt-Smith and Hercules Maguma), thanks for showing me that there really is a light at the end of the tunnel. As for previous members of the lab, I would like to thank Dr. Denis Columb for his support and keeping my focus targeted to the goal of completion of this thesis. I would also like to thank our collaborator Dr. Shanthi Srinivasan for providing the enteric neuron cell lines that were an integral part of this work. Finally I would like to thank my family for always being there to support me and keep me going in my efforts to become a scientist. Mom, Dad, both of you are accomplished scientists and I thank you for your support and understanding throughout all of my training. To my wife Daniela, your love and patience has been incredible and I know that you too will soon accomplish your dreams of completing your Ph.D. in Chemical Biology. To all of you Thank You.

Table of Contents

List of Tables

List of Figures

List of abbreviations

$5\text{-}HT_3$ – serotonin receptor

ACh – acetylcholine

AHP - afterhyperpolarization

AH-type – afterhyperpolarization type

AMPAR – α-amino-3-hydroxy-5-methyl-4-isoxazolepropionic acid receptor

AS-C – acaete-scute complex

ATX – Ω-agatoxin IVA

BK – big conductance calcium-activated potassium channels

BMP-2 – bone morphogenic protein 2

CGRP – calcitonin gene related peptide

Cl_{Ca} – Calcium activated chloride current

CTX - Ω-conotoxin GVIA

DCPIB – 4-[(2-Butyl-6,7-dichloro-2-cyclopentyl-2,3-dihydro-1-oxo-1*H*-inden-5-yl)oxy]butanoic acid

EN – enteric neuron

E_{rev} – reversal potential

ET-3 – endothelin 3

ET_B – endothelin receptor B

fEPSP – fast excitatory post-synaptic potential

GABAR – γ-Aminobutyric acid receptor

GDNF – glial cell derived neurotrophic factor

GI – gastrointestinal

HCN – hyperpolarization activated cyclic nucleotide gated ion channel

IBS – irritable bowel syndrome

IK – intermediate conductance K_{Ca} channel

IM-FEN – immortalized fetal enteric neurons

IM-PEN – immortalized post-natal enteric neurons

IPAN – intrinsic primary afferent neuron

I_r – input resistance

ISH – in situ hybridization

LGIC – ligand gated ion channel

LMMP – longitudinal muscle myenteric plexus

MASH1 – mammalian acaete-scute complex 1

NA – niflumic acid

nAChR – nicotinic acetylcholine receptors

NMDAR – N-Methyl-D-aspartate receptor

NMDG – N-methyl-D-glucamine

nNOS – (NOS1) neuronal nitric oxide synthase

NPC – neuronal progenitor cell

pCGM1 – pCMV6-A-GFP-MASH1

PKA – protein kinase A

PKC – protein kinase C

PNS – parasympathetic nervous system

Prb – retinoblastoma protein

RMP – resting membrane potential

ROS – reactive oxygen species

RT-PCR – reverse transcription polymerase chain reaction

sEPSP – slow excitatory post-synaptic potential

SEVC – single electrode voltage clamp

SK – small conductance calcium-activated potassium channels

SNS – sympathetic nervous system

SP – substance P

S-type – synaptic type

TAg – large T antigen

Tau – time constant

TEA – tetraethylammoniom

TGF-β – transforming growth factor β

TRP – transient receptor potential

TRPV1 – transient receptor potential vanilloid 1

TTX – tetrodotoxin

$V_{1/2}$ – Voltage of half activation/inactivation

VGCC – voltage gated Ca^{2+} channels

VGNC – voltage gated Na^{+} channels

Abstract

ELECTROPHYSIOLOGICAL CHARACTERIZATION OF ENTERIC NEURONS ISOLATED FROM THE IMMORTOMOUSE

By Edward Gregory Hawkins
Bachelor of Science, Animal Physiology and Neuroscience,
University of California, San Diego, 2000

A dissertation submitted in partial fulfillment of the requirements for the degree of Doctor of Philosophy at Virginia Commonwealth University.

Virginia Commonwealth University, 2011

Director: Hamid I. Akbarali, Ph.D.
Professor
Department of Pharmacology and Toxicology

The availability of murine genetic models is extremely advantageous to studying gastrointestinal function, but the benefits afforded by studying enteric neurons in mice has been hindered by their accessibility. Fetal (E13) and 2 day post-natal (P2) enteric neuron cell lines (IM-FEN and IM-PEN, respectively) were recently developed from the H-2Kb-tsA58 immortomouse. Our goal was to identify the electrophysiological properties of these cell lines and clarify their utility as a model of enteric neurons.

IM-PEN cells stained positively for the neuron specific markers βIII-tubulin and PGP9.5 and were negative for the glial cell marker S100. Detection of mRNA for TRPA1, TRPV1, ClCa1, $K_{Ca}3.1$, $Na_V1.3$ and $Na_V1.9$ were present while $Ca_V2.2$ and TASK1 were very faint. No significant difference was observed in the passive membrane properties of IM-FEN and IM-PEN. The cells had depolarized resting membrane potentials -29.8 ± 0.9mV (n=30) and high input resistances ranging from 552 ± 104MΩ (IM-FEN, n=6) to 728 ± 128MΩ (IM-PEN, n=20).

In current clamp, hyperpolarizing current was given to obtain a holding potential of -60mV or -80mV, yet neither IM-FEN (n=6) nor the IM-PEN cells (n=20) were able to generate action potentials in response to depolarizing pulses. In whole cell voltage clamp depolarization induced an inward current which was identified as an L-type Ca^{2+} channel. Niflumic acid inhibited the outward current as well as the tail currents indicating a Cl_{Ca} current supporting the mRNA data. A volume sensitive chloride channel was also identified that was DCPIB sensitive (n=7) and removed when chloride was replaced with gluconate (n=4), displaying characteristics of $I_{Cl,swell}$. As a result IM-PEN cells had a high chloride conductance resulting in a depolarized membrane potential, which is a characteristic of immature neurons.

The transcription factor MASH1 has been found to be required for enteric neuron differentiation. Transfection of MASH1 after 4 and 8 days did not alter the electrophysiological characteristics of IM-PEN (n=6). We conclude that IM-PEN may represent immature enteric neurons and are a useful model to examine the effect of factors required for the development of enteric neurons.

I. Introduction

The gastrointestinal system of the adult consists of several types of specialized cells that secrete, digest, absorb, and move chyme through an organism. A large number of diseases and treatments can affect gastrointestinal (GI) function and cause serious, painful, and in some cases, lethal side effects. Many of these disorders are the result of detrimental effects on enteric neurons. A complete understanding of how enteric neurons function in the GI tract could help scientists and clinicians identify and target better therapeutics for GI disorders. The major focus of this thesis is on the electrophysiological characteristics of murine enteric neurons isolated from the immortomouse. These studies will therefore provide important information regarding the electrical excitability of a novel model of enteric neurons.

A. GI anatomy and physiology

Understanding the structural anatomy of the GI is important to comprehending how a specialized group of neurons and smooth muscle cells function to generate peristaltic contractions. Figure 0-1 shows how specialized cells are segregated into layers in the GI system in order to perform their specific tasks. The lumen of the lower GI system (ileum and colon) is encased by mucosal cells dedicated to secretion and absorption. These cells are surrounded by the submucosa that is covered by circular smooth muscle cells. Between the submucosa and the circular smooth muscle is the first layer of the enteric nervous system, the submucosal plexus (Meissner's plexus). The submucosal plexus innervates the muscosa regulating secretion of GI constituents. The layers of smooth muscle and neurons that control peristaltic contractions surround these inner layers. Thick circular smooth muscle cells run in a perpendicular fashion forming a ring around the gut when they contract. They are covered and innervated by the outer

layer of the enteric nervous system that makes up the myenteric plexus (Auerbach's plexus). The myenteric plexus innervates the circular muscle and a thin layer of longitudinal muscle that is surrounded by a protective layer called the serosa. Both the submuscosal plexus and the myenteric plexus make up the enteric nervous system which is a subdivision of the peripheral nervous system. Central nervous system (CNS) innervation of the GI tract occurs through the parasympathetic (PNS) and sympathetic nervous systems (SNS). Vagal input from the PNS increases GI secretion and motility whereas splanchnic and pelvic innervation by the SNS slows gastric motility (Johnson 2006).

A series of three articles published between 1899 and 1901 by Bayliss and Starling established the law of the intestine (Bayliss et al., 1899; Bayliss et al., 1900; Bayliss et al., 1901). The law of the intestine states that, "…stimulation of the gut produces excitation above and inhibition below the excited spot." (Bayliss et al., 1899). They concluded that conditions in neighboring parts of the intestine send both inhibitory and excitatory signals through the enteric nervous system to the CNS as well as to the smooth muscle. Another major finding of their studies is that peristalsis occurs in the absence of innervation by the CNS. This meant that the enteric nervous system, specifically the myenteric plexus, contains all the components necessary to coordinate and regulate a complex series of contractions. Peristalsis occurs when the longitudinal muscle contracts caudad (descending) in order to shorten the distance chyme needs to travel. In conjunction, the circular muscle contracts orad to the bolus pushing the chyme into the contracted longitudinal segment (Figure 0-2) (Grider 2003a).

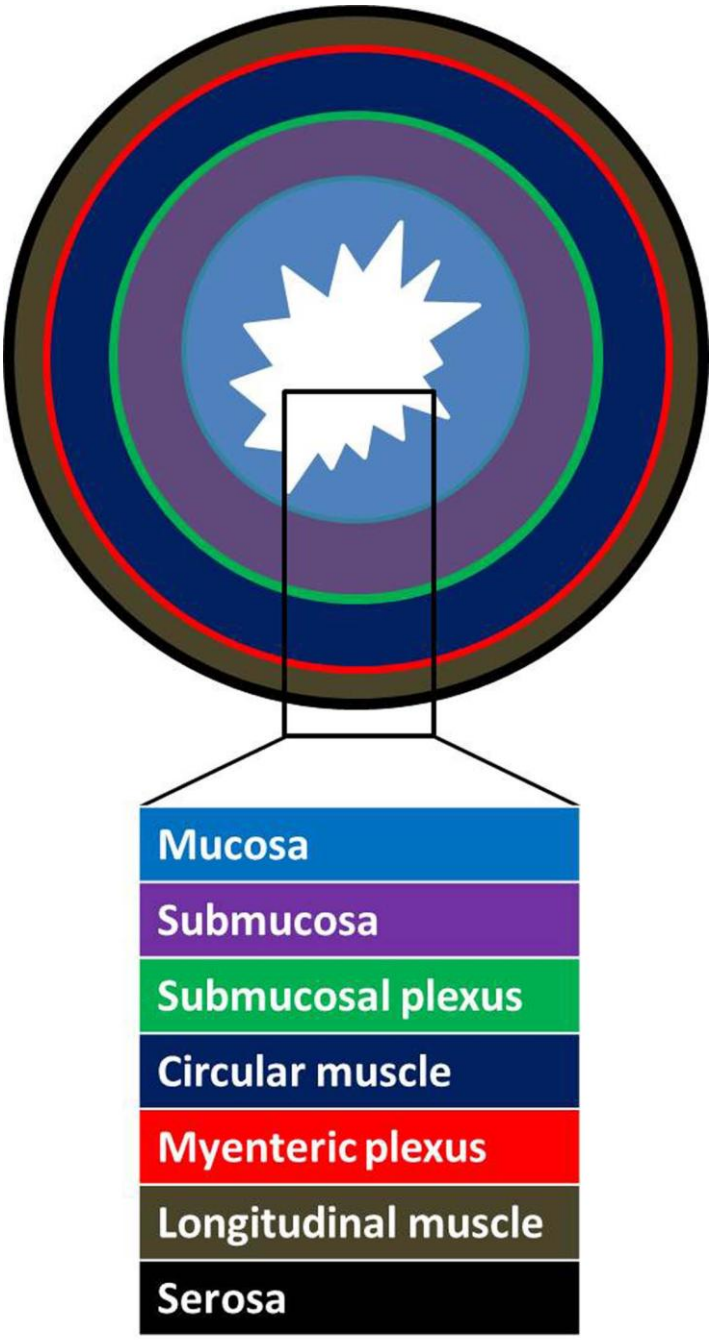

Figure 0-1 Diagram representing cross section of the gastrointestinal tract. Several layers of specialized tissue compose the labeled regions each with a specific phsyiological function. The enteric nervous system is composed of both the submucosal plexus and the myenteric plexus.

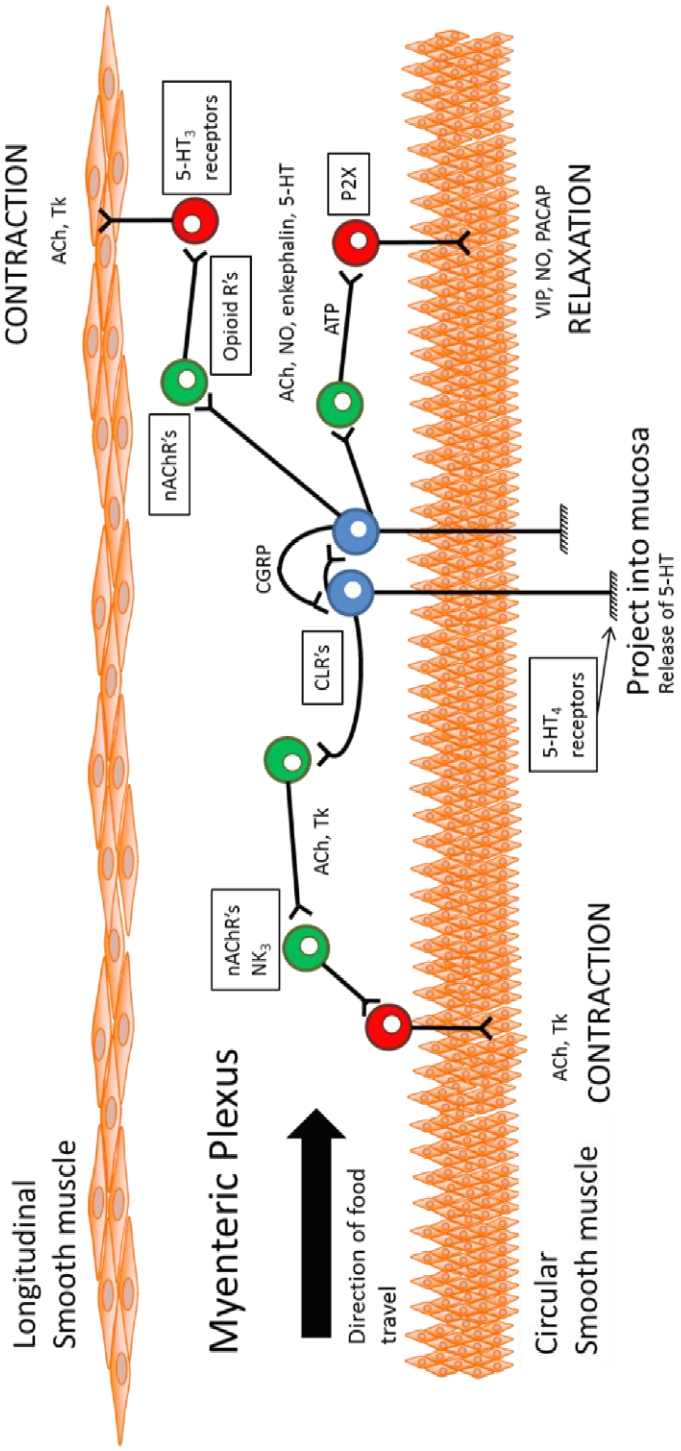

Figure 0-2 Composition of neurons in the myenteric plexus and how they control peristalsis. See text for details.

B. Enteric neurons

Enteric neurons of the myenteric plexus cluster into ganglia and are linked by interganglionic fiber tracts forming a network between the two smooth muscle layers. The cell bodies in the ganglia lay end to end in a flat 2-dimensional plane and are a mixture of sensory, inter and motor neurons (Brookes 2001). Many classification schemes have been developed to describe the structure of enteric neurons, however, one of the most commonly used was established by the neuroanatamist A. S. Dogiel identifying both type 1 and type 2 neurons (Nurgali et al., 2004). Dogiel type1 neurons have a single long axon and a series of short dendrites that extend from the soma. These neurons consist of interneurons and motor neurons that have orally or anally projecting axons that release acetylcholine (ACh) and substance P or nitric oxide (NO) and vasoactive intestinal peptide (VIP), respectively (Grider 2003b)(Nurgali et al., 2004). Dogiel type 2 neurons consist of sensory neurons that contain multiple axonal projections. Sensory neurons project towards the mucosa and typically contain the neurotransmitters calcitonin gene related peptide (CGRP), substance P and ACh (Figure 0-2) (Furness et al., 2004) (Grider 2003b).

1. Afterhyperpolarization-type (AH-type)

Another type of classification has been described by determining the electrophysiological properties of enteric neurons. The passive properties of myenteric neurons are provided in Table 0-1. The electrophysiological characteristics of sensory neurons that synapse in the enteric nervous system were first studied using microelectrodes and have been termed intrinsic primary afferent neurons (IPAN's). These neurons were termed AH-type neurons resulting from a large afterhyperpolarization (AHP) in their action potentials. AH neurons have several unique characteristics:

1) generally have a more hyperpolarized membrane potential than Synaptic type neurons

2) prolonged afterhyperpolarization inhibited by clotrimazole

3) a hump in the falling phase of the action potential

4) expression of I_K channel

5) expression of calbindin

6) they are the majority of neurons expressed in the myenteric plexus (60%) (Johnson 2006).

Action potentials in AH neurons are complex with the rising phase carried by Na^+ and Ca^{2+} ions leading to a shoulder in the falling phase (North 1973). As with neurons in the CNS, the falling phase is regulated by time and voltage dependent K^+ channels. Critical to the characteristics of the action potential for AH neurons is the development of an AHP which prevents further excitation of the neuron that can last for up to 30 seconds. Several studies determined the AHP to be Ca^{2+}-dependent and the result of a K_{Ca} channel (Vogalis et al., 2002b).

2. Synaptic type (S-type)

The electrophysiological properties of inter- and motor neurons differ sufficiently from sensory neurons to categorize them as synaptic-type neurons (S-type). It was found that a majority of the so called S-type neurons demonstrated fast excitatory post-synaptic potentials (fEPSP's) in response to acetyl choline (ACh) (Hirst et al., 1974). Other features differentiating S-type neurons include:

1) more depolarized membrane potentials compared to AH

2) increased excitability

3) no afterhyperpolarization (leads to increase in excitability)

4) rising phase of action potential was carried only by Na^+ ions.

When given depolarizing pulses, long spike trains of actions potentials are elicited and depend on the amplitude of the depolarization (Nurgali 2009).

The significance of the different characteristics in the action potentials of AH and S type neurons becomes apparent when we think about signal transmission and coding. In AH neurons, the afterhyperpolarization lengthens the refractory period thereby limiting the number of action potentials a neuron can produce. The length of the AHP has been found to be modulated by intracellular messaging of the IK channel (Neylon et al., 2006). As a result, regulation of an ion channel is an important determinant of how sensory information is transmitted to the inter- and motor- neurons (S-type). The response of the S-type channels is directly mediated by the stimulus received, and therefore, changes in sensory information (from AH) alter the response in the smooth muscle through S-type neurons (Ferens et al., 2007).

Table 0-1 Passive properties of enteric neurons

Passive properties

Cell type	RMP (mV)	Ir (MΩ)	Species	Age	Method	Tissue	Ref
AH-type	-57±4	502±27	guinea pig	adult	patch clamp	duodenum	1
	-59±8	260±110	guinea pig	adult	microelectrode	colon	2
	-59.2±10.6	150±91	guinea pig	adult	microelectrode	ileum	3
	-50 to -65	125±7	guinea pig	adult	microelectrode	ileum	4
	-63±1.2	194±16	mouse	adult	microelectrode	colon	5
	-56±5	104±63	mouse	adult	microelectrode	colon	6
	-55±7	500±52	mouse	adult	patch clamp	ileum	7
	-69±5	136±35	mouse	adult	microelectrode	intestine	8
	-63±4	172±35	mouse	--	microelectrode	ileum	9
S-type	-47±6	713±49	guinea pig	adult	patch clamp	duodenum	1
	-49±5	290±120	guinea pig	adult	microelectrode	colon	2
	-54.0±13	153±118	guinea pig	adult	microelectrode	ileum	3
	-48±0.5	155±8	mouse	adult	microelectrode	colon	5
	-46±6	123±62	mouse	adult	microelectrode	colon	6
	-63±2	112±9	mouse	adult	microelectrode	intestine	8
	-62±2	121±14	mouse	--	microelectrode	ileum	9
myenteric	-56.3 ± 2.7	--	mouse	adult	perforated patch	colon	10
myenteric	-46 ± 13	392 ± 203	guinea pig	adult	patch clamp	small intestine	11
submucosal	-40/-70	60/190	guinea pig	adult	microelectrode	small intestine	12
myenteric	-44.5±0.5		rat	post-natal	patch clamp	small intestine	13, 14
myenteric	-47±3		rat	post-natal	patch clamp	small and large intestine	15
myenteric	-35.8±3.8		rat	post-natal	patch clamp	small and large intestine	16
myenteric	-54±9	150±0.59	human	--	microelectrode	distal colon	17

1 (Rugiero et al., 2002); 2 (Lomax et al., 2001); 3 (Hodgkiss et al., 1983); 4 (Hirst et al., 1985); 5 (Nurgali et al., 2004); 6 (Furukawa et al., 1986); 7 (Mao et al., 2006); 8 (Ren et al., 2003); 9 (Bian et al., 2003); 10 (Kang et al., 2003); 11 (Hanani et al., 2000); 12 (Hirst et al., 1975); 13 (Murakami et al., 2007); 14 (Franklin et al., 1992); 15 (Haschke et al., 2002); 16 (Hamodeh et al., 2004); 17 (Brookes et al., 1987)

C. Ion channels

Information on ion channel function from electrophysiology, molecular and structural biology, as well as behavioral studies, has greatly increased our knowledge of their importance throughout the body. Structural studies have found that ion channels are typically composed of an α pore-forming subunit that is then modulated by a series of accessory subunits. These accessory subunits can regulate a multitude of channel properties including activation, inactivation, voltage dependence, and membrane trafficking. Some ion channels have several subunits that form the pore of the channel and each of these subunits can be targets for different drugs. Ion channels also undergo post-translational modifications that alter their characteristics leading to the development of specialized subtypes. Several methods have been employed to determine the type of ion channels expressed in enteric neurons. Voltage-clamp studies on myenteric neurons have identified several voltage gated ion channels in enteric neurons (Table 0-2). Focusing mostly on electrophysiological evidence I will review voltage gated ion channels that have been identified in enteric neurons to date. This is important since ion channels have potential as therapeutic targets in the treatment of GI disorders (Akbarali et al., 2010).

Table 0-2 Ion channels currently expressed in enteric neurons

Voltage gated ion channels							
Ion Channel	Species	Age	Tissue	Method	Neuron	Regulation	Ref
Sodium							
$Na_v1.3$	guinea pig	post-natal	duodenum, colon	PCR, ISH	AH, S		1
$Na_v1.7$	guinea pig	post-natal	duodenum, colon	PCR, ISH	AH, S		2
$Na_v1.9$	guinea pig, rat	adult	duodenum	PCR, whole cell, single channel	AH	senktide, PKC	3
Calcium							
N-type ($Ca_v2.2$)	guinea pig	adult; post-natal	duodenum	ISH, microelectrode, whole cell	AH, myenteric, submucosal	pregabalin, adenosine	4
L-type ($Ca_v1.X$)	guinea pig, rat	adult; post-natal	small intestine	whole cell	myenteric		5
P/Q-type ($Ca_v2.1$)	guinea pig	post-natal	small intestine	whole cell	myenteric		6
R-type ($Ca_v2.3$)	guinea pig	adult; post-natal	small intestine	ISH, microelectrode, whole cell	myenteric		7
Potassium							
A-type (K_vX)	guinea pig	adult	intestine	perforated patch, whole cell, SEVC	AH, S	histamine, cAMP	8
delayed rectifier (K_{dr})	guinea pig	adult	intestine	whole cell	AH		9
inward rectifier (K_{ir})	guinea pig	adult	intestine	whole cell, SEVC	AH, S		10
IK ($K_{ca}3.1$)	guinea pig,rat	adult; post-natal	intestine	SEVC, whole cell, cell attached	AH	butyrate, cAMP, PKA	11
Leak conductance	guinea pig	adult	intestine	SEVC	AH, S		12
TASK1 ($K_{2p}3.1$)	guinea pig	adult	ileum	microelectrode	AH		13
Chloride							
ClCa	mouse	adult	colon	perforated patch	myenteric		14
Other							
HCN 1	rat, mouse	adult	ileum	IHC	myenteric, submucousal		15
HCN 2	guinea pig, rat, mouse	adult	ileum	SEVC, IHC, microelectrode	myenteric, submucousal		16
HCN 4	guinea pig	adult	ileum	SEVC, IHC, microelectrode	myenteric, submucousal		17
TRPA1	mouse	adult	intestine	contractility, PCR, IHC	myenteric, submucousal		18
TRPV1	mouse	adult	colon	IHC	extrinsic		19

1-2 (Sage et al., 2007); 3 (Copel et al., 2009; Coste et al., 2004; Rugiero et al., 2003); 4 (Barajas-Lopez et al., 1996; Bian et al., 2004; Chen et al., 2002; Hirning et al., 1990; Needham et al., 2010; Rugiero et al., 2002); 5 (Bian et al., 2004; Chen et al., 2002; Franklin et al., 1992; Hanani et al., 2000; Hirning et al., 1990); 6 (Bian et al., 2004; Vogalis et al., 2002a); 7 (Bian et al., 2004; Needham et al., 2010);8 (Galligan et al., 1989; Starodub et al., 2000a; Starodub et al., 2000b; Zholos et al., 1999); 9 (Zholos et al., 1999); 10 (Galligan et al., 1989; Zholos et al., 1999); 11 (Baidan et al., 1995; Galligan et al., 1989; Vogalis et al., 2001; Vogalis et al., 2002a; Vogalis et al., 2003); 12 (Galligan et al., 1989); 13 (Matsuyama et al., 2008); 14 (Kang et al., 2004) ; 15-16 (Galligan et al., 1990; Xiao et al., 2004); 17 (Xiao et al., 2004); 18 (Penuelas et al., 2007); 19 (Matsumoto et al., 2011)

1. Sodium channels

In general, voltage gated Na^+ channels (VGNC) were found to be responsible for the upstroke of the action potential, and they can be classified as being TTX-sensitive or TTX-resistant (Narahashi et al., 1964). The TTX-sensitive channels tend to have fast activation and inactivation properties compared to their TTX-resistant counterparts. As a result, TTX-sensitive VGNC are thought to be intimately involved with the rising phase of the action potential while the TTX-resistant channels are assumed to serve more of a modulatory function increasing cellular excitability (Campbell 1992).

As previously mentioned, the rising phase of the action potential in enteric neurons is largely attributed to a Na^+ conductance although, in AH neurons, a Ca^{2+} conductance has also been found (Nurgali 2009). In situ hybridization (ISH) performed by Sage et al., sought to determine which TTX-sensitive Na^+ channels were expressed in myenteric neurons of the guinea pig duodenum and colon. Preparations of longitudinal muscle myenteric plexus (LMMP) were made and incubated with specific oligo probes for the α subunits of several voltage gated sodium channels. RT-PCR analysis showed positive mRNA expression of $Na_v1.2$, $Na_v1.3$, $Na_v1.6$, and $Na_v1.7$. However, the ISH data was only positive for $Na_v1.3$ and $Na_v1.7$ in the ileum and colon. They explained the abundance of channels found in their RT-PCR data by the ability of this

approach to detect very low and possibly non-functional mRNA as well as the heterogeneity of the cells in a LMMP preparation (Ginzinger 2002)(Bartoo et al., 2005)(Sage et al., 2007).

Sensory neurons of the CNS have been found to contain TTX-resistant voltage-gated sodium channels of which two are known, $Na_v1.8$ and $Na_v1.9$ (Beyak et al., 2004). Rugiero et al. used guinea pig and rat duodenum to ascertain if these channels were present in the myenteric plexus. AH neurons were identified by their unique Dogiel type II morphology using biocytin as a histological stain for nerve cells. These neurons elicited a slow activating and inactivating current in the presence of 300nM TTX and the Ca^{2+} channel blocker Cd^{2+} (500µM). The electrophysiological properties of the channel were similar to that of $Na_v1.9$ previously measured in dorsal root ganglion. A $V_{1/2}$ of activation was calculated as -32 ± 1mV, and RT-PCR confirmed the expression of $Na_v1.9$. They concluded that AH neurons of the myenteric plexus expressed $Na_v1.9$ and that this channel may help modulate cellular excitability by increasing depolarization at synapses (Rugiero et al., 2003). Research on the rat duodenum myenteric plexus found a $V_{1/2}$ of -34.6 ± 0.4mV, similar to that of the guinea pig. Furthermore a 7 transmembrane G-protein coupled receptor (GPCR), neurokinin 3, was found to transiently increase the $Na_v1.9$ current in guinea pig duodenum. Whole cell patch clamp recordings on LMMP preparations with the application of senktide, an NK_3 receptor agonist, and a PKC agonist, phorbol, demonstrated an increase in the peak current and a negative shift of the window current (Coste et al., 2004)(Copel et al., 2009). The overall effect of this response increased activation of AH neurons.

We may conclude from these data that several types of VGNC's are functionally expressed in enteric neurons, each of which has a specific role in excitation of the cell. The fast activating TTX sensitive $Na_v1.3$ and $Na_v1.7$ were found to be responsible for the upstroke of the

action potential in both AH- and S- type enteric neurons. The slow activating and TTX insensitive $Na_v1.9$ was located in AH neurons and is thought to play a role in cellular excitability. Neurokinin, a member of the tachykinin family of neuropeptide neurotransmitters, shifted the window current of $Na_v1.9$, thereby increasing the excitability of AH neurons.

2. Calcium channels

Calcium ion regulation is critical to cellular function. The Ca^{2+} cation is known to regulate contraction and secretion, and to be a major component of several second messenger cascades. As a result, several studies have sought to determine the methods by which Ca^{2+} enters the cell through transporters, voltage gated Ca^{2+} channels, and cation selective channels. The voltage-gated Ca^{2+} channels (VGCC) were first defined by their activation properties, high voltage activated (HVA) or low voltage actived (LVA), and then by specific characteristics (Hille 2001). Modulation of VGCC by specific neurotransmitters therefore became an important avenue of research.

One of the leading published reports that defined the characteristics of the Ca^{2+} conductance through VGCC in AH neurons of the myenteric plexus used LMMP preparations obtained from adult guinea pigs. Currents were measured in the presence of TTX using microelectrodes in both current clamp and single electrode voltage clamp (SEVC). An inward current was present that was sensitive to changes in external Ca^{2+} and the peak current was unchanged in the presence of Ba^{2+} (Hirst et al., 1985). Building on this work, another study found multiple inward Ca^{2+} conductance in cultured myenteric neurons. The cultures were grown from the small intestine of 3 day-old rats and electrophysiological recordings were made in the whole cell configuration. Two types of currents were isolated based on their inactivation

properties. The L-type channel blocker nitrendipine suppressed the decaying component but not the sustained component of the inward current (Franklin et al., 1992).

Whole cell recordings on isolated enteric neurons from the guinea pig revealed an inward current that was blocked by Cd^{2+}, resistant to nifedipine, and sensitive to Ω-conotoxin GVIA (CTX) characteristic of N-type Ca^{2+} channels. Similar to $Na_v1.9$, a GPCR was found to modulate the channel. Activation of the adenosine receptor inhibited N-type Ca^{2+} channels in enteric neurons. This was found to be a pertussis toxin-sensitive effect, but inhibition of the kinases PKA and PKC did not alter the inhibition caused by adenosine (Baidan et al., 1995)(Barajas-Lopez et al., 1996). A similar study found that group II metabotropic glutamate receptors inhibited N-type Ca^{2+} channels in cultured myenteric neurons established from 1 week old guinea pigs (Chen et al., 2002).

To identify which VGCC were present, a focused study on the isolation of functional VGCC in the myenteric plexus was conducted. Whole cell patch-clamp recordings on primary cultures from 1-2 day old guinea pig were made and successive elimination of possible VGCC channels was performed pharmacologically. A 25% reduction was seen in the overall inward current upon the administration of 100nM Ω-agatoxin IVA (ATX), a blocker of P/Q-type channels. The contribution of N-type channels to the total inward current was calculated as 34% upon the administration of CTX. The L-type channel antagonist nifedipine also produced a small decrease (<20%) in the total current. The rest of the inward current was found to be inhibited by 50μM $NiCl_2$ a blocker of R-type Ca^{2+} channels (Bian et al., 2004).

The complexity of VGCC in enteric neurons has led to several studies describing possible mechanisms of regulation in vivo. Pregabalin is used to treat neuropathic pain and was found to be beneficial in patients with irritable bowel syndrome (IBS) (Camilleri 2007). It targets the

α2δ1 subunit of N-type Ca^{2+} channels decreasing their conductance, leading to the hypothesis that the mechanism of action was through a decrease in the excitability of IPAN's. This hypothesis was supported by microelectrode measurements in which the action potential duration was decreased and the amplitude and length of the AHP were reduced. These studies were conducted on LMMP preparations of the guinea pig duodenum. The effect was confirmed to be N-type Ca^{2+} channel-dependent by the addition of CTX, which mimicked the response of pregabalin (Needham et al., 2010). In the rat, using the whole cell patch clamp procedure on cultured myenteric neurons, it was found that bradykinin-induced depolarizations occurred through non-selective cation channels and VGCC's. The effect of bradykinin was present in both AH- and S-type neurons and was potentiated by PGE2 (Murakami et al., 2007).

Evidence has therefore been collected for the presence of N, L, P/Q, and R type Ca^{2+} channels in the enteric nervous system of the guinea pig. It is clear from electrophysiological recordings that these channels can be modulated in several ways and may serve diverse roles as a result. One of these functions is modulation of the internal Ca^{2+} concentration, which indirectly affects the excitability of AH neurons through a K_{Ca} channel.

3. Potassium channels

Voltage gated K^+ channels are one of the largest and most diverse families of ion channels. Their importance in maintenance of the membrane potential and lowering of cellular excitability is evident, especially in enteric neurons. An example of this is the afterhyperpolarization in AH neurons, which is the result of a calcium-activated potassium channel (K_{Ca}, IK) that can keep the cell quiescent for several seconds after an action potential. The large functional diversity of these ion channels makes them one of the most studied families of all voltage-gated ion channels.

One of the most significant ion channels for gastrointestinal electrophysiologists is a K_{Ca} channel. This ion channel was found to be involved in the characteristic afterhyperpolarization of the AH sensory neuron. Since its discovery, many researchers have focused their efforts on its function and modulation during different disease and inflammatory states (Ferens et al., 2007). Several studies used current clamp experiments on myenteric neurons from guinea pigs (250-400g) using LMMP preparations and the microelectrode technique to study the afterhyperpolarization of AH neurons. The first clue as to the effect of Ca^{2+} was that the hyperpolarizing response was TTX resistant (Hirst et al., 1973). This led to the conclusion that AH neurons have a Ca^{2+} component in the rising phase of their action potentials and was confirmed by use of Ca^{2+} channel antagonists. Vogalis et al. used cell attached patch clamp recordings on LMMP preparations from the guinea pig to demonstrate that K_{Ca} channels open following a spike. Furthermore, calculations from cell-attached recordings noted the unitary conductance of the K_{Ca} channel to be 20-40pS suggesting they belong to the family of intermediate conductance K_{Ca} (IK) channels. The IK channels were found to be resistant to external TEA, which block BK channels, and apamin, which blocks SK channels (Vogalis et al., 2001). Clotrimazole in low micromolar concentrations blocked the IK channel, inhibiting the hallmark AHP of AH neurons in the myenteric plexus. These researchers later found that the IK channel was down regulated by PKA through a cAMP dependent pathway leading to increased excitability of the neuron. In the whole cell patch clamp configuration, they used LMMP preparations from the adult guinea pig and measured a decrease in IK with forskolin treatment and an increase when PKA was blocked (Vogalis et al., 2002b). The abundance of signaling molecules and the receptor systems through which they function in the enteric nervous system leave open a variety of pathways through which IK can be modulated (Vogalis et al., 2003).

Other researchers found that short chain fatty acids like butyrate were able to cause a hyperpolarization in isolated enteric neurons (Haschke et al., 2002). Whole cell voltage clamp recordings on cultured rat myenteric neurons (1-10 days old) demonstrated that hyperpolarization was caused by a K^+ conductance since it was blocked by intracellular Cs^{2+}. The hyperpolarization was also inhibited by thapsigargin indicating that the hyperpolarization was dependent on intracellular Ca^{2+} stores. They concluded that butyrate indirectly activates K_{Ca} channels through the release of intracellular Ca^{2+} thereby hyperpolarizing the cell.

Several types of K^+ currents have been identified in enteric neurons, most of which involve maintenance of the resting membrane potential or modulation of the action potential. Rectifying currents are those in which the conductance is voltage-dependent:

1) inwardly rectifying currents have a small outward conductance

2) outwardly rectifying currents have a small inward conductance.

Patch clamp experiments obtained on cultured myenteric neurons from the guinea pig intestine, in conditions that inhibited a K_{Ca} channel, isolated three distinct K^+ currents:

1) A-type current (K_A)

2) delayed outwardly rectifying current (K_{dr}) and

3) an inwardly rectifying current (K_{ir})(Zholos et al., 1999).

Inwardly and outwardly rectifying channels were observed to depolarizing and hyperpolarizing command potentials. The experiment was performed under conditions in which the holding potential was made progressively more hyperpolarized. The most depolarized holding potential elicited K_{dr} however as the holding potential was hyperpolarized, the holding current decreased demonstrating K_{ir}. Further hyperpolarization of the holding potential elicited a fast activating transient current characteristic of K_A. Confirmation of the channel type was

performed by measurements of their activation and inactivation properties along with specific channel blockers. Block of the K_{dr} channel by TEA or 4-AP broadened the action potential duration. These data show that K_{dr} is responsible for the repolarization of the action potential. K_{ir}, on the other hand, played a small role in the afterpolarization of AH neurons; therefore it is one of the factors keeping AH channels in a low excitability state. The conclusion drawn from this work was that the generation of sEPSP's by neurotransmitters functions as a modulator, decreasing the resting K^+ conductance and allowing spike generation (Zholos et al., 1999).

Initial research using single electrode voltage clamp (SEVC) concluded that ascending interneurons contained a transient outward current when depolarized (Brookes et al., 1997). To further analyze the current, Starodub et al. focused specifically on A-type currents in guinea pig neuronal cultures established from myenteric neurons of the small intestine. Perforated patch recordings were conducted to maintain the intracellular contents. The authors found that A-type channels are expressed in both S and AH neurons, although channel density was higher in S type cells. The activation kinetics was such that the channel was inactive at rest. Therefore activation of the channel was theorized to occur by depolarization, leading to a shortening of the fEPSP and increased excitability (Starodub et al., 2000a). Further studies determined that A-type currents were inhibited by histamine through the H2 receptor; however, the channel was inhibited in AH and not in S-type neurons (Starodub et al., 2000b).

A study using SEVC of guinea pig LMMP preparations sought to determine the effect of muscarine, a cholinergic receptor agonist, on K^+ channels in enteric neurons. In this study, 4 different K^+ conductances were measured relating to K_{Ca}, an inward rectifier, an A-type current, and a "leak" conductance. Their conclusion was that muscarinic agonists had no effect on the inward rectifier or the A-type current. However the K_{Ca} channel and the leak conductance in AH

cells were both reduced. Since S neurons do not contain K_{Ca} only the leak conductance was reduced through M1 receptors in these cells. Therefore, the overall effect of a muscarinic agonist was to increase the excitability of enteric neurons (Galligan et al., 1989).

A major contribution of the excitation of any neuron relies on its ability to establish and maintain a RMP negative enough to remove the deactivation of ion channels. As a result of their negative equilibrium potential, potassium ions are typically responsible for maintaining the RMP through outwardly rectifying K^+ channels. Of this large family, TASK1 was identified in AH neurons in the guinea pig ileum using PCR, immunohistochemistry, and intracellular microelectrode recordings (Matsuyama et al., 2008). Blockers of TASK1, bupivacaine and methanadamide depolarized the cells and increased their input resistance (I_r) indicating that a background channel was being blocked. Although not confirmed by electrophysiology for activity, TASK2 and TASK3 were found in sympathetic and S-type neurons respectively. This research concluded that just as regulation of K_{Ca} alters AH excitability so might regulation of TASK1 (Matsuyama et al., 2008). This conclusion is supported by evidence suggesting inhibition of TASK1 and increased excitability by muscarinic GPCR activation in cerebellar neurons (Mathie 2007).

Potassium channels play a key role in every neuronal cell type currently known including enteric neurons. The dependence of the coding of sensory information by IK in an AH neuron maintains the peristaltic reflex by preventing over excitation of S-type neurons. The K_{dr} current also plays an important role by shortening the duration of the action potential. On the other hand, K_{ir} is partially responsible for maintenance of the membrane potential and keeping the cells hyperpolarized. The contribution of the family of voltage gated K^+ channels to modulating cellular excitability is critical to normal GI function.

4. Chloride channels

Studies of Cl^- conductance have found channels that stabilize the membrane potential, modulate cell volume, and regulate pH. Clearly, this anion is important in several cellular processes and is a major permeating anion in both voltage and ligand gated ion channels. Research to date has classified a wide variety of chloride channel families to match their diverse roles, however, studies on the effects of voltage-gated chloride channels in enteric neurons remain relatively few.

One group has identified a Cl_{Ca} current using cultured myenteric neurons harvested from the adult mouse proximal colon. Using the perforated patch technique, depolarizing pulses exhibited an inward current that was blocked by TTX and Cd^{2+}, indicating the presence of Na^+ and Ca^{2+} channels. When these channels were inhibited, a time-dependent outwardly rectifying current was present along with the appearance of slowly deactivating tail currents when the neuron was repolarized. Substitution of the Cl^- anion shifted the reversal potential while removal of Ca^{2+} inhibited the current suggesting the presence of a Cl_{Ca} channel. This was confirmed with niflumic acid, which had no effect on the Ca^{2+} conductance; however it reduced the identified Cl^- current (Kang et al., 2003). The exact identity of the Cl_{Ca} channel responsible for these currents remains unknown, although CLCA1 and 2 were found in mouse epithelial cells using immunohistochemistry, lending credence to their presence in myenteric neurons (Roussa et al., 2010).

Myenteric neurons most likely contain other Cl^- channels that have yet to be identified. One of the most ubiquitous Cl^- channels is VRAC or $I_{Cl,swell}$ which is involved in the maintenance of cell size and volume (Ackerman et al., 1994). Theories persist as to whether this channel is stretch-activated or an osmolarity sensor; either way enteric neurons need to adapt to both

conditions (Kozlowski 1999). The knowledge of voltage gated Cl^- channels in the myenteric plexus is incomplete.

5. Other channels

Several other ion channels that may have important physiological functions are present in enteric neurons. Some of these include non-selective cation channels and ligand gated ion channels. The first targeted recordings of hyperpolarization-activated cyclic nucleotide gated (HCN) ion channels in the enteric nervous system were performed by Galligan et al. They identified a sag in the electrotonic potential of AH neurons when the cells were hyperpolarized beyond -70mV. The recordings were performed on myenteric and submucousal preparations of the ileum of adult guinea pigs using microelectrodes and whole cell patch clamp. The HCN channels had differential permeability to Na^+ and K^+ as was demonstrated in a series of experiments in which the concentrations of these ions was altered (Galligan et al., 1990). Direct identification was first made by transcripts of HCN, 1, 2 and 4 being expressed in the enteric nervous system by immuno-reactivity. Measurements taken from the adult guinea pig ileum using SEVC indicated HCN currents. Immuno-reactivity post recording found that AH neurons contained HCN 2 and 4. Interestingly the rat ileum and mouse distal colon showed positive immuno-reactivity for HCN 1 and 2 indicating differential expression of HCN amongst species (Xiao et al., 2004).

TRPV1 is a polymodal sensor of both heat and inflammatory pain and has been found to be upregulated in patients with IBS. Conversely, TRPV1 antagonists have been shown to decrease colonic hypersensitivity in inflammatory and post-inflammatory models. The identification and distribution of TRPV1 found that the channel co-localized with calcitonin gene related peptide (CGRP) and SP. Although TRPV1 immuno-reactivity was positive and found to

innervate the mucosa and smooth muscle layers, cell bodies could not be located leading to the assumption that they are on extrinsic primary afferent fibers. TRPA1 is also expressed on sensory neurons and seems to follow the expression pattern of TRPV1 as desensitizing contractions to TRPA1 cause cross-desensitization with TRPV1 contractions (Penuelas et al., 2007). This dictates some kind of overlap in signaling, however, if this effect is neurogenic or myogenic is unknown. Most research on these channels is focused on their modulation by pain and inflammation in sensory afferent neurons (Matsumoto et al., 2011; Storr 2007).

6. Ligand gated ion channels

Years of research have been conducted on ligand-gated ion channels (LGIC) because of their importance in neurotransmitter and hormone signaling throughout the GI system. It was not until relatively recently that electrophysiologists were able to accurately measure ionic currents and identify proteins that respond to voltage as opposed to a ligand. A comprehensive review on ligand gated ion channels of the enteric nervous system was assembled by Galligan, J.J., 2002. In summary, S and AH neurons were found to contain nAChR, P2X, 5-HT3, NMDA, and AMPAR, which are non-selective cation channels and GABA and Glycine which are permeable to Cl^-. Our studies focused mainly on voltage sensitive ion channels, although, due to their diversity and abundance, the LGIC's deserve mention. Please refer to the following review for further information on LGIC (Galligan 2002).

D. Development of IM-PEN and IM-FEN

The importance of studying murine enteric neurons derives from the hundreds of mouse models that are available to researchers. For example, a search of The Jackson Laboratory's website for colitis returns 19 different mouse strains, each having a genetic alteration with the propensity to develop some type of colitis. Used as a general term to state an inflammatory

condition in the gastrointestinal tract, colitis can be divided into IBD, Chrohn's disease, ulcerative colitis and several other syndromes. However, these 19 models are not available in other species and electrophysiology of the murine gastrointestinal tract is complicated by several issues. Development of a method by which to study these enteric neurons could be invaluable to the gastrointestinal field to developing treatments and understanding how those and other treatments affect the GI in return. Complications in the single cell voltage clamp approach range from difficulty in the isolation of mouse enteric neurons to the varied electrophysiological techniques and limitations used to record them. A recent protocol to patch clamp mouse enteric neurons in situ results in a challenging procedure that takes approximately 4 hours to isolate the LMMP (Osorio et al., 2010). Although there are several positives about this technique, the recordings must be done in the presence of L-type Ca^{2+} channel blockers and muscarinic antagonists (ie. nicardipine and atropine). The protocol states that care must be made to ensure these blockers do not alter the currents one wishes to measure. Although a major step forward for electrophysiologists studying the enteric nervous system there are still limitations which require other methods.

An additional example is the result of genetic manipulation of the mouse genome. This led to the development of an enteric neuron cell line (EN cell) isolated from the stomach and intestine of the H-2kb-tsA58 mouse (immortomouse) (Anitha et al., 2008). This transgenic mouse has an immortalizing gene, the tsA58 large T antigen (TAg), which is controlled by a temperature sensitive promoter H-2kb, permissive at 33°C and not 39°C. This promoter can be further initialized by the addition of interferon, a class I antigen. The Tag functions by inhibiting the tumor suppressor genes P53 and retinoblastoma (Prb) thereby causing the cell to continue from G1 to S phase and divide (Ludlow 1993). The normal body temperature of the mouse is

approximately 39°C and very few cells express high levels of interferon, making the transgene inactive in vivo. As a result, in situations where it has been difficult to isolate primary cultures because of low cell recovery, one can isolate the cells from the H-2kb-tsA58 mouse. Growing them at the permissive temperature of 33°C, and then placing the cells at 39°C in a low serum media slows the cell cycle and allows the cell to grow/differentiate for study (Jat et al., 1991)(Noble et al., 1995). A cell line development core facility at Vanderbilt University has demonstrated how valuable the immortomouse mouse can be by developing a series of GI epithelial cell lines from transgenic mice. Like enteric neurons, epithelial cells have been notoriously difficult to culture, and the immortomouse circumvents this issue, and crossbreeding allows for the development of a transgenic cell line (Whitehead et al., 2009).

Both fetal (IM-FEN) and post-natal (IM-PEN) cell lines of enteric neurons isolated from the stomach and small intestine of the H-2kb-tsA58 mouse (immortomouse) have been developed. Several neuronal specific markers were assayed including PGP9.5, cRet, and SERT expression at both 33°C and 39°C. Several of these markers showed increased expression after incubation in 1% low serum media at 39°C after 7 days. To prove functionality of the cell line, the IM-FEN cells were transplanted into both a C57BL/6 nNOS KO mouse strain and a Piebald mouse strain. One week later, longitudinal muscle strips were removed (with the attached myenteric plexus) and colonic relaxation or contraction was measured in the respective strains in response to neurogenic stimulation. The relaxation to neuronal stimulation in the $nNOS^{-/-}$ mice was improved in the transplanted mice. On the other hand, the heterozygote Piebald mice have a known reduction in the number of enteric neurons in the distal portion of the colon resulting from a spontaneous mutation (Spencer et al., 2008). The transplanted Piebald mice regained their contractile properties as measured by a bead expulsion assay recovering to wildtype

C57BL/6 levels (Anitha et al., 2008). More recently, research from the same lab demonstrated the ability of bone morphogenic protein-2 (BMP-2) to increase the differentiation characteristics of IM-FEN over that of treatment with glial cell line derived neurotrophic factor (GDNF). An increase in neurite length, βIII-tubulin expression, and nNOS, tyrosine hydroxylase (TH), and NPY expressing neurons were all apparent with BMP-2 (Anitha et al., 2010). These findings suggested that IM-FEN cells have the propensity to develop into functional neurons in vivo. However, the basic electrical properties, or the composition of sensory to motor neurons during culture are not known.

II. Goals and specific aims

The major long-term goal of this study was to discern the electrophysiological properties of the IM-PEN cell line. This included measurements of the passive and active properties of the cells. Identification of ion channels responsible for these properties is of utmost importance to researchers because once characterized, this cell line may well provide an excellent model for pharmacological and therapeutic studies on enteric neurons.

III. Materials and Methods

Cell Culture

Frozen stocks of both the IM-FEN and IM-PEN cell line were obtained from our collaborator Dr. Shanthi Srinivasan, Emory University (Anitha et al., 2008). IM-FEN and IM-PEN cell propagation and differentiation occurs in 2 steps: Propagation: 1) Cells were cultured in Dulbecco's Modified Eagle/F12 (DMEM/F12) media, N2 supplement, interferon-γ (20U/ml of recombinant mouse interferon-γ), Glial cell-line derived neurotrophic factor (GDNF) (100ng/ml), antibiotic and 10% fetal bovine serum (FBS) at the permissive temperature of 33°C in 10% CO2. The permissive temperature and interferon-γ caused expression of the transgene containing TAg and promoting proliferation of the cell lines. The cells were passaged when confluent using trypsin-EDTA 0.25% with cells plated at 33°C and others at 37°C. Differentiation: 2) To differentiate these cells towards a neuronal lineage, the medium was changed to Neurobasal–A medium containing B-27 supplement, 1 mM glutamine, 1% FBS, antibiotic and GDNF (100 ng/ml) and incubated at 37°C with 5% CO2 for 5-9 days. It is on these cells that experiments were performed. Fresh media was added every 3 days to maintain a healthy cell population. No change in the cell line was demonstrated over the course of 40 passages. As a result, thawing of earlier stocks to maintain the continuity of the cell line was conducted at this time point.

Immunocytochemistry

The protocol to perform the immunocytochemistry on the IM-PEN cells involved several steps. Table 0-3 is a list of the primary and secondary antibodies used along with their dilutions. The cells were first fixed with 4% formaldehyde solution for 1 hour and washed 3 times with

PBS for 5 minutes each. The permeabilization step was conducted with 1% Triton X-100 diluted in PBS and incubated for 2 hours. The cells were then washed 3 times in PBS for 5 minutes each before addition of 10% goat serum for 1 hour. Another wash step with PBS preceded the addition of the primary antibody which was either incubated for 2 hours at room temperature (23°C) or overnight at 4°C. The primary antibody was diluted in 0.3% Triton X-100 in PBS (Table 0-3). Another series of wash steps preceded incubation of secondary antibody (Table 0-3) which was also diluted in 0.3% Triton X-100 in PBS. For controls the primary antibody was omitted and the secondary antibody was given alone. Visualization was made using an Olympus FluoView FV300 confocol microscope (Olympus America Inc., Center Valley, PA,).

Table 0-3 Antibodies used for Immuno-reactivity

Antigen	Primary antibody	Dilution	Source	Secondary antibody	Dilution
βIII tubulin	rabbit, polycolonol	1/1000	Abcam Inc.	Alexa Flour 488	1/500
PGP9.5	rabbit, polycolonol	1/1000	Abcam Inc.	Alexa Flour 568	1/500
S100	rabbit, monoclonal	1/500	Chemicon,	Alexa Flour 488	1/500
ChAT	rabbit, polycolonol	1/200	Santa Cruz Biotech	Alexa Flour 488/568	1/500
NOS-1	mouse, monoclonal	1/200	Santa Cruz Biotech	Alexa Flour 488/568	1/500
TRPV1	goat, polyclonol	1/500	Santa Cruz Biotech	Alexa Flour 488	1/500

Electrophysiology

Whole-cell currents were measured in IM-PEN cells by the patch clamp technique. External and internal patch pipette solutions were experiment dependent and are detailed in Tables 0-4 and 0-5. The pH of the external solutions was adjusted with NaOH and the internal solution with KOH, except for the Cs^{2+} containing solution in which CsOH was used. The

osmolality was determined using freezing point depression on an Advanced Model 3300 Micro-Osmometer from Advanced Instruments, Inc. (Norwood, MA).

Table 0-4 External solutions (Concentration in mM)

	1	2	3	4	5	6	7	8
Purpose	normal	Na^+	Ca^{2+}	No Ca^{2+}	Cl^- removal	isoosmotic	hypoosmotic	hypoosmotic
NaCl	135	-	125	135	29	110	110	-
KCl	5.4	5.4	5.4	5.4	5.4	-	-	-
NaH_2PO_4	0.3	0.3	0.3	0.3	0.3	-	-	-
HEPES	5	5	5	5	5	10	10	10
$MgCl_2$	1	1	1	1	1	1	1	1
$CaCl_2$	2	2	-	-	2	1	1	1
$BaCl_2$	-	-	10	-	-	-	-	-
glucose	5	5	5	5	5	-	-	-
NMDG	-	135	-	-	-	-	-	-
TEA	-	-	5	-	-	-	-	-
Gluconic acid	-	-	-	-	106	-	-	110
mannitol	-	-	-	-	-	300mOsm	230mOsm	230mOsm
pH	7.4	7.4	7.4	7.4	7.4	7.3	7.3	7.3

Table 0-5 Internal solutions (Concentration in mM)

	A	B	C	D
Purpose	normal	low EGTA	Ca^{2+}	Isotonic Cs
K-aspartate	100	100	-	-
KCl	30	30	-	-
ATP-Mg	4.5	4.5	4.5	-
$MgCl_2$	1	1	2	1
HEPES	10	10	10	10
EGTA	6	0.1	10	-
Cs-aspartate	-	-	100	-
CsCl	-	-	30	50
NaCl	-	-	-	-
mannitol	-	-	-	290mOsm
pH	7.2	7.2	7.2	7.3

External solution (Table 0-4) 1 was physiological in nature, solution 2 had Na^+ replaced with NMDG, solution 3 contained 10mM Ba^{2+}, solution 4 had Ca^{2+} removed, and solution 5 had Cl^- removed. The isoosmotic and hypoosmotic solutions (6-8, Table 0-4) for the recording of $I_{cl,swell}$ were adapted from (Harvey et al., 2010). The internal solutions are numbered in Table 0-5: solution 1 was physiological (high EGTA), solution 2 was the same as 1 with low EGTA, solution 3 contained Cs^{2+}, and solution 4 was adapted from (Harvey et al., 2010). Each experiment required specific solutions which are referenced in the text by their respective letter or number. Any compounds or drugs used were perfused in the same solutions and concentrations defined in the text. Patch-clamp recordings in the whole-cell configuration were made at room temperature with an Axopatch 200B amplifier (Molecular Devices, Sunnyvale, CA). Patch pipettes with resistances of 3-5MΩ were pulled from thick walled borosilicate glass tubes (1B150-6, WPI, Sarasota, FL) on a Flaming-Brown P97 electrode puller (Sutter instruments, Novato, CA). Pulse generation and data acquisition were achieved using Clampex and Clampfit 10.2 software through an Axon Digidata 1440A and a Minidigi 1A (Molecular Devices, Sunnyvale, CA). The stimulus and holding potentials were experiment-dependent and are mentioned with their respective data in the Results section. Data were acquired at 5kHz and low pass filtered at 1-2kHz. Series resistance did not exceed 5MΩ and was not compensated. All of the data were collected after the cell was allowed 5 minutes to stabilize to the recording conditions.

Reverse Transcription – Polymerase Chain Reaction (RT-PCR)

Expression of mRNA was examined by RT-PCR. The IM-PEN cells were cultured as previously mentioned in 10 cm tissue culture dishes for 7 days at 37°C. RNA was purified using the Invitrogen Purelink™ Micro-to-Midi total RNA purification system following the

recommended protocols for cellular isolation (Invitrogen, Carlsbad, CA). The concentration was determined using a spectrophotometer and preceded DNAase1 treatment which was also conducted following recommended protocols by Invitrogen. Approximately 200ng of RNA was used in the Quantace One-step Sensi-mix (Bioline, Taunton, MA) to perform the RT-PCR. The primers were obtained from the literature or created using the basic local alignment search tool (BLAST) (Altschul et al., 1990) and are in Table 0-6. The following accession numbers were used in the primer search for BLAST; Cav2.2 (NM_007579), Nav1.3 (NM_018732), and Nav1.9 (NM_018852). RT-PCR protocols were run using an MJ MiniOpticon from BioRad (Hercules, CA). A gradient RT-PCR run from 50-68°C determined an optimal annealing temperature of 57°C using mouse brain as a control. The protocol consisted of an initial 30 minute incubation at 42°C to generate a cDNA template. A ten minute incubation at 95°C was then conducted to activate the polymerase and deactivate the reverse transcriptase. The PCR was conducted over 35 cycles of: 1) denaturation (95°C for 30s), 2) annealing (57°C for 30s), and 3) extention (72°C for 30s). A melt curve was run at for each product from 50°C to 99°C. The resultant oligonucleotides were visualized on a 3.5% agarose gel containing ethidium bromide and pictures were taken using a UVP transilluminator (Upland, CA).

Table 0-6 Primers used for RT-PCR

Product	Primer	Sequence (5' - 3')	Reference
TRPA1	Forward	ACAAGAAGTACCAAACATTGACACA	(Penuelas et al., 2007)
	Reverse	TTAACTGCGTTTAAGACAAAATTCC	
TRPV1	Forward	AGCGAGTTCAAAGACCCAGA	(Penuelas et al., 2007)
	Reverse	TTCTCCACCAAGAGGGTCAC	
$Ca_v2.2$	Forward	CTGTGGGTGACTTTCCCTGT	BLAST
	Reverse	CAACCAGTTCCATGTGTTGC	
TASK1	Forward	CATCGGCGCAGCTGCCTTCT	(Matsuyama et al., 2008)
	Reverse	CGATGACCGTGAGGCCCGTG	
$Cl_{Ca}1$	Forward	GTGGACCAGCCGGGCTACATGTCTAG	(Roussa et al., 2010)

	Reverse	TGTGACACAGTTGCCTCTCTCA	
$K_{Ca}3.1$	Forward	CAACAAGGCGGAGAAACACG	(Neylon et al., 2004)
	Reverse	GCATCTTGGAGATGTCCAC	
$Na_v1.3$	Forward	GCCTTCTTATCGCTGTTTCG	BLAST
	Reverse	TCAACTGCTCCAACATCTGC	
$Na_v1.9$	Forward	TGGATTCCCTTCGTTCACAGA	BLAST
	Reverse	GTCGCAGATACATCCTCTTGTTT	

Data Analysis

Electrophysiological data were obtained using the Clampex 10.2 software from Molecular Devices, Sunnyvale, CA. Current-Voltage relationships for the inward current were measured as the peak negative inward current from the start of the pulse to the 50ms time point. The outward currents were measured at the end of the stimulation pulse. The data were graphed and analyzed using SigmaStat 11. Results are reported as means ± standard error of the mean for n number of samples. To normalize for cell size the current (pA) is reported as the peak current density (pA/pF). Statistics were performed using a Students t test using an α of 0.05 with significance of $p < \alpha$.

Calculation of the equilibrium potential using the Nernst equation involved the following formula: $E = \frac{RT}{zF} ln \frac{[ion\ outside]}{[ion\ inside]}$; where R = the ideal gas constant, T = temperature in Kelvin, z = valence, and [X] denote concentrations of the ion outside and inside the cell.

The time constant of the electrotonic potential was calculated using a standard exponential fit of the curve between the stimulus in Clampex 10.2 with equation $f(t) = \sum_{i=1}^{n} A_i e^{-t/t_i} + C$; whereby A = amplitude, τ = the time constant, and C is an offset constant. The fitting method used was Chebyshev and is described in detail in the pCLAMP 10 User Guide.

Construction of the steady state voltage inactivation curve involved a two pulse protocol. A Vh of -80mV was used with a prepulse starting from -80mV to +10mV in 10mV increments

for 100ms. The test pulse, to activate the inward current was -30mV for 100ms. Measurements of the evoked test pulse current were divided by the maximum current in order to normalize the data. The fraction of test current still available was plotted against the pre-pulse potential. These points were fitted using the Boltzmann charge-voltage fit yielding the steady-state voltage inactivation curve and activation curve. $I = I_{\max}/[1 + \exp((V_{\text{mid}} - V)/V_c)]$ and $g = g_{\max}/[1 + \exp((V_{\text{mid}} - V)/V_c)]$.

MASH1

Chemical transfection of the cell line was conducted following the specified protocol for GeneJammer from Agilent Technologies. A pCDNA3 vector was used as the shuttle for GFP transfection to confirm transfection of the cells. The vector for MASH1 transfection was constructed by OriGene Technologies, Inc., using the mouse Ascl1 gene NM_008553 and placed in vector PS100026. Dishes were transfected at 70-80% confluency with 300ng of vector. Co-transfections were performed with equal amounts of both plasmids. GFP was only able to be visualized for 4-5 days on the upright microscope (10X), however confocal images seemed to see GFP out to eight days.

Drugs

Unless otherwise noted the compounds used to make the various buffers were obtained from Sigma-Aldrich Corp., (St. Louis, MO). The 4-[(2-Butyl-6,7-dichloro-2-cyclopentyl-2,3-dihydro-1-ox o-1H-inden-5-yl)oxy]butanoic acid (DCPIB) was obtained from Tocris Bioscience, (Ellsville, MO).

IV. Results

A. Chapter 1: Neuronal background of cells from the small intestine of the H-2kb-tsA58 transgenic mouse (immortomouse)

1. 1.1 Growth

The IM-PEN cell line has two phases in culture; 1) propagation at 33°C and 2) differentiation at 39°C. The cells appeared to have clear morphological distinctions when grown at the 33°C proliferative stage versus the 39°C differentiation stage. As seen in Figure 1-1A, cells grown at the permissive stage appear to be rounded with little neurite outgrowth. These cells were incubated in DMEM media containing 10% fetal bovine serum, N2, and interferon gamma (IFNγ), which were present to increase transcription of the H-2kb-tsA58 transgene (Anitha et al., 2008). It has been demonstrated that placing cells in serum starved conditions can help them differentiate (Seidman et al., 1996). In Figure 1-1B IM-PEN cells grew neurites, as indicated by black arrows, and appear to fit the classical morphology of a neuron, with a cell body and possible axon and/or dendrites. Differentiated IM-PEN cells were incubated at 37°C for 7 days in Neural basal A media, with B-27 supplement and 1% FBS. Under conditions of low serum and inactivation of the transgene (39°C) development dictates the neuronal background of the IM-PEN cell line (Anitha et al., 2008).

2. 1.2 Immunocytochemical evidence of neuronal background

The second method used to determine if IM-PEN cells were neuronal in origin was immunocytochemistry. Several specific antibodies are available for the identification of both neurons and the cells

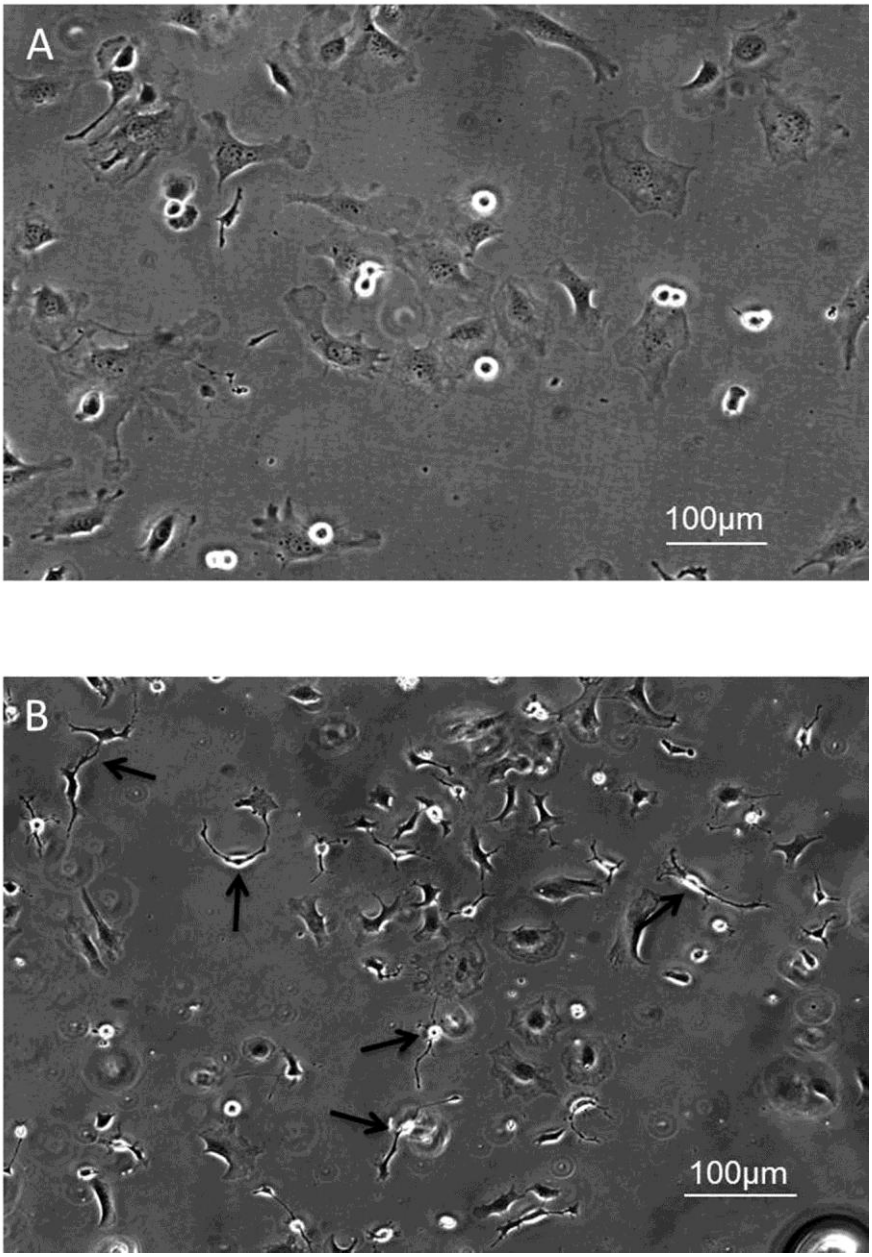

Figure 1-1 Phase contrast images of IM-PEN at 33°C and 39°C A) IM-PEN at the permissive culture conditions of 33°C with interferon-γ appear circular. B) Growth of neurites (black arrows) seen under differentiating conditions (39°C without interferon-γ) after 7 days. Images were taken at 10X magnification

that surround them in the gastrointestinal system such as glial and smooth muscle cells. Information on the dilutions of primary and secondary antibodies used is provided in the Methods section. The IM-PEN cells were stained for two neuronal markers, βIII-tubulin and the pan-neuronal marker PGP9.5 (Takehara et al., 2009)(Ritter et al., 2009). Figure 1-2A and 1-2B show positive immuno-reactivity of PGP9.5 and βIII-tubulin respectively (20X). In panel 1-2C at 60X the immuno-reactivity of βIII-tubulin appears in long strands surrounding the nucleus of the cell, characteristic of a microtubule protein. As a control, the primary antibody of βIII-tubulin was not added, and demonstrated the specificity of the secondary antibody (Figure 1-2D). The same control was performed for PGP9.5 with the identical result (data not shown). Clear immuno-reactivity of the microtubule protein βIII-tubulin was also present when the cells were grown on laminin, Figure 1-2E. The glial cell marker S100 (Figure 1-3) showed no immuno-reactivity in IM-PEN cells incubated at 37°C for 7 days, consistent with the conclusion that IM-PEN are neuronal cells, and confirming previous findings (Anitha et al., 2008).

Enteric neurons are known to communicate through a complex grouping of hormones and neurotransmitters (Hansen 2003)(van Nassauw et al., 2010). Of the many possible neurotransmitters, two of the most studied in the gut are ACh and nitric oxide (NO) (Grider 1989)(Mustafa et al., 2009). Since neurotransmitters are typically short lived, it is common to search for enzymes involved in their synthesis to establish their presence. For ACh, this enzyme is choline acetyl transferase (ChAT) and for nitric oxide (NO) the enzyme is neuronal nitric oxide synthase (nNOS or NOS-1)(Oda 1999)(Knowles et al., 1994). In Figure 1-4, panel A shows the nuclei stained with Hoechst nuclear stain (blue) showing the presence of viable cells and panel B shows negative immuno-reactivity for NOS and ChAT respectively. In conclusion it appears that the IM-PEN cell line is neuronal in nature; positive immuno-reactivity of PGP9.5

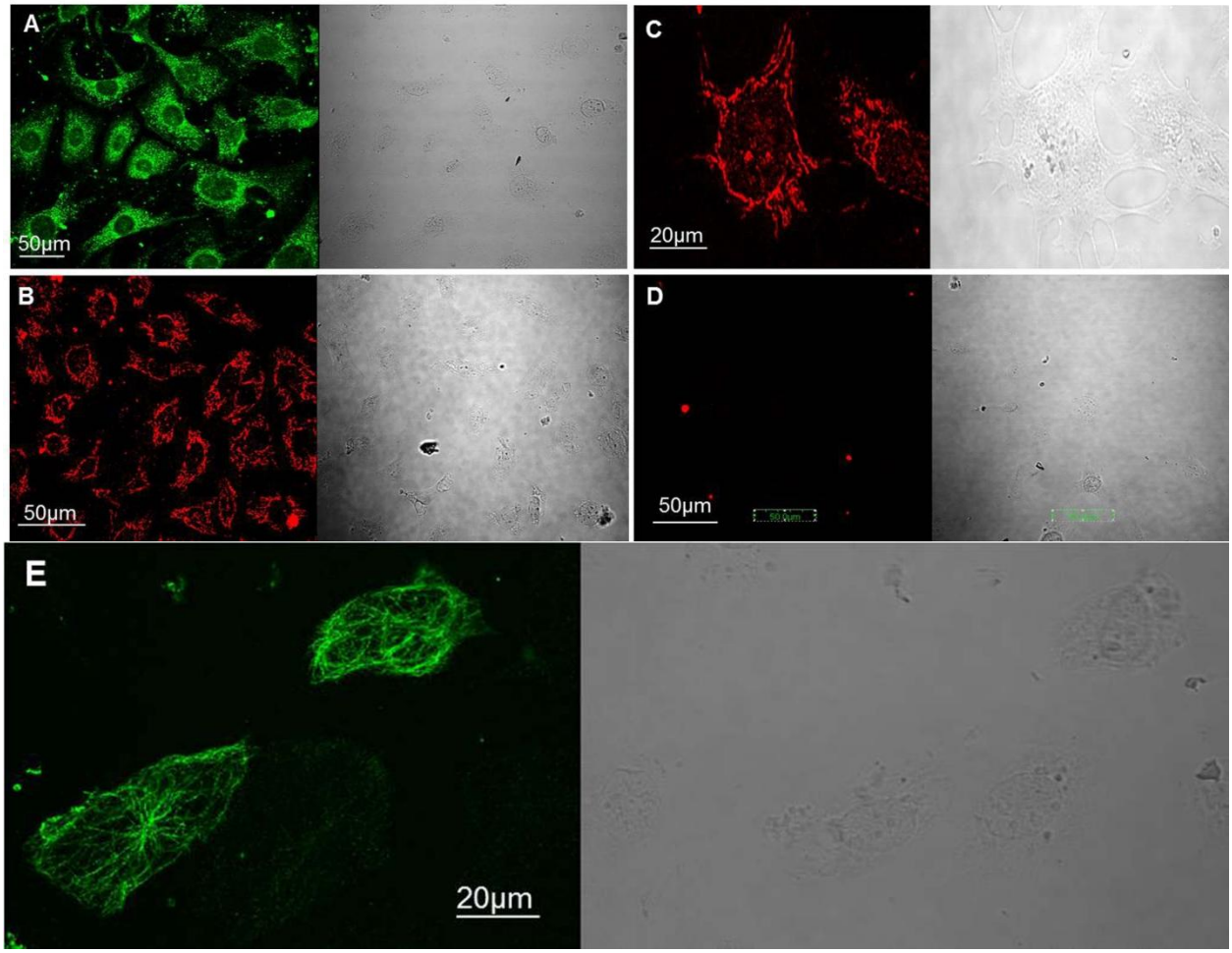

Figure 1-2 IM-PEN exhibits positive immuno-reactivity for the neuronal marker βIII-tubulin (Tuj1) and PGP9.5 A) PGP9.5 immuno-reactivity (green) 20X B) βIII-tubulin immuno-reactivity (red) 20X C) higher magnification of βIII-tubulin (red) 60X D) control in the absence of primary antibody 20X E) IM-PEN grown on laminin also showed positive immuno-reactivity for βIII-tubulin (green) 60X. Each experiment is shown in conjunction with its respective brightfield image.

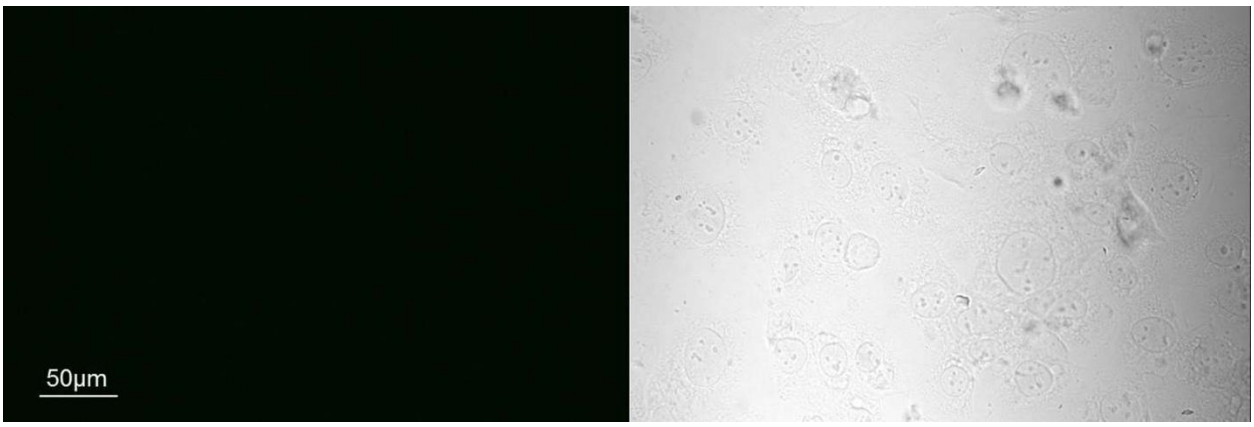

Figure 1-3 immuno-reactivity of glial marker immuno-reactivity for the glial cell marker S100 was negative 20X in IM-PEN cells after 7 days at 39°C (differentiation conditions).

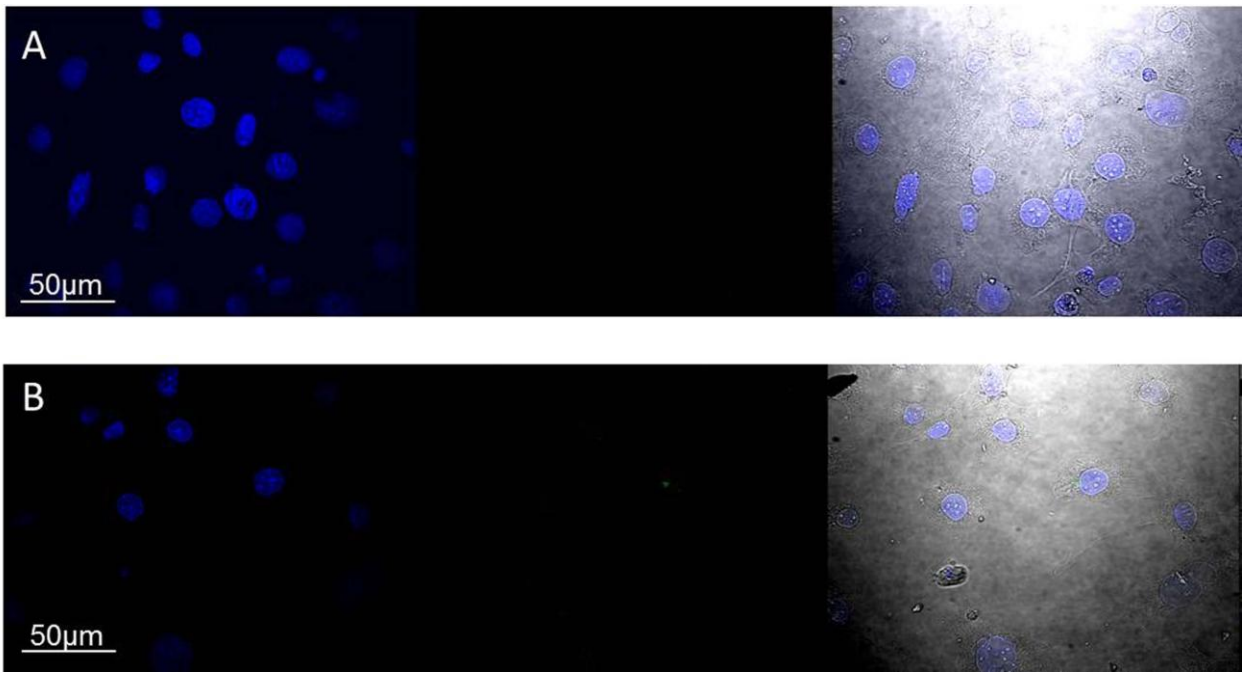

Figure 1-4 Presence of neurotransmitters A) horizontally across panal A; immuno-reactivity for nuclei with Hoechst, NOS-1 and an overlay with the brightfield image 20X. B) Same as A showing negative immuno-reactivity for ChAT 20X.

and βIII-tubulin, and negative immuno-reactivity of S100. However, IM-PEN cells did not express the necessary enzymes to produce the neurotransmitters ACh and NO. Although many neurotransmitters/hormones could be present in this cell line our goal was to characterize IM-PEN's electrophysiological properties and therefore the possible presence of other neurotransmitters was not investigated.

3. 1.3 PCR of ion channels expressed in IM-PEN

To determine if ion channels expressed in enteric neurons are present in IM-PEN cells, reverse transcription PCR (RT-PCR) was performed. Primer sequences were obtained from the literature or constructed in BLAST and can be found in the Methods section (Altschul et al., 1990). Optimization of the protocol was achieved using mouse brain mRNA as a control. We examined the gene expression of the transient receptor potential cation channels (TRPA1 and TRPV1), N-type calcium channel ($Ca_v2.2$), acid-sensitive K^+ channel (TASK1), calcium activated chloride channel (Clca1), intermediate conductance potassium channel (IK, $K_{ca}3.1$), and voltage sensitive sodium channels ($Na_v1.3$, and $Na_v1.9$). As seen in Figure 1-5, mRNA for TRPA1, TRPV1, ClCa1, $K_{ca}3.1$ (IK), $Na_v1.3$ and $Na_v1.9$ were present while $Ca_v2.2$ and TASK1 were very faint, indicating little to no expression. These data are important in two ways;

1) they demonstrated that a number of ion channels that are expressed in enteric neurons are also expressed in IM-PEN and

2) mRNA for some ion channels known to be responsible for characteristics of the action potentials of enteric neurons are also expressed (e.g., $Na_v1.3$, $K_{Ca}3.1$) .

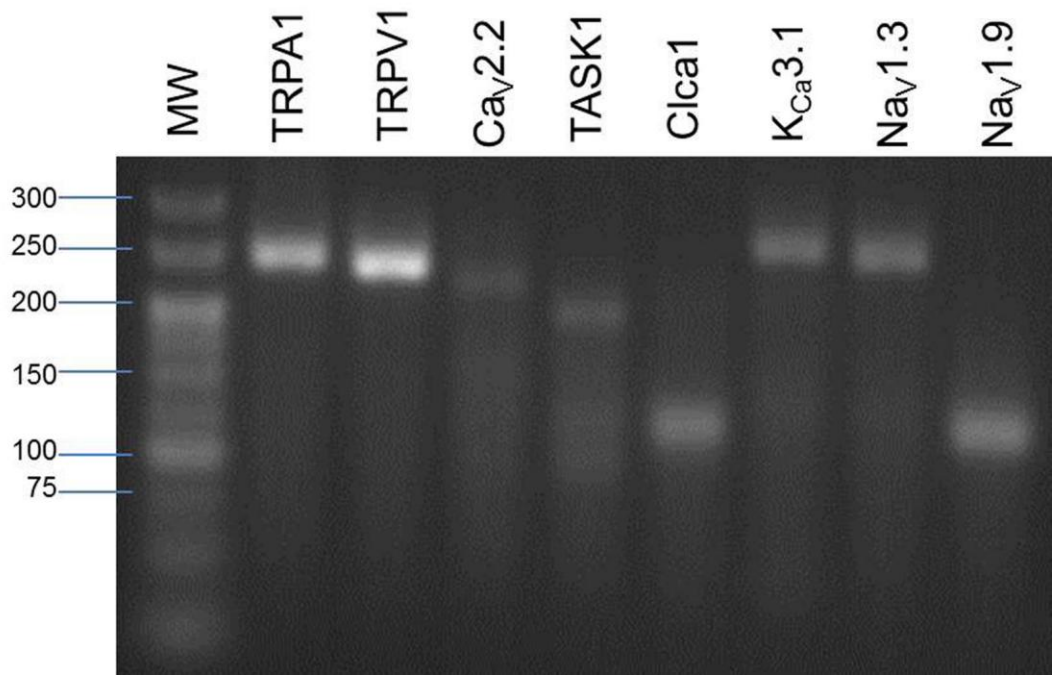

Figure 1-5 mRNA of ion channels from IM-PEN cells 2.5% agarose gel of RT-PCR fragments from IM-PEN after 7 days at 39°C identifying specific ion channels known to be expressed in enteric neurons.

B. Chapter 2: Electrophysiological characteristics of IM-PEN

1. 2.1 Passive membrane properties

At rest the electrical properties of a cell can yield information which can be used to delineate cell types. The measurement of these properties stems from our ability to model the cell as an electrical circuit. An electrotonic current is defined as a current that proceeds and eventually dissipates within the cell because it is too weak to "activate" the cell. However, because, in theory, no channels are activated by an electrotonic current, several inherent properties of the cell can be measured such as its input resistance and the membrane time constant. Other passive membrane properties include the resting membrane potential generated by ionic pumps creating an electrochemical gradient between the internal and external environments, and the cell size (Hille 2001)(Osorio et al., 2010).

Using the whole cell current clamp technique, the resting membrane potential (RMP) of the IM-FEN cell line was measured as -24.6 ± 2.1mV (n=6) and for IM-PEN as -28.9 ± 0.9mV (n=30). An important caveat in measuring RMP in single cells is that the seal resistance needs to be at least 10X greater than the input resistance to avoid shunt artifacts. Although there was no statistical difference between the RMP's of IM-FEN and IM-PEN, using a Student's t test, the cell lines are clearly more depolarized than enteric neurons measured in vivo (Table 0-1). The input resistance is a measure of how "leaky" an extra-cellular membrane is during the course of an electrotonic potential. There was no significant difference between the input resistance of IM-FEN (552.2 ± 104.8MΩ, n=6) and IM-PEN (728 ± 128MΩ, n=20) using a Student's t test. These measurements are also near the previously measured input resistance of 497 ± 52MΩ of mouse AH enteric neurons (Mao et al., 2006). Measurement of cell capacitance or how much

Table 2-1 Passive properties of IM-FEN and IM-PEN.

	IM-FEN	IM-PEN	Laminin IM-PEN
Resting membrane potential	-24.6 ± 2.1 mV (n=6)	-29.8 ± 0.9 mV (n=30)	-23.7 ± 4.8 mV (n=5)
Input resistance	552.2 ± 104.8 MΩ (n=6)	728 ± 128 MΩ (n=20)	307.5± 29.2MΩ (n=4)
Membrane area		37.2 ± 1.9 pF (n=30)	27.6 ± 4.7 pF (n=5)
Action potentials	No (n=6)	No (n=20)	No (n=4)
Time constant of electrotonic potential	70.9 ± 14.1 ms (n=6)	89.9 ± 18.6 ms (n=4)	90.8 ± 46.6 ms (n=4)

charge can be stored on the membrane is directly proportional to membrane area. Enteric neurons have an average size of approximately 55pF depending on type (Osorio et al., 2010)(Rugiero et al., 2002). The IM-PEN cells are smaller at 37.2 ± 1.9pF, n=30 after 7 days in 37°C.

2. 2.2 Action potentials

The *sin qua non* of a neuron is the ability to fire action potentials. As previously mentioned in the Introduction, this was one method used to distinguish two different sub-types of enteric neurons, AH from S (Wade et al., 1988). In the experiment illustrated in Figure 2-1A, hyperpolarizing current was superimposed on the holding current to bring the resting membrane potential of an IM-PEN cell to -80mV. This was to confirm that the inactivation of any VGNC's present was removed. Both hyperpolarizing and depolarizing pulses were given in order to generate an electrotonic potential and action potential respectively. As seen in table 2-1, neither the IM-FEN (n=6) nor IM-PEN cells (n=20) were able to generate action potentials. It is important to note that all six of the IM-FEN cells tested were given a hyperpolarizing current to have a resting membrane potential of -60mV. This was in contrast to the IM-PEN cells in which the same number of cells was held at -60mV and 14 cells were held at -80mV. The dotted line box in Figure 2-1A marks the electrotonic potential in response to a hyperpolarizing pulse used to measure the electrotonic time constant (τ). An example of the exponential fit used to calculate τ is shown in Figure 2-1B with values given in Table 2-1. There was no statistical difference in the τ of the electrotonic potential in IM-FEN (70.9 ± 14.1ms, n=6) versus that of IM-PEN (89.9 ± 18.6ms, n=4) as measured by a Student's t test.

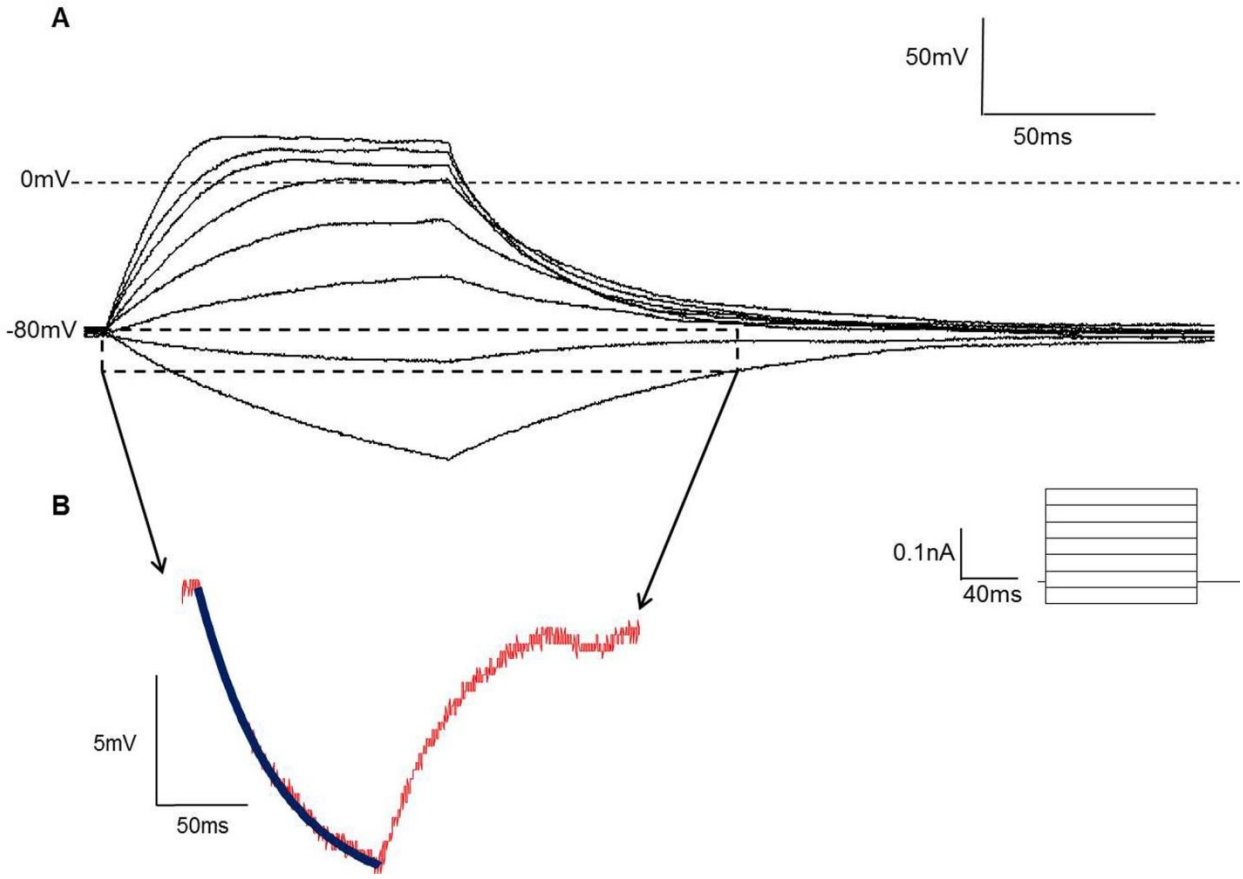

Figure 2-1 Whole cell current clamp recording of IM-PEN cell. A) Depolarizing current pulses elicited passive responses and large electrotonic potential with hyperpolarizing pulses. B) An amplification of the electrotonic potential in A (red) with an overlay of the exponential fit (blue) used to calculate the time constant (τ) of the electrotonic potential in Table 2-1.

Several studies have shown that primary cultures of isolated neurons appear to grow better when there was a binding surfactant for adhesion of the cells (Gershon 2010). One such surfactant is the glycoprotein laminin, which forms part of the basal lamina and produces a protein network for cell attachment (Ratcliffe 2010)(Wade et al., 1988). Growing IM-PEN cells on laminin-coated cover slips resulted in no significant changes in the passive membrane properties of the IM-PEN cell line as determined by a Student's t test (Table 2-1). The resting membrane potential remained depolarized at -23 ± 4.8mV (n=5), and the mean cell size was similar to cells not grown on laminin at 27.6 ± 4.7pF (n=5). No action potentials were produced and the time constant of the electrotonic potential remained equivalent at 90.8 ± 46.6ms (n=4). The largest change was in the input resistance, which decreased from 728 ± 128MΩ to 307.5 ± 29.2MΩ. This change could be a result of the conditions under which the electrophysiological recordings were made. The IM-PEN cells were harvested using trypsin prior to patching whereas the laminin cells were not. As there were no significant differences in the passive or active membrane properties of IM-FEN and IM-PEN we turned our attention to the investigation of the ion channels expressed in IM-PEN cells. Our hypothesis being that the IM-PEN cells are further differentiated because they are 2 day post-natal as opposed to E13 (Burns et al., 2009; Roberts et al., 2010).

3. 2.3 Ion Channels

a) 2.3a Sodium

Several ions contribute to the overall electrical characteristics of a cell. These typically include Na^+, K^+, Ca^{2+}, and Cl^-, each of which flow in or out of the cell depending on their equilibrium potential estimated by the Nernst equation. We know from the RT-PCR experiment that IM-PEN express mRNA for at least two different voltage gated sodium channels ($Na_v1.3$

and $Na_v1.9$). Since we were unable to stimulate an action potential in these cells, our first priority was to ascertain if active VGNC's were present in IM-PEN. From a holding potential (Vh) of -80mV, 10mV step depolarizations were given for 350ms with external solution 1 and internal solution A (Tables, 0-4 & 0-5). In Figure 2-2A the current-voltage relationship (IV curve) showed a small inward current. The current voltage relationship was constructed by measuring the peak amplitude negative current (pA) between the beginning of the pulse and 50ms, normalizing by cell size (pA/pF) and plotting against its respective voltage. In Figure 2-2B the downward deflection/inward current was magnified and clearly showed that a depolarization to -20mV produced a maximum average current density of –0.85 ± 0.17pA/pF (n=11). Two methods were used to determine whether the inward current was sodium dependent;

1) replacement of the Na^+ cation with NMDG, which does not permeate sodium channels and

2) block with 2µM tetrodotoxin.

As shown in Figure 2-2, neither of these methods blocked the observed current. In the presence of NMDG at -20mV an average current density of -0.56± 0.27pA/pF (n=3) was produced compared to -0.73±0.19pA/pF (n=4) in 2µM TTX. These data show that while Na^+ channels were transcribed, the resulting mRNA does not produce functional ion channels, supporting the finding that these cells do not fire Na^+-dependent action potentials.

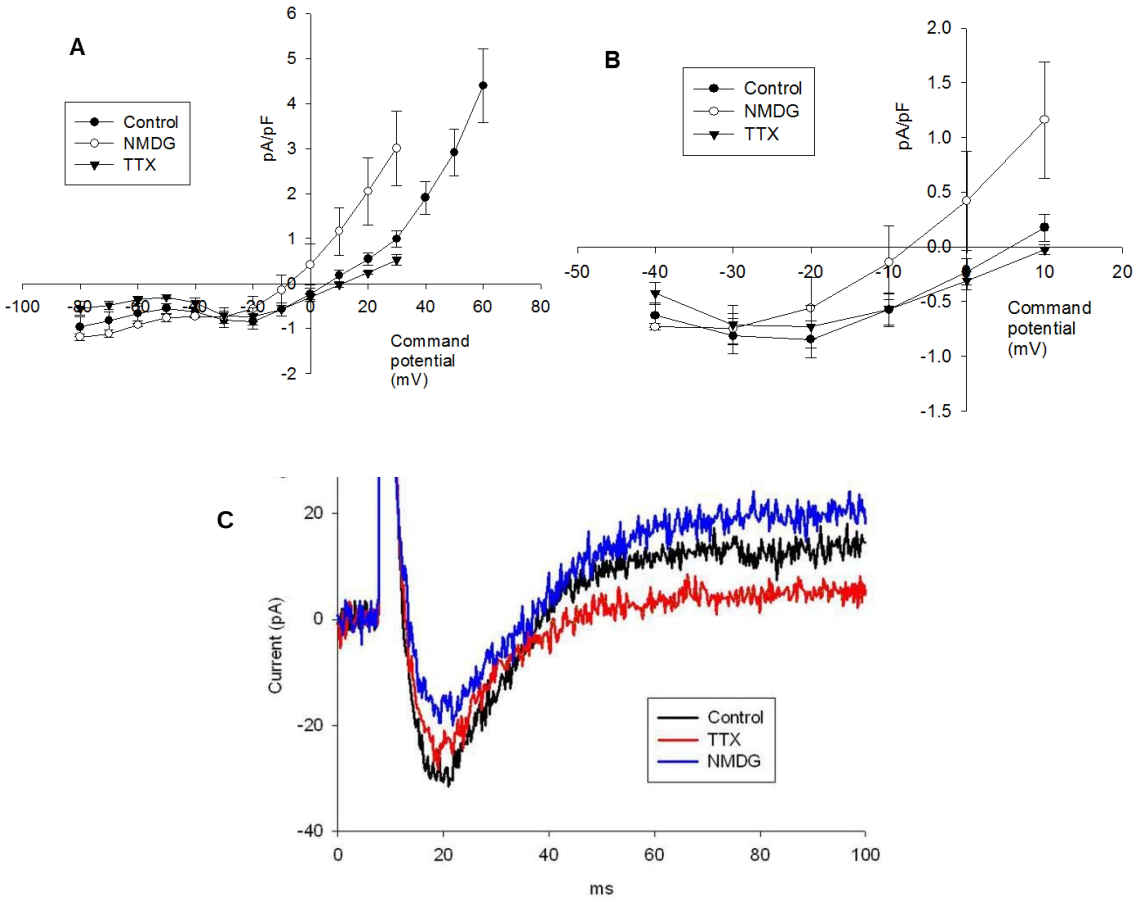

Figure 2-2 Sodium channel A) Current-Voltage relationship developed from peak negative current indicate a small inward channel (closed circles, n=11). B) An enlargement of A shows that the inward current is insensitive to NMDG replacement (open circles, n=3) and 2μM TTX (upside down triangles, n=4). C) Overlap of control, NMDG, and TTX treatment of the same cell at -20mV.

b) 2.3b Calcium

A common method to identify whether or not a specific class of ion channel is present is to remove or replace the permeant ion with one that does not permeate the channel. Accordingly, the cells were maintained at a holding potential of -80mv and given depolarizing pulses in 10mV steps. Unless otherwise noted the extracellular solution used was 1 and the internal solution was B in Tables 0-4 & 0-5. Raw traces in Figure 2-3A show the inward current which was abolished when the cell was perfused with a Ca^{2+} free external solution (#4 in Table 0-4) and reappeared when the cells were re-perfused with 2mM Ca^{2+}. Using a Student's t test, a significant difference was found between the current densities of the control and wash versus Ca^{2+} free plot (pA/pF) when measured at -20mV (control -0.85 ± 0.17pA/pF, Ca^{2+} free -0.2 ± 0.05, wash -1.1 ± 0.31, $p<0.05$, n=3) (Figure2-3B and 2-3C). In general, Ca^{2+} channels can also be blocked by cadmium (200µM), confirming that the inward current is Ca^{2+} dependent (Mueller et al., 2009). It was clear from the raw traces of the same cell that treatment with 200µM Cd^{+} blocked the inward current (Figure 2-4). This was confirmed by the IV curve (Figure2-4B) where the inward current (open circles) was completely blocked by 200µM Cd^{+} (closed circles) (n=2). Although Cd^{+} established the presence of a Ca^{2+} channel, it did not identify which subtype of Ca^{2+} channel was present.

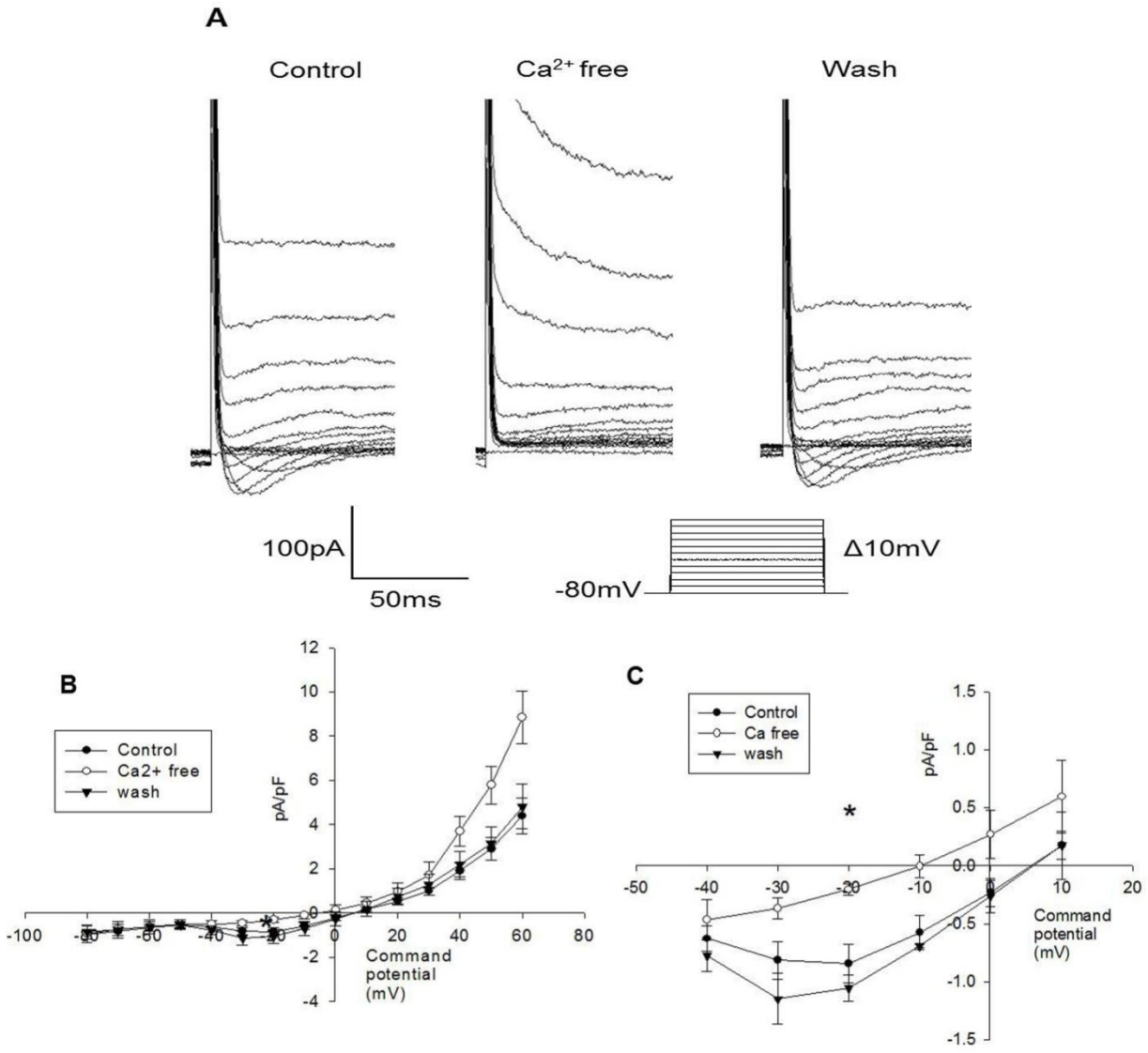

Figure 2-3 Calcium channel A) Raw trace in which the inward current was removed with a Ca^{2+} free solution and returned when Ca^{2+} was reperfused. B) Current voltage relationship showing inhibition of the inward current (n=3) (closed vs open circles). C) Magnified inward current from B showing a significant difference in the Ca^{2+} free current at -20mV ($p<0.05$).

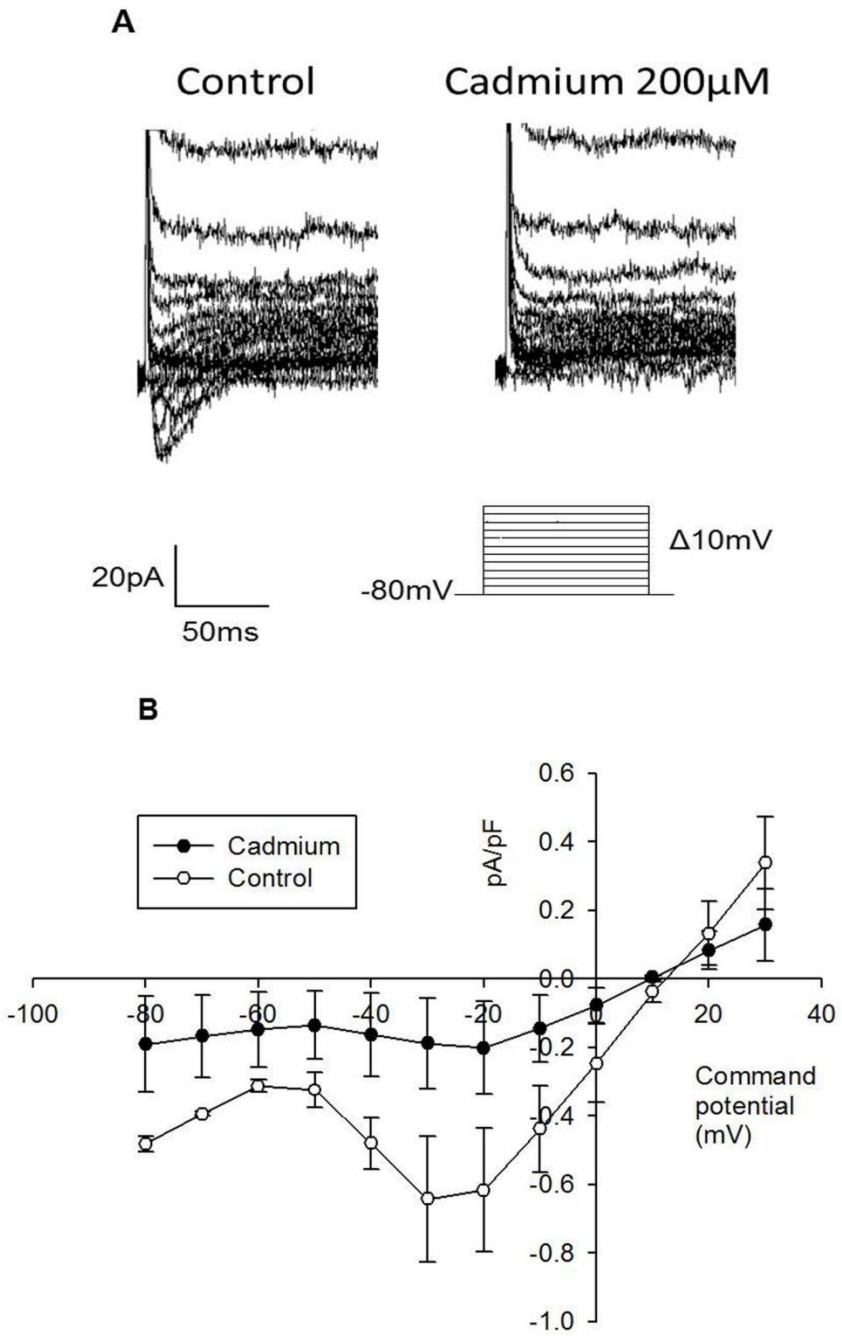

Figure 2-4 Confirmation of the Calcium current A) Raw trace of whole cell voltage clamp showing inward current induced by depolarizing pulses and inhibition by 200µM Cd2+. B) Current-Voltage relationship of the inward current (closed circles) and in the presence of 200 µM Cd2+ (open circles)(n=2).

Calcium channel subtypes can be identified by their pharmacological sensitivity to specific agonists and antagonists. These include different toxins and venoms which are some of the most efficacious tools at our disposal, mostly because of their high affinity and potency. One of the many toxins produced by the cone snail is ω-conotoxin GVIA which is a specific inhibitor of neuronal type (N-type) Ca^{2+} channels expressed in neurons (Mueller et al., 2009). Since IM-PEN cells are neuronal, we proceeded to determine if ω-conotoxin would block the Ca^{2+} channel. The raw traces in Figure 2-5A clearly demonstrate that ω-conotoxin at 100nM did not effectively block the inward current. An enlarged image of the IV relationship, Figure 2-5C, demonstrates that there is an insignificant 10mV shift to the right in the presence of ω-conotoxin. The maximum mean control current at -20mV was -0.86 ± 0.5pA/pF (closed circles) while that for ω-conotoxin at -20mV was -0.97 ± 0.61pA/pF (open circles)(n=3). These data indicate that the inward current was not the result of N-type Ca^{2+} channels.

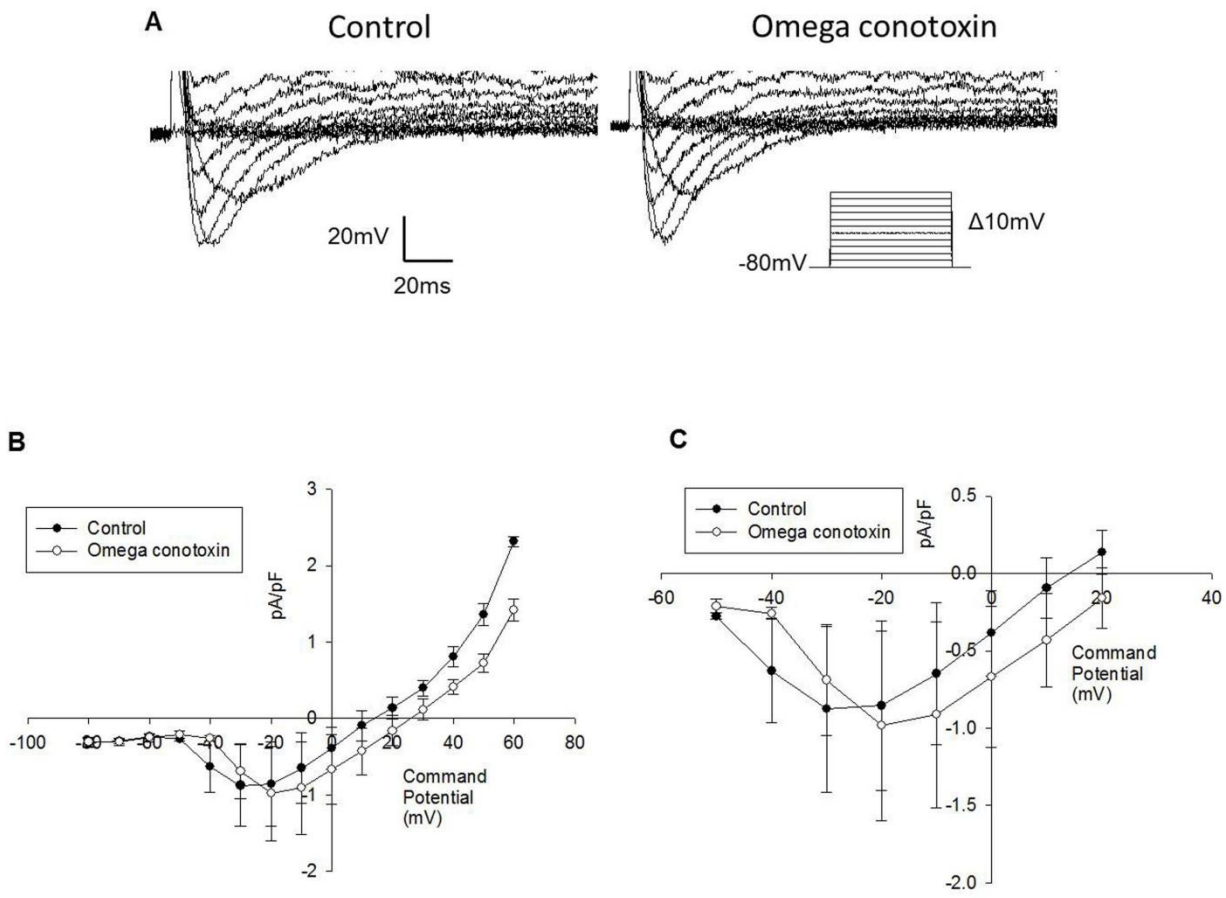

Figure 2-5 Calcium current sensitivity to ω-conotoxin A) Response to whole cell voltage clamp recording of IM-PEN to depolarizing pulses; control and in the presence of ω-conotoxin. B) Shows a rightward shift in the current-voltage relationship; however there is no change in the amplitude of the current (C)(n=3).

Sensitivity to the dihydropyridine, nifedipine, can help distinguish long lasting (L-type) Ca^{2+} channels from other subtypes in the VGCC family (Sitmo et al., 2007). IM-PEN cells were held at -80mV and given 10mV depolarizing pulses. Inhibition of the inward current was apparent with treatment of 1μM nifedipine as indicated by the raw traces in Figure 2-6A. The IV curve and inward current was magnified in Figure 2-6B as shown in Figure 2-6C. Although a significant difference in the currents was not obtained (Student's t test), it appears that there may be a trend showing inhibition when compared to the control -0.85 ± 0.17pA/pF (closed circles) vs. nifedipine treatment -0.42 ± 0.12pA/pF (open circles) at -20mV (n=3).

Barium is sometimes used, in place of Ca^{2+}, to measure L-type calcium channels as it yields larger current amplitudes and minimizes run down of the channel. The IM-PEN cells were given the same protocol previously described to stimulate the inward current. Replacement of 2mM external Ca^{2+} with 10mM Ba^{2+} resulted in a slight shift to the right of the current but did not increase the current amplitude (Figure 2-7A) (solutions 1 and 3 in Table 0-4 and solution A in Table 0-5). The peak Ca^{2+} current density at -20mV was -1.25 ± 0.9mV and the Ba^{2+} current density was -1.18 ± 0.8mV (n=4). The outward current appeared to decrease. There are several possible reasons for this (see Discussion). Raw currents for the same cell measured in both Ca^{2+} and Ba^{2+} are represented in Figure 2-7B.

The steady state voltage inactivation curve was constructed from a two pulse protocol comprised of a pre pulse and a test pulse. The duration and amplitude of the pre-pulse was sufficient to measure the current in a fully active state to a fully inactive state. The test pulse was at a fixed duration at an amplitude large enough to evoke the current after the pre-pulse. To produce the steady state voltage activation curve a single pulse protocol was used. This

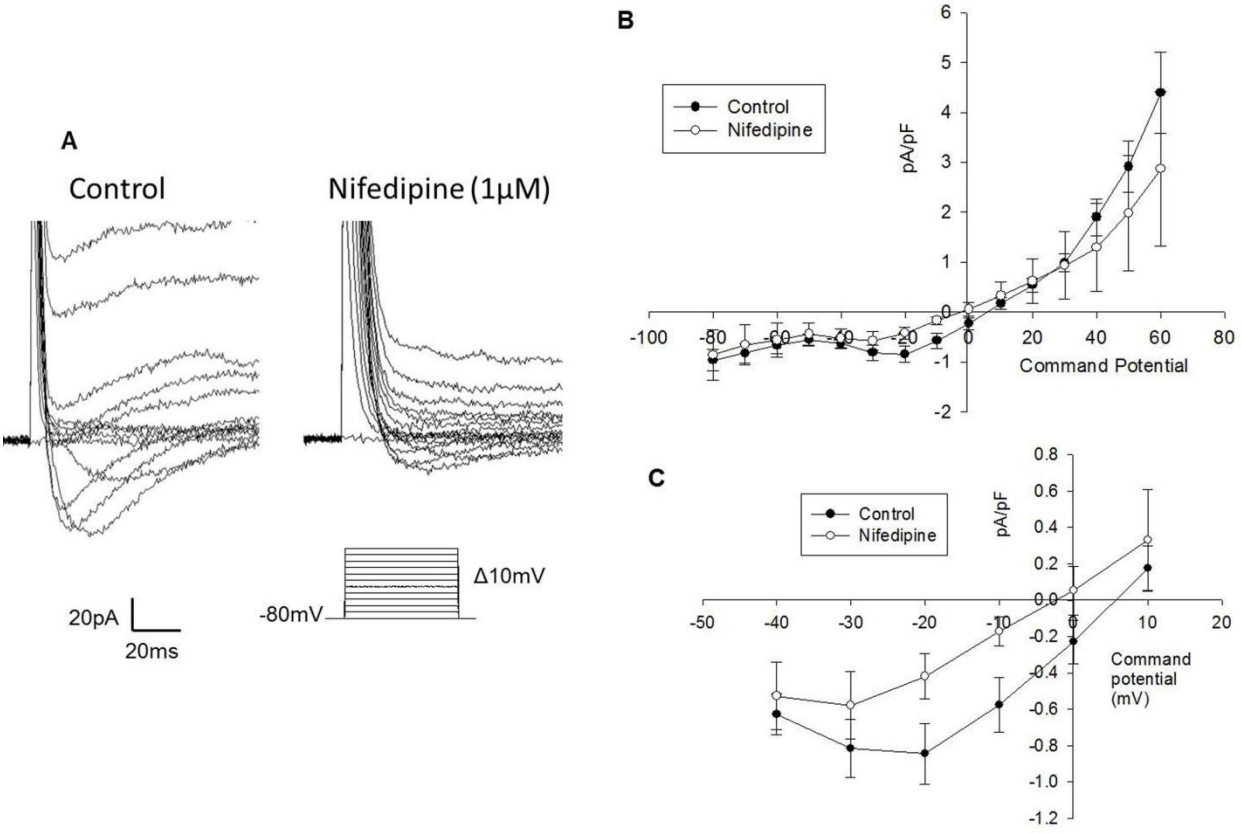

Figure 2-6 Nifedipine inhibits the inward current A) Raw trace shows inhibition of the inward current with 1µM Nifedipine. B) Current-voltage relationship, control (closed circles) and inhibition with nifedipine (open circles)(n=3). C) The inward current from B enlarged.

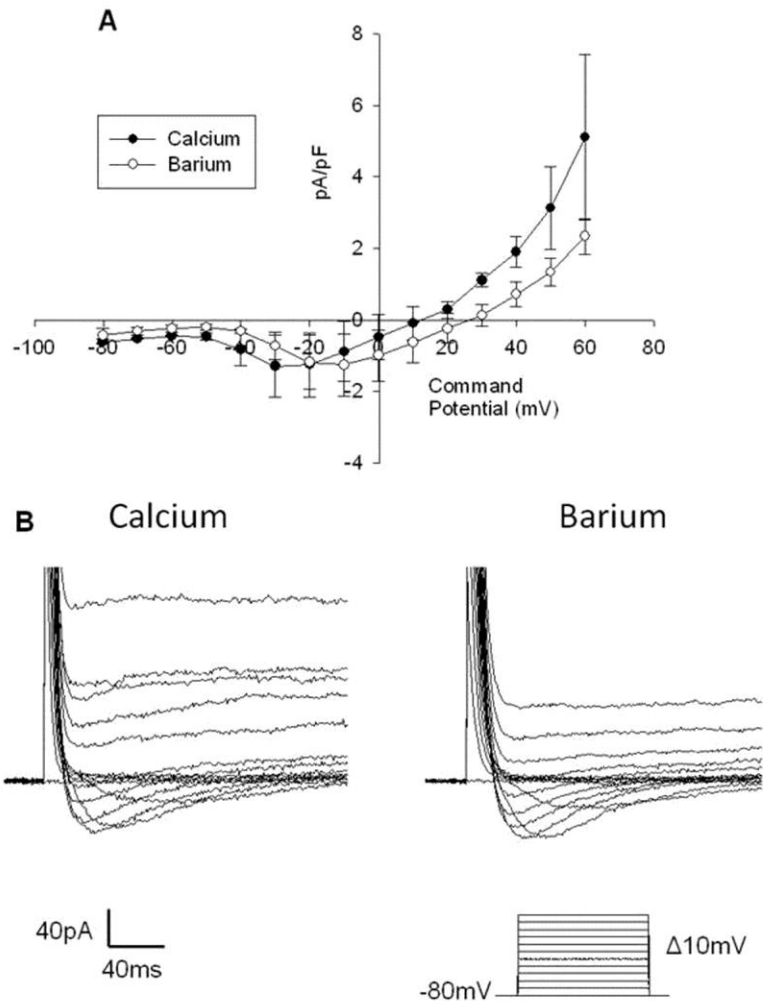

Figure 2-7 Inward current Ca^{2+} vs. Ba^{2+} A) Current-voltage relationship of inward current measured with Ca^{2+} (closed circles) and Ba^{2+} (open circles)(n=4). B) Representative voltage clamp recording from the same cell perfused first with Ca^{2+} then with Ba^{2+}.

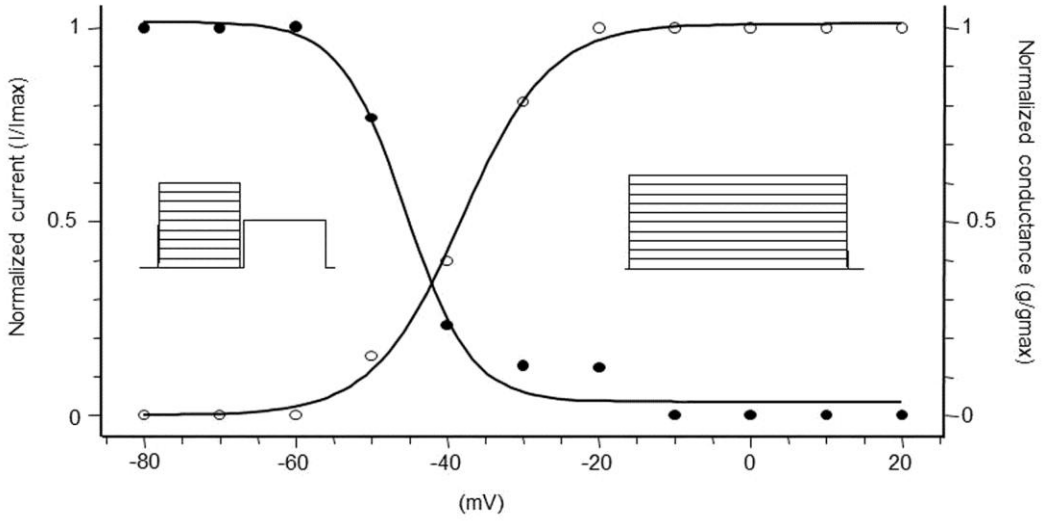

Figure 2-8 Steady state voltage activation and inactivation as measured from the inward current

protocol was the same as that used to measure the inward currents whereby IM-PEN was held at -80mV and pulses were given in 10mV increments up to 30mV. The overlap of these two curves generates a "window current" due to incomplete inactivation in the steady state at voltages that can cause activation (Figure 2-8). The $V_{1/2}$ for steady state voltage inactivation of the inward current was -45.3±0.84mV and for voltage activation was -38 ± 0.39mV (n=3). A caveat to this measurement is that the Ca^{2+} current was not isolated by block of K^+ channels. As a result these measurements are of the whole cell current and may be different from that of the actual Ca^{2+} channel.

When Ca^{2+} was removed from the external solution we noticed an increase in the outward current. The amplitude of the current was measured at the end of the stimulation pulse where the Ca^{2+} current should not have an effect as a result of inactivation of the channel. Using the same raw data from the cells used to measure the inward Ca^{2+} current, IV curves were constructed from the end of the stimulation pulse at the 350ms time point. In Figure 2-9A an outward current was present at positive potentials and this current was significantly increased at 60mV when Ca^{2+} was removed from the solution with a Vh of -80mV (control, closed circles, 4.7 ± 0.5pA/pF, n=6 and Ca^{2+} free, open circles, 8.4 ± 1.4pA/pF, $p<0.05$, n=3). When Ca^{2+} was reintroduced to the external solution the current was reduced to its control value (closed triangles at 60mV, 5.3 ± 0.6pA/pF, $p<0.05$, n=3). In the presence of 1μM nifedipine, a blocker of L-type Ca^{2+} channels and a compound that blocks the inward current of IM-PEN, the current decreased from 4.7±0.5pA/pF, n=6 to 2.9±1.6pA/pF, n=3 at 60mV (control versus nifedipine respectively) (Figure 2-10). Possible reasons for why removing Ca^{2+} increases the outward current while blocking Ca^{2+} channels decreases the current will be considered in the Discussion section.

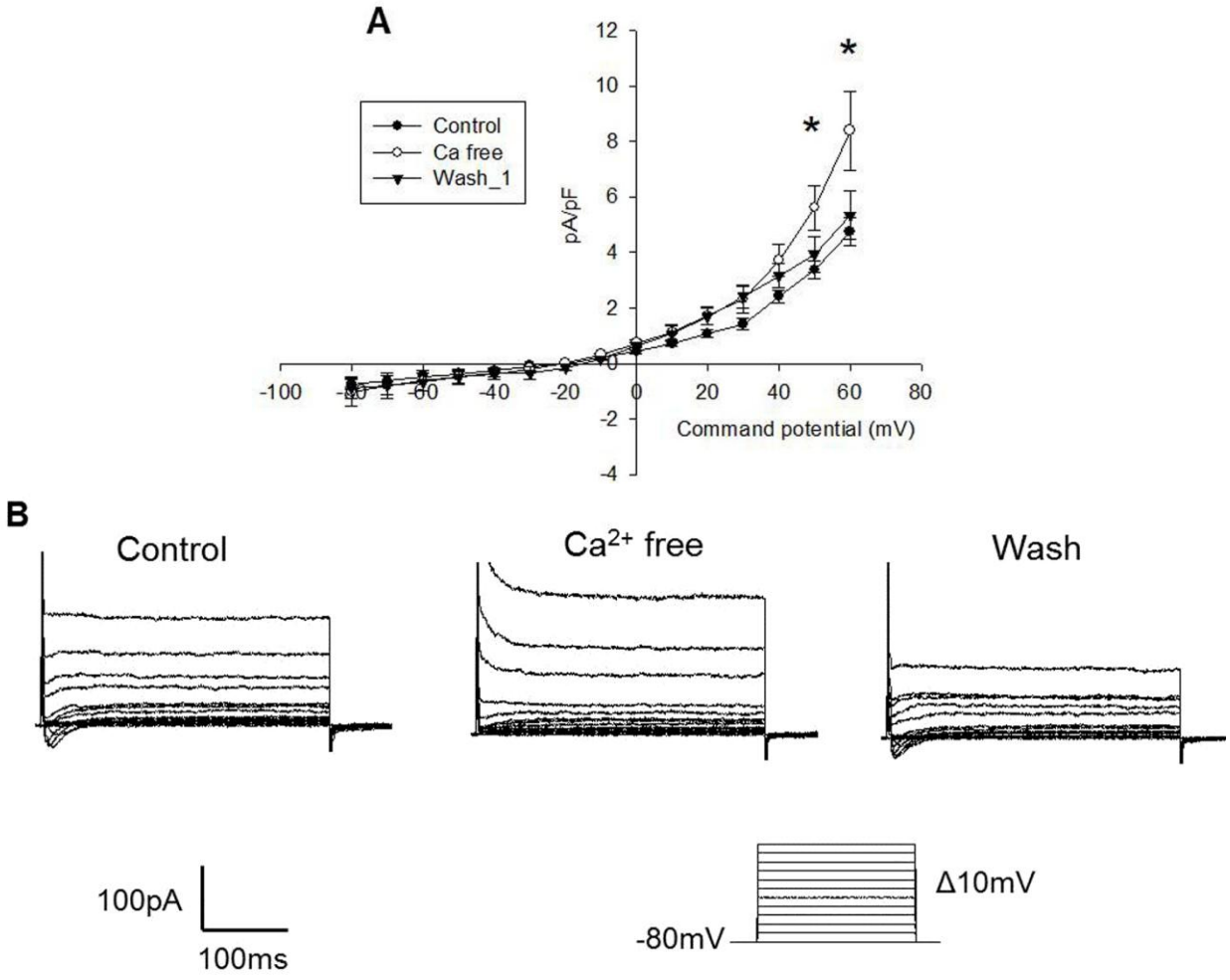

Figure 2-9 Ca^{2+} free solution increases an outward current A) Current-voltage relationship taken from the end of stimulation pulse shows a significant increase in the outward current which was removed when Ca^{2+} was replaced (n=3, $p<0.05$). B) Representative whole cell voltage clamp recording showing the change in amplitude of the outward current.

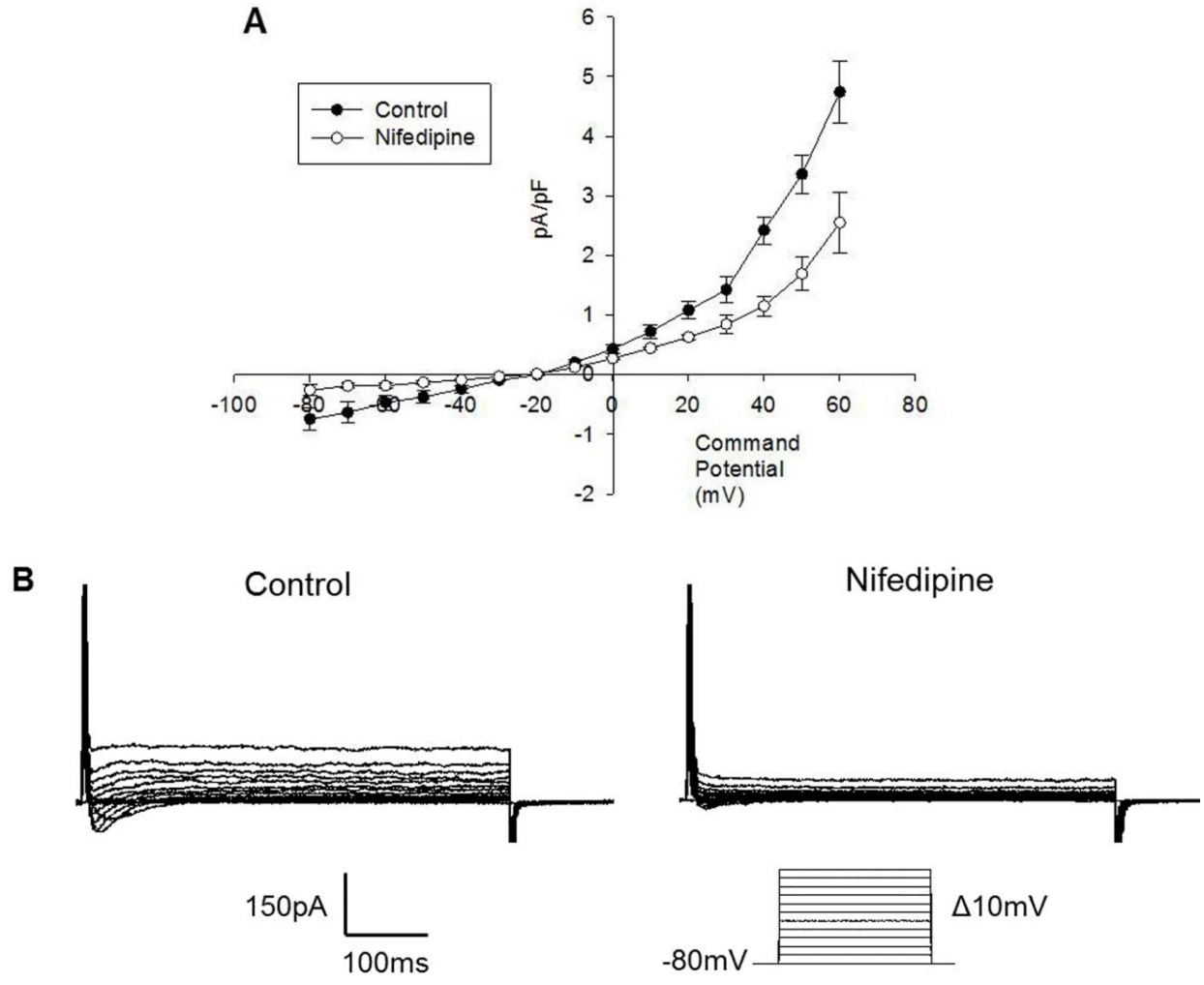

Figure 2-10 Nifedipine decreased the outward current A) IV relationship depicting 1μM nifedipine (open circles) significantly decreasing the outward current (closed circles)(n=3, $p<0.05$). B) Representative raw traces from the same IM-PEN cell showing a decrease in the Ca2+ and the outward current.

c) 2.3c Potassium

Using solutions 1 and A (Tables, 0-4 & 0-5 respectively) an outward current was inhibited by the quaternary ammonium 4-aminopyridine (4-AP) (n=5). The raw traces seen in Figure 2-11A show inhibition of the outward current to 3mM 4AP clamped at -60mV when given depolarizing pulses at 10mV intervals. Importantly, because it attests to the heterogeneity of IM-PEN cells, this current was only seen in 5 out of 20 cells tested. The IV curve, measured at the end of the pulse (350ms), still exhibited an outward current (Figure 2-9B). The calculated Nernst equilibrium potential for K^+ with these solutions is -83.7mV. In contrast, the reversal potential in the cells expressing K^+ currents was depolarized from this value at -40 ± 0.5mV (n=5) indicating the presence of other currents.

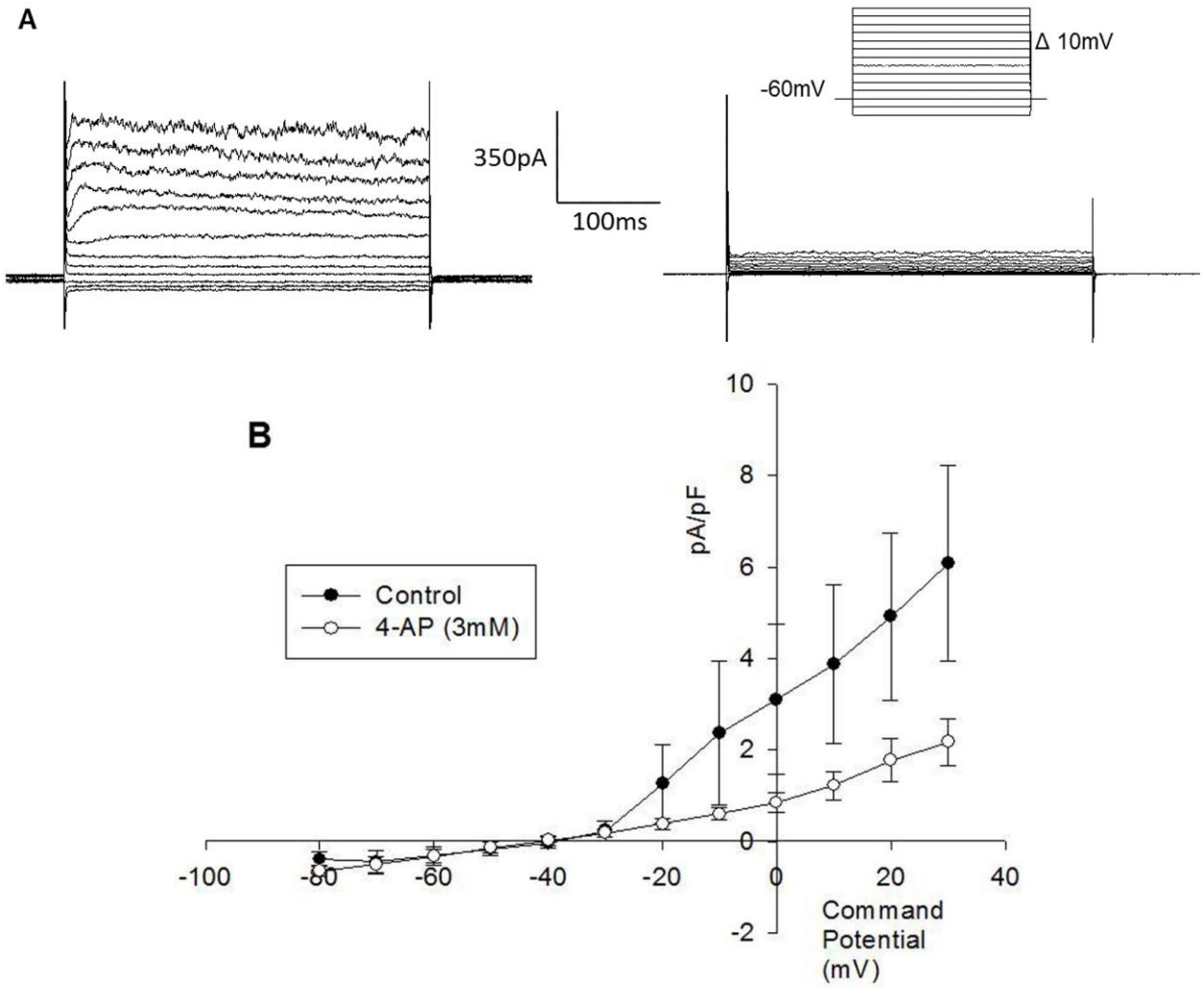

Figure 2-11 4-aminopyridine sensitive potassium channel A) Representative trace of whole cell voltage clamp outward current inhibited by 3mM 4AP. B) IV curve showing inhibition of outward current (n=5).

d) 2.3d Chloride

Several lines of evidence suggest the presence of chloride channels in IM-PEN cells:

1) outward currents were present with130mM internal Cs^{2+} (when measuring Ca^{2+} channels)

2) outward current in the presence of 4AP and

3) the reversal potential in the IV relationship for the K^+ channel recordings was near the calculated equilibrium potential of Cl^- using the Nernst equation (-38mV).

The existence of Cl^- channels was confirmed with the replacement of 100mM Cl^- in the external solution with 100mM gluconate which does not permeate Cl^-channels. Whole cell voltage clamp experiments were carried out with external solution 1 as the control and replacement of 100mM Cl^-, solution 5 in table 0-4, in conjunction with internal solution C from Table 0-5. The IM-PEN cells were held at -60mV and pulsed in 10mV voltage steps to obtain the raw data seen in Figure 2-12A. The currents were significantly reduced when perfused with a low chloride solution (Figure 2-12B). Subtraction of the raw data (Figure 2-12A – 2-12B) yielded the chloride current seen in Figure 2-12C which was graphed in the current voltage relationship Figure 2-12D (n=6). The calculated equilibrium potential for Cl^- using the Nernst equation was -38mV, near that of the reversal potential of the IV curve of -36.8mV, suggesting that Cl^- was the major anion responsible for this current.

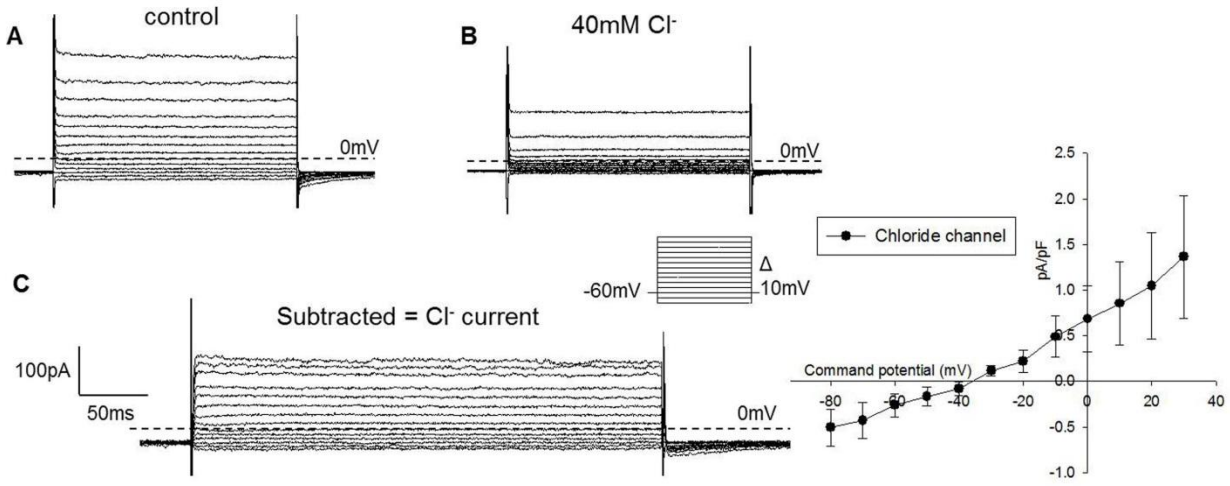

Figure 2-12 IM-PEN cells contain Cl^-currents A) Voltage clamp experiment in the whole cell configuration with K^+ channels blocked by 140mM CsCl in the internal solution and 144mM Cl^- in the external solution. B) Same cell recorded with 40mM Cl^- in the external solution produces smaller currents. C) Cl^-sensitive current obtained by subtraction. D) IV curve of chloride channel (n=6).

Of note was the presence of slowly deactivating tail currents suggesting expression of a calcium-activated Cl^- channel. Whole cell voltage clamp recordings were performed in the presence of solutions 1 and C (Tables, 0-4 & 0-5) and a Vh of -60mV with test potentials in 10mV increments. The administration of 1μM niflumic acid to the external solution decreased the outward current as well as significantly inhibited the tail current. The boxes in Figure 2-13A depicts a reduction of the tail current upon the administration of niflumic acid (NA) at depolarizing pulses. Inhibition of the tail current is made more apparent in Figure 2-13B which is an enlargement of the superimposed tail currents at +30mV. Figure 2-13C shows that the overall amplitude of the control current (closed circles) was significantly reduced (Student's t-test, $p<0.05$, $n=4$) with 1μM NA (open circles) confirming the expression of a Clca channel seen in the RT-PCR.

Volume-regulated anion channels (VRAC, $I_{Cl,swell}$) tend to be ubiquitously expressed as cells need to regulate their size and osmolarity (Okada 1997). IM-PEN cells were held at either -60mV or +30mV to induce swelling-activated inward or outward currents respectively. As seen in Figure 2-14A, perfusing a hypoosmotic solution (solution 8 in Table 0-4 with internal solution D in Table 0-5) from a Vh of -60mV elicited an inward current that was blocked by the $I_{Cl,swell}$ channel blocker DCPIB (10μM)(Decher et al., 2001). The current voltage relationship showed a reversal potential of -21.3 ± 4.5mV (n=7) compared to the calculated equilibrium potential of chloride with these solutions of -19.7mV showing Cl^- to be the major permeating ion. As expected, when cells were held at +30mV, swelling activated currents were outward (9/11) (5/9 had a transient outward current) (Figure 2-15). Ion channels can also be categorized by the selectivity they have to specific ions. It has been reported that replacement of Cl^- with gluconate, should decrease the current (Ackerman et al., 1994). In Figure 2-15 the $I_{Cl,swell}$ current was

activated by treatment with a hypoosmolar external solution (7 in Table 0-4) at +30mV. When the Cl^- anion was replaced with gluconate (solution 8, Table 0-4) the current was inhibited and only returned when Cl^- (solution 7, Table 0-4) was perfused (n=4).

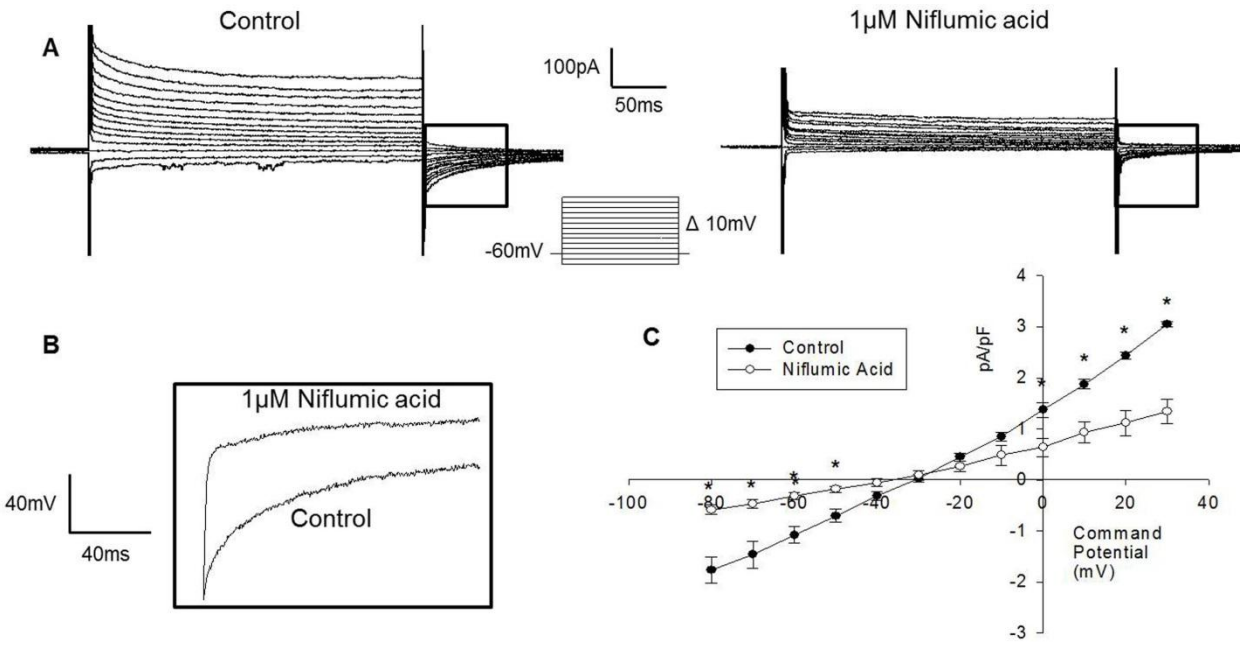

Figure 2-13 Niflumic Acid sensitive current. A) Whole cell voltage clamp recordings in the presence of internal Cs^{2+} showed outward currents and slow deactivating tail currents. B) Niflumic acid (1μM NA) inhibited both the outward currents and tail currents. C) Expanded traces of tail currents at -60 mV from test pulse of +30 mV in the absence and presence of 1μM NA. D) IV relationship of amplitude of end of pulse current in the absence and presence of 1μM NA.

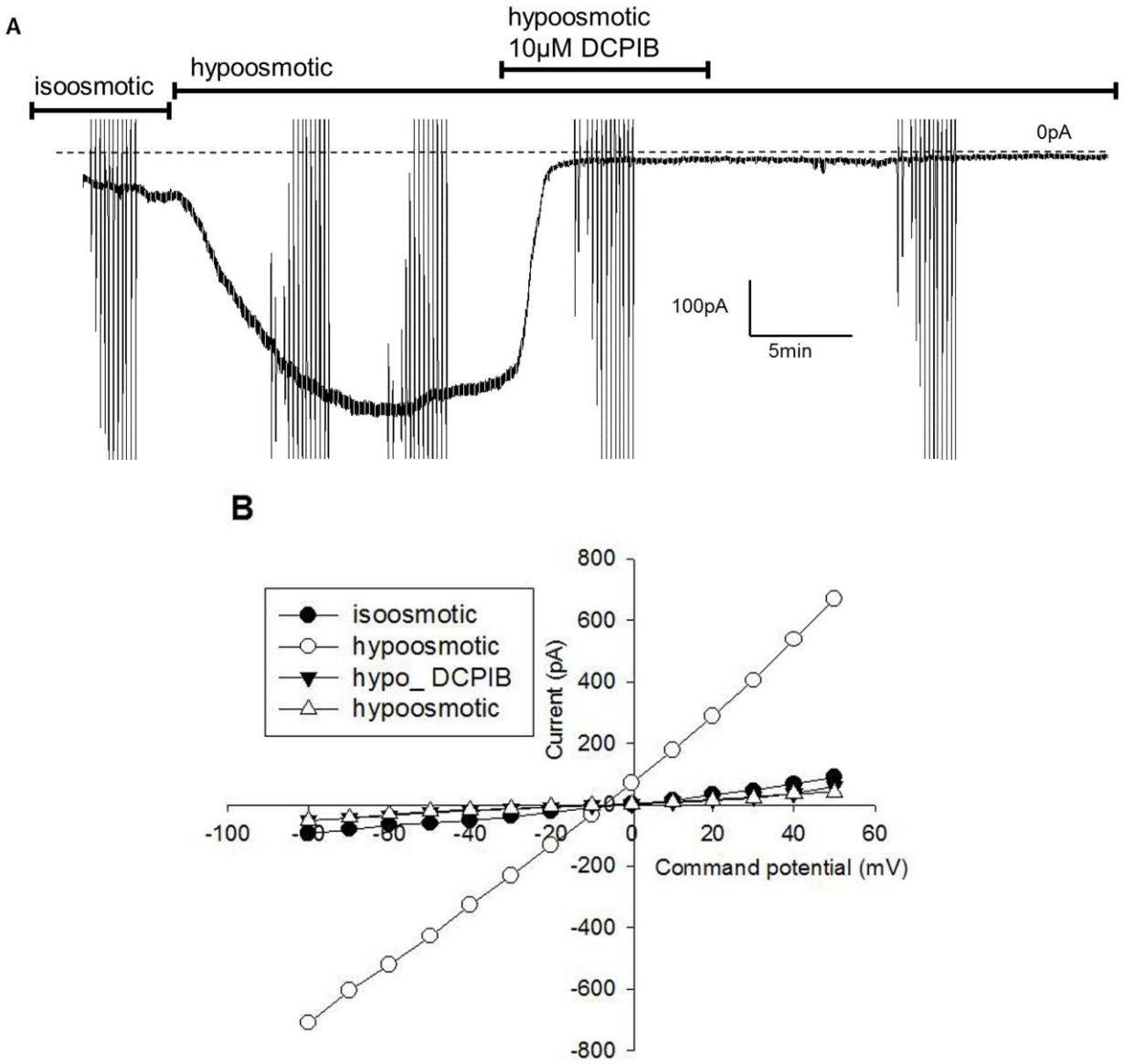

Figure 2-14 A hypoosmotically activated chloride current A) Whole cell voltage clamp recording at Vh= -60mV initiated an inward current upon the perfusion of hypoosmotic solution (230mOsm). This current was inhibited and remained inhibited after treatment with 10μM DCPIB (n=7). B) IV-relationship showing swelling activated current and inhibition by DCPIB.

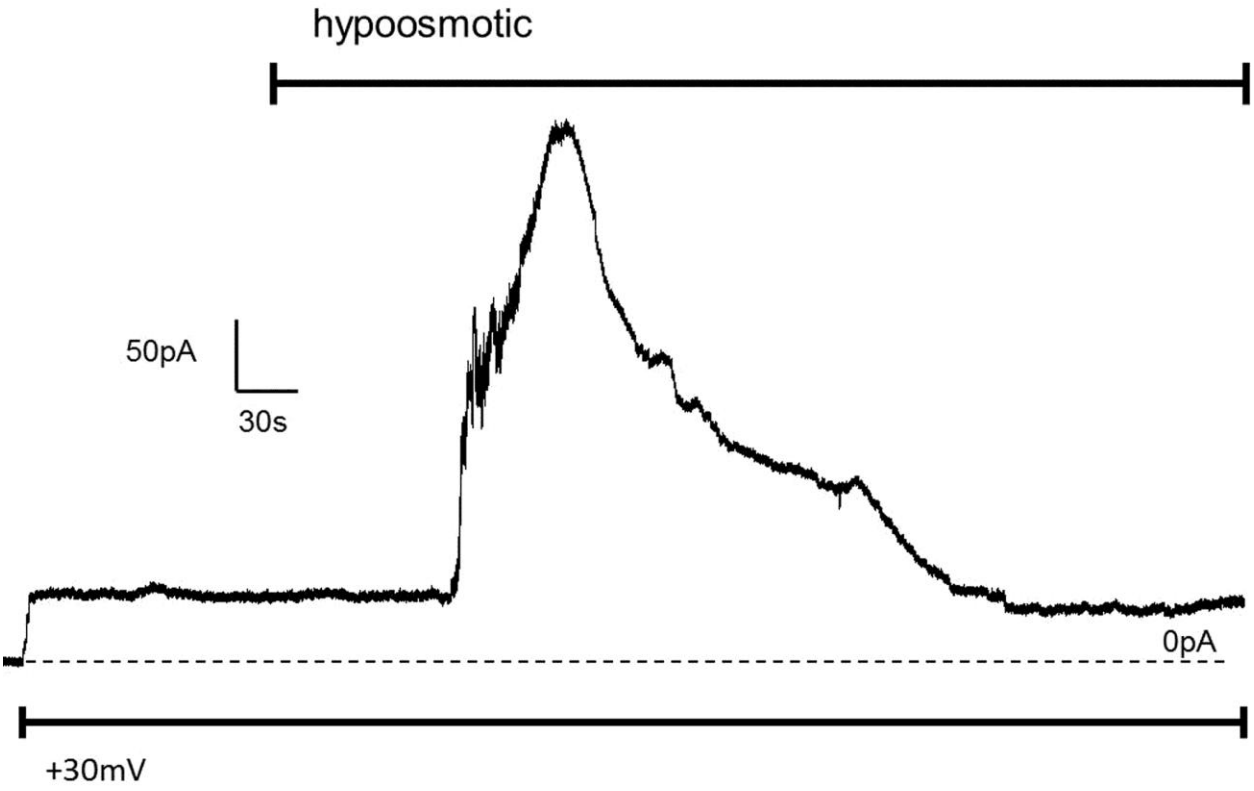

Figure 2-15 Swelling activated current at +30mV. Perfusion of a hypoosmotic external solution initiated an outward current at +30mV. In 5/9 cells the current was transient in nature (n=9/11).

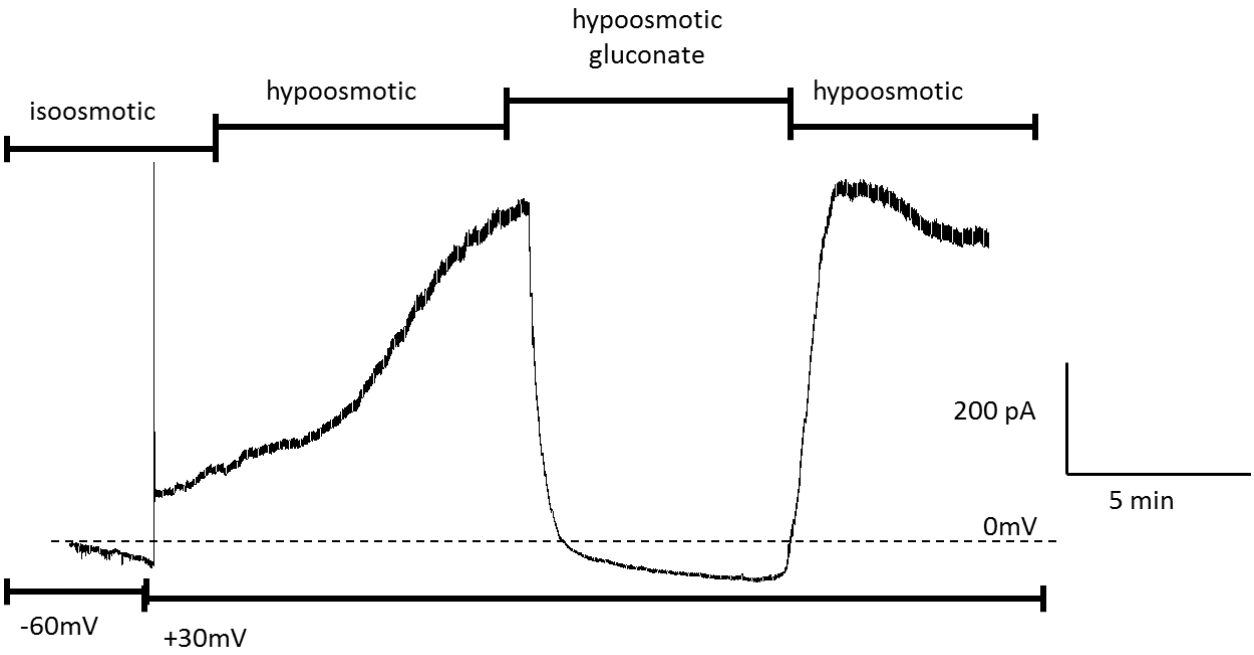

Figure 2-16 Solubility of swelling activated current. Whole cell recording of IM-PEN with Vh = +30mV. Addition of hypoosmotic solution initiated an outward current which was inhibited when Cl^- was replaced in the external solution with gluconate. The current returned when Cl^- was returned to the external solution (n=4).

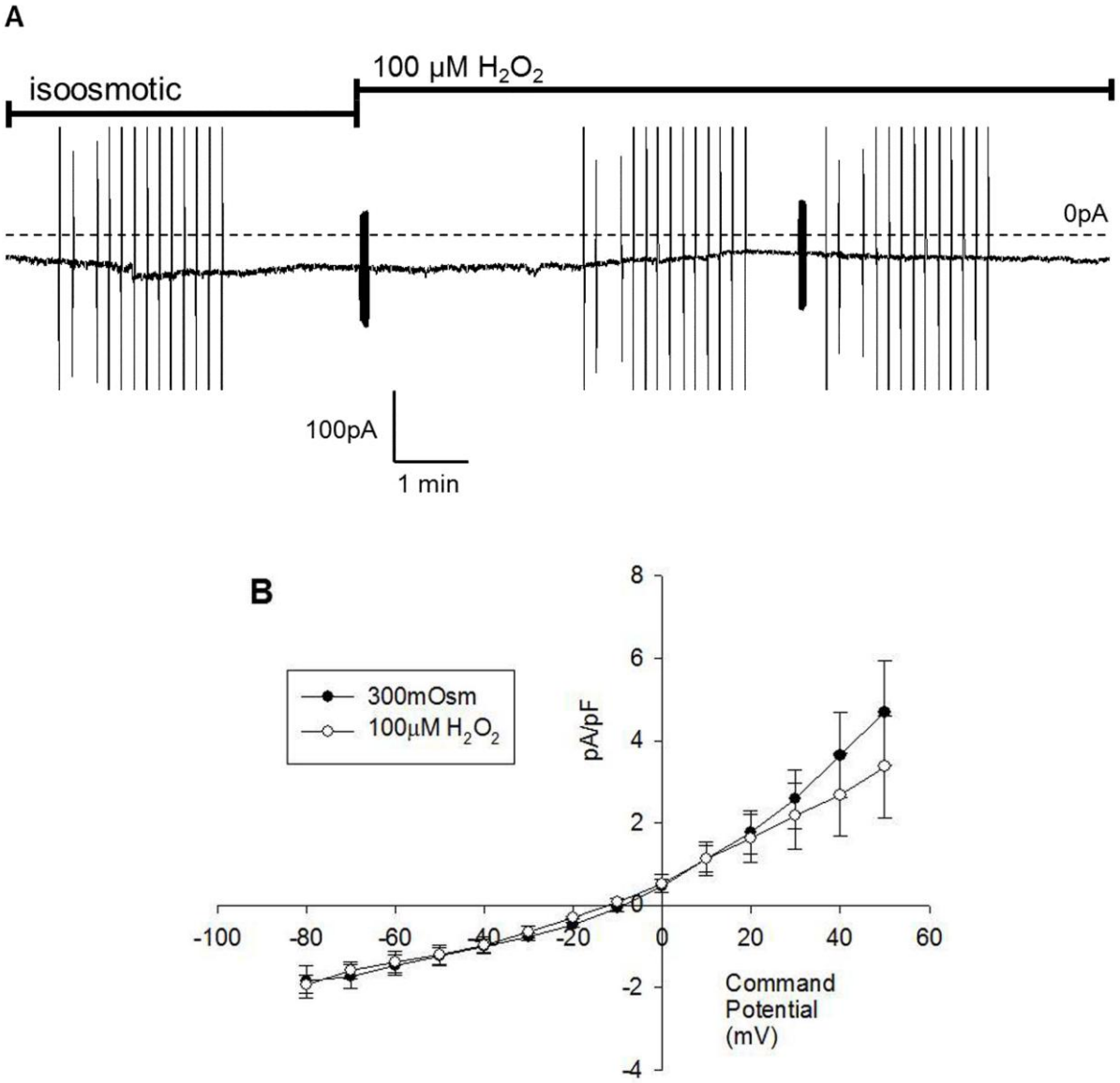

Figure 2-17 H_2O_2 and swelling activated currentA) Raw trace of IM-PEN given 100µM H_2O_2 in isoosmotic solution did not ellicit $I_{Cl,swell}$. B) IV relationship showing isosmotic (closed circles) and 100µM H_2O_2 (open circles)(n=5).

The $I_{Cl,swell}$ channels have also been shown to be activated through a reactive oxygen species pathway (Ren et al., 2008). Whole cell continuous recordings with a Vh of -60mV and solutions 6 and C (Table 0-4 & 0-5) were performed. The $I_{Cl,swell}$ channel in IM-PEN was unaffected by the addition of 100µM hydrogen peroxide (H_2O_2) added to solution 6 as shown in Figure 2-17A. An IV relationship was constructed before (closed circles) and after (open circles) the administration of H_2O_2 (n=5) (Figure 2-17B) and confirms H_2O_2 had no effect.

e) 2.3e TRPV1

The RT-PCR data indicated likely transcription of TRPV1 expression which was confirmed using immunocytochemistry (figure 2-18A). In these images at 40X and 60X the protein appeared to be internalized in small vesicles in the cytoplasm. Whole cell voltage clamp experiments with solutions 1 and A (Table 0-4 & 0-5respectively) confirmed that TRPV1 was inactive on the cellular membrane of IM-PEN. A continuous recording holding the cell at -60mV for several minutes in the presence of 10µM capsaicin failed to yield a current (Figure 2-18B)(n=4). We were able to measure capsaicin-induced inward currents in dorsal root ganglion neurons (DRG) to confirm that the recording conditions were adequate to stimulate TRPV1 (data not shown).

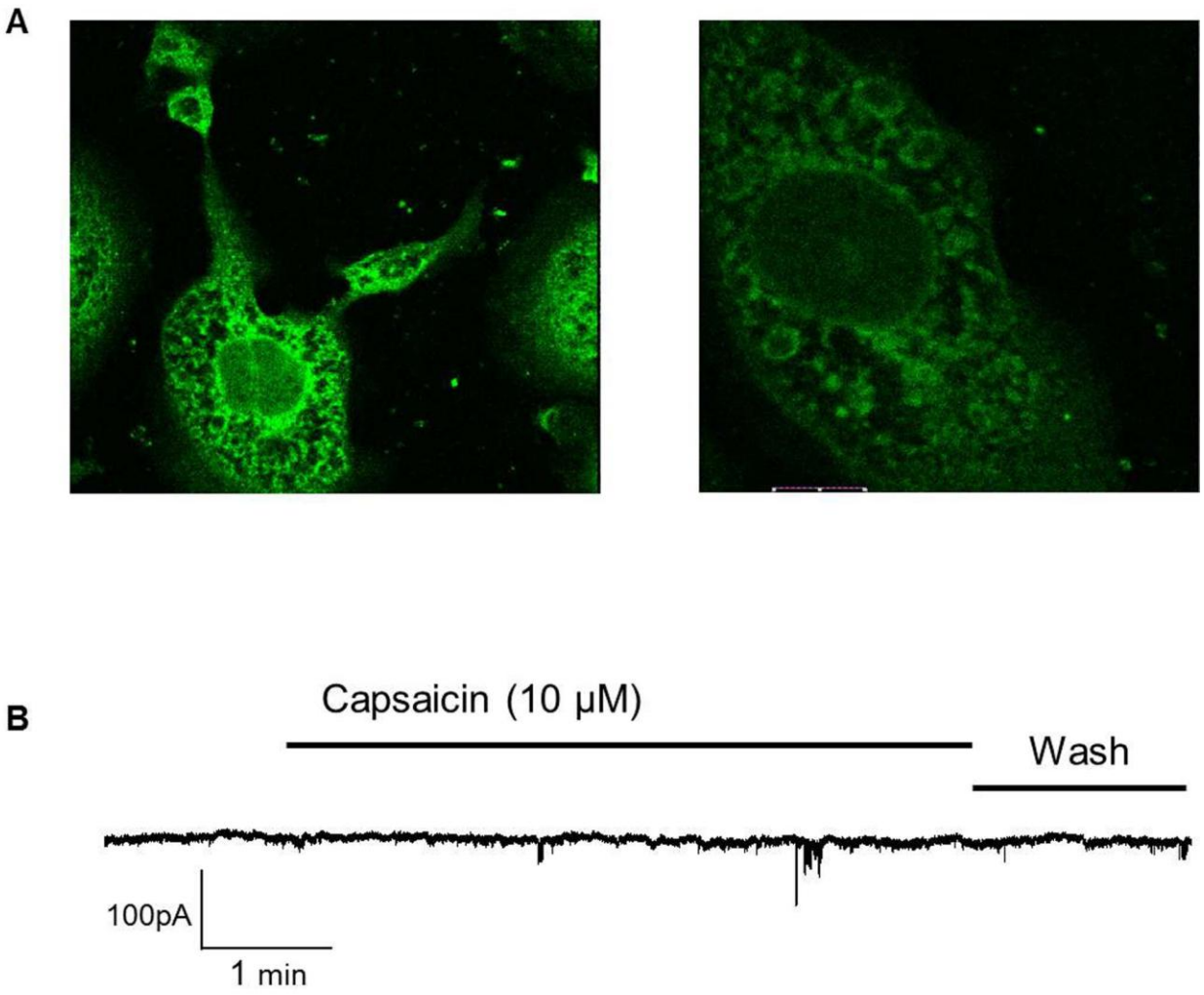

Figure 2-18 TRPV1 channel A) TRPV1 positive immuno-reactivity of IM-PEN after 7 days at 37°C. Side panel shows immuno-reactivity in intracellular vesicles at higher magnification. B) Whole cell voltage clamp recording from IM-PEN cell held at -60 mV and treated with 10µM capsaicin. No currents were elicited in the presence of capsaicin.

f) 2.3f Ligand gated ion channels

Although our studies focused mainly on voltage gated ion channels, enteric neurons also contain a variety of ligand gated ion channels. The following measurements were made in the whole cell configuration with external solution 1 (Table 0-4) and internal solution A (Table 0-5) except for GABA which was measured with internal solution C (Table 0-5). A summary is shown in Table 2-2;

1) GABA (100µM) did not activate currents (0/8)

2) Acetylcholine (500µM) did not activate currents (0/4)

3) Nicotine (1mM) did not activate currents (0/3) and

4) Serotonin (10µM) did not activate currents (0/3).

The lack of currents stimulated by ACh and nicotine was consistent with the immunohistochemistry data, which was negative for ChAT. However, it is possible that other neurotransmitter/hormone receptor systems are present in IM-PEN.

Table 2-2 Ligand gated ion channels.

Ligand ([X])	n/total	Solutions
GABA (100µM)	0/8	1 and C
Acetylcholine (500µM)	0/4	1 and A
Nicotine (1mM)	0/3	1 and A
Serotonin (10µM)	0/3	1 and A

C. Summary

To briefly summarize the previous data, immunocytochemistry indicated the IM-PEN cell line was neuronal in origin; however the cultured cells did not express ChAT or NOS1. Both IM-FEN and IM-PEN cells were also depolarized with high membrane resistances and lacked the ability to fire action potentials to depolarizing pulses even when held at hyperpolarized membrane potentials. A possible reason for this is that the Na^+ channels necessary for the upstroke of the action potential were not functionally active, even though they were transcribed. A majority of the cells expressed a very small L-type Ca^{2+} channel. A high Cl^- conductance was found to result in the depolarized RMP's seen in IM-PEN. These data taken together agree with those from immature neurons studied in the CNS (Mongiat et al., 2009). Although several compounds (e.g., GDNF and N2) known to be involved in the development of enteric neurons were added to the differentiation media, it is possible that the cells are missing a critical factor. Our view is that the addition of one or more of these factors may be what is necessary to trigger action potentials in IM-PEN.

D. Chapter 3: Differentiation into an excitable enteric neuron

1. 3.1 Introduction

Many regulators and transcription factors are involved in the maturation of the enteric nervous system. Interest in this field has renewed as investigators begin to understand the number of GI disorders resulting from EN-associated impairments (i.e. Hirschsprung's disease HSCR, megacolon, and GI obstruction). At best, these syndromes cause pain and inflammation to the patient and can sometimes result in death. Therapies developed to reestablish enteric nervous system function could potentially cure these patients; an understanding of how enteric neurons develop is likely to aid in the identification of such treatments. Current knowledge indicates that the transcription factors PHOX2B and SOX10 initiate proliferation of uncommitted progenitor neural crest cells into the developing GI tract. The gut is thought to be permeated by vagal neural crest cells following a GDNF gradient down to the cecum. The lower gut is infiltrated by sacral neural crest cells which travel proximally and are mediated by endothelin-3 (ET-3) and the endothelin receptor B (ET_B). Deletion of ET-3 or ET_B causes anganglionosis of the distal gut, a syndrome that mimics HSCR and is present in two mouse models as well as some patients with the resultant disease. The signaling pathway in Figure 3-1 shows that ET-3 maintains the crest derived cells in an uncommitted state through a SOX 10 mediated pathway (Bondurand et al., 2006). Keeping neurons in an uncommitted state may allow them to permeate the entire gut before fully differentiating into enteric neurons. GDNF then binds to the receptor kinase RET which dimerizes and stimulates proliferation, migration, survival, and differentiation of neural crest cells from which enteric neurons develop. The MASH1 transcription factor seems to have two waves of expression, the first cause's termination of SOX10 and differentiation into esophageal EN's (Blaugrund et al., 1996). HAND2, like

MASH1, is a basic helix-loop-helix transcription factor that is required for the terminal differentiation of enteric neurons. A second wave of MASH1 is then involved with differentiation and maturation in the hindgut (Gershon 2010).

Mammals express homologues of the acaete-scute complex (AS-C), which have been named MASH1 and MASH2 and are found in neurons or trophoblasts respectively. MASH1 KO mice were originally thought to be viable, yet pups died within 12 hours of birth. It was observed that MASH1$^{-/-}$ mice had no milk in their stomachs, enteric neurons did not develop around the esophagus, and there was a delay in the development of enteric neurons in the hindgut (Guillemot et al., 1993a). In Drosophila, AS-C genes encode for basic helix-loop-helix transcription factors that promote the development of neurons in the CNS and PNS (Guillemot et al., 1993b). Furthermore, Vierbuchen et al. determined that a single transcription factor, Ascl1, was necessary to promote the conversion of fibroblasts into cells expressing neuronal markers (Vierbuchen et al., 2010). Although additional factors were shown to greatly increase the efficiency of the conversion of fibroblasts to neurons, of the factors tested, only Ascl1 has been found to be involved in EN development. As shown in Figure 3-1, neuronal markers begin to appear after the first wave of Ascl1/ MASH1 expression. IM-PEN expressed PGP9.5 and βIII-tubulin (aka Tuj1) and had depolarized RMP's, supporting evidence that they may not be fully mature EN's (red). Because of the importance of MASH1 in EN development and its ability to generate neuronal cells out of fibroblasts, we transfected IM-PEN with MASH1 to determine if we could generate mature EN's.

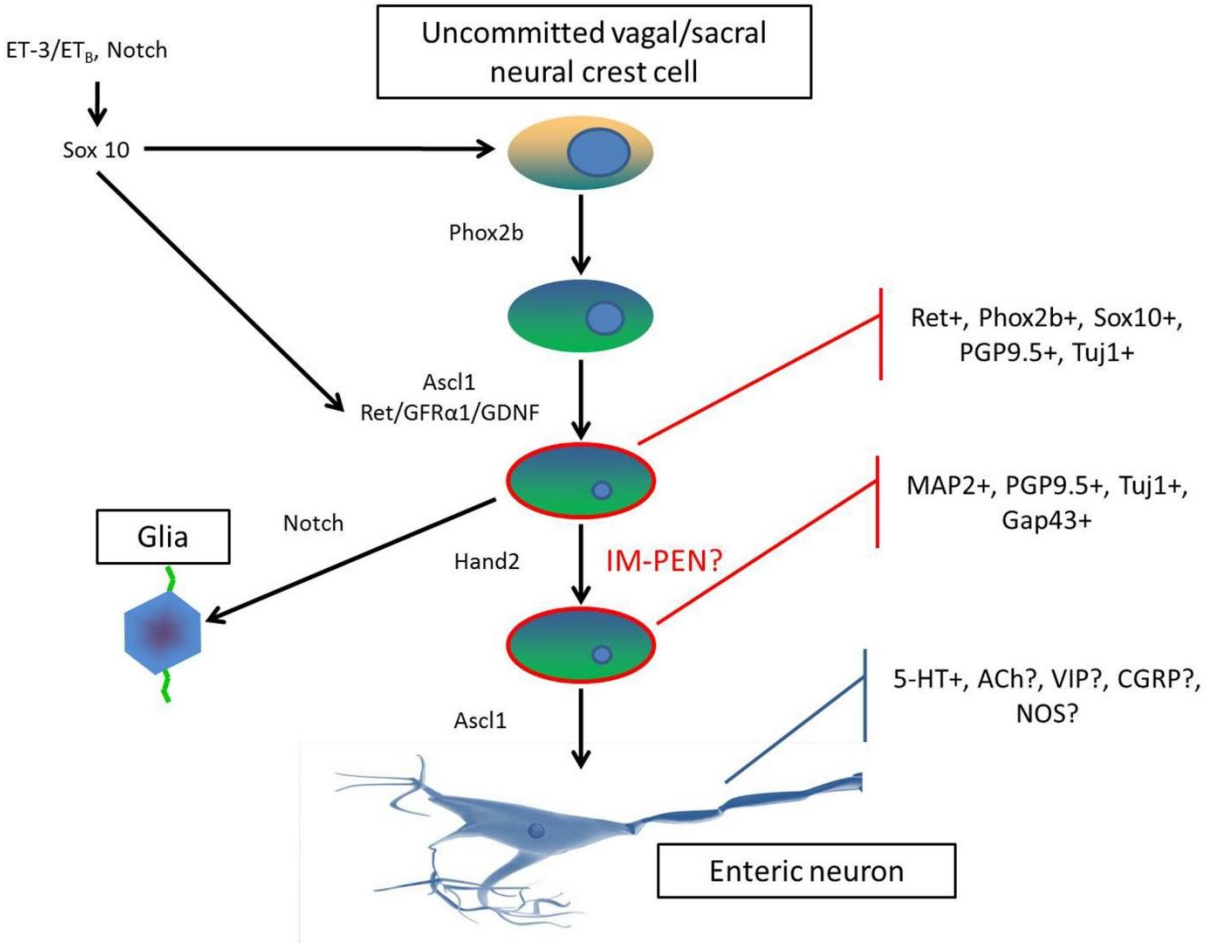

Figure 3-1 Schematic of differentiation of enteric neurons from nueral crest cells. Each stage requires a set of transcription factors or growth factors. These stages are delineated by the neuronal markers they express (right). Positive expression of PGP9.5 and βIII-tubulin (also known as Tuj1) and the lack of fully mature neuronal biophysical properties (action potentials) led to the conclusion of IM-PEN as immature enteric neurons (circled in red). In the diagram above Ascl1 (MASH1) is necessary for the final conversion into mature enteric neurons. Our hypothesis is that MASH1 transfection of IM-PEN may generate mature enteric neurons. This diagram was adapted from (Gershon 2010).

2. 3.2 Transfection of MASH1

The first step was to confirm whether or not it was possible to transfect IM-PEN cells. This was confirmed with the transfection of green fluorescent protein (GFP) in cells grown at 37°C for 4 days. Figure 3-2A is an image of GFP positive IM-PEN cells adjacent to the brightfield image in Figure 3-2B. In order to confirm that whole cell recordings were obtained from transfected IM-PEN cells, we had the transcription factor inserted into the vector pCMV6-A-GFP (pCG) which would co-express GFP. Empty pCG vector was transfected into IM-PEN with the result seen in Figure 3-2C. It was apparent that the empty pCG vector expressed GFP but not nearly as well as GFP alone. Panel E and F of Figure 3-2 represent MASH1 transfected cells (pCGM1) and even less GFP fluorescence was seen, and therefore MASH1 positive cells. Many electrophysiologists perform a double transfection whereby the ion channel/target is placed in one vector and a reporter, e.g., GFP, is placed in an alternative vector. It is then assumed that if the cell is expressing the reporter it is also expressing the gene of interest (Holt et al., 1990). As a result, we performed double transfections with pCGM1 and GFP. Figure 3-3G is an example of the cells that were double transfected. Confocal microscopy showed very low transfection efficiency for IM-PEN. However, we were subsequently able to perform electrophysiology experiments on these cells.

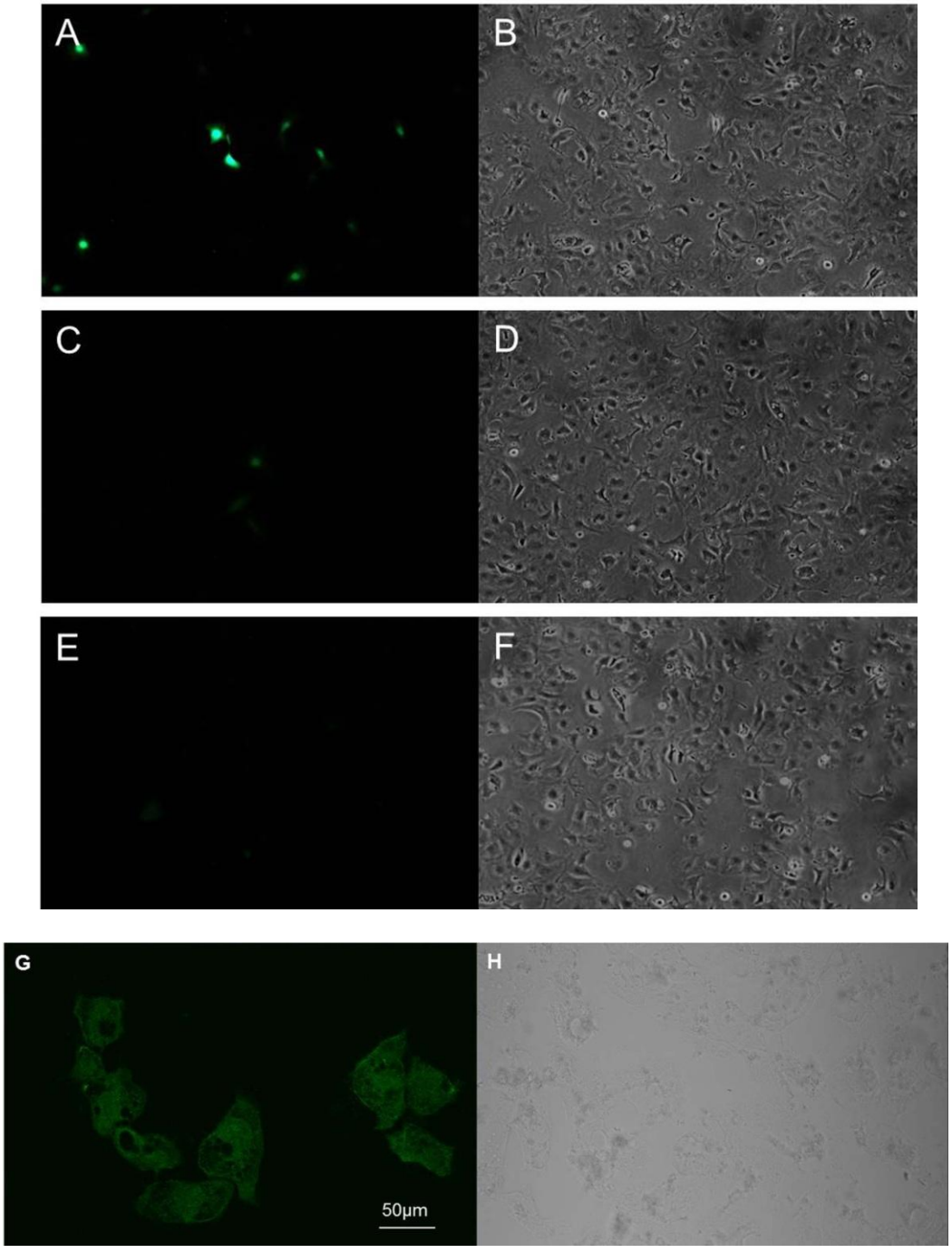

Figure 3-2 MASH1 transfection A) IM-PEN transfected with GFP C) Transfection with empty vector pCG and E) transfection with MASH1.G) Same as E visualized on confocal microscope. All images are shown with their corresponding brightfield image.

3. 3.3 Immuno-reactivity of MASH1 transfected cells

One indication that MASH1 can differentiate the IM-PEN cell line would be the demonstration of the presence of neurotransmitters. Our data in Chapter 1 showed that the IM-PEN cell line did not contain ChAT or NOS1 immunoreactive cells after 7 days in the differentiation conditions. IM-PEN cells were therefore stained for both ChAT and NOS1 after 8 days of MASH1 transfection in the same differentiation conditions. Figure 3-5A shows no ChAT immunoreactive cells in untransfected cells after 8 days. Figures 3-5B and C are also negative for ChAT and NOS1 respectively after MASH1 transfection for 8 days.

4. 3.4 Passive properties of MASH1transfected IM-PEN cells

There was a significant difference in the RMP of IM-PEN cells; -29.8 ± 0.9mV (n=30) and MASH1 transfected cells -18 ± 3.6mV (n=6, $p<0.05$). There was also a statistical difference in the much larger size of the IM-PEN cells of 37.2 ± 1.9 pF (n=30) versus the smaller MASH1 transfected cells 17.3 ± 1.2 pF (n=6, $p<0.05$). When maintained at -80mV, depolarizing current pulses in whole cell current clamp did not generate action potentials. However IM-PEN cells transfected with MASH1 did have a significantly higher input resistance (1706 ± 178.4MΩ, n=3) and slower time constant (37.8 ± 2.2ms, n=3) than the control IM-PEN cells. The current clamp recording depicted in Figure 3-4 and the exponential fit used to calculate the time constant of a MASH1 transfected cell is represented in Figure 3-4B. The exponential fit of the time constant was the same as that explained described earlier for calculating the time constant in Figure 2-1B.

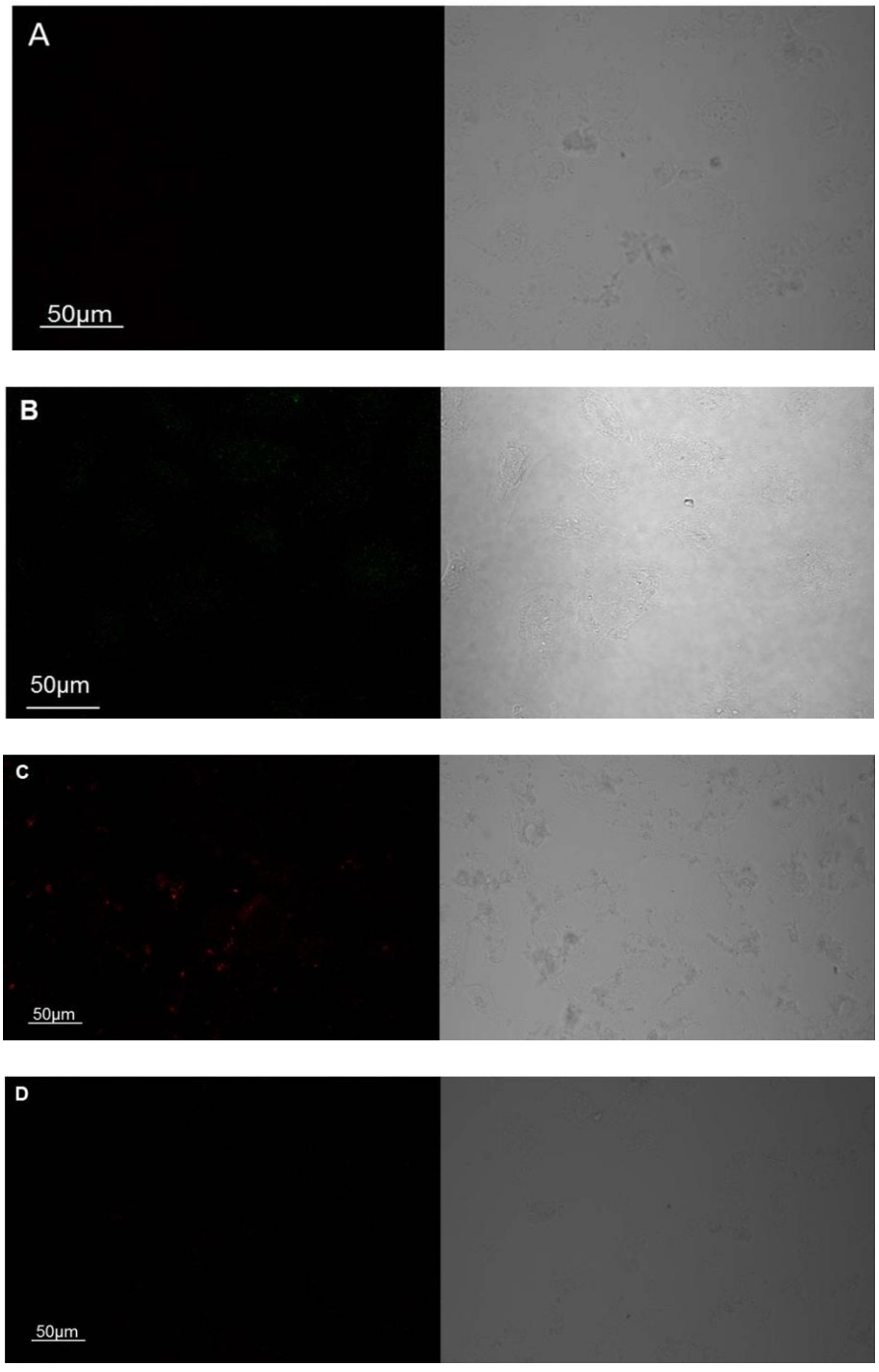

Figure 3-3 ChAT and NOS expression in IM-PEN transfected for 8 days with MASH 1 A) ChAT after 8 days untransfected B) NOS1 after 8 days untransfected C) ChAT after 8 days D) NOS1 after 8 days (C and D were transfected with MASH1).

5. 3.5 Ionic currents of IM-PEN transfected with MASH1

Studies by Vierbuchen et al. demonstrated that 8 days after MASH1 transfection, voltage gated Na^+ currents could be measured (Vierbuchen et al., 2010). We performed whole cell voltage clamp studies on IM-PEN cells using external solution 1 and internal solution A (Table 0-4 & 0-5). The loss of GFP as a marker required that recordings be performed after 4 days to identify IM-PEN/MASH1 transfected cells. The raw data in Figure 3-5A is representative of one of the MASH1 transfected cells tested, showing no evidence of inward currents. The IV relationship in Figure 3-5B was constructed from the maximum negative value between cursors set at the beginning of the pulse to 50ms into the pulse and confirms that no inward current was measured in these cells (n=6). However, like untransfected IM-PEN there seemed to be an increase in the outward current when 2mM Ca^{2+} was removed, as seen in the raw data. The IV curve assembled from the current at the end of the pulse in Figure 3-5C demonstrates that, although not statistically significant, there was an increase in the outward current when 2mMCa^{2+} was removed from the external solution. This current was not evident when Ca^{2+} was replaced (n=3). A difference of note in Figure 3-5 was that the outward current significantly increased in the MASH1 transfected cells (n=6) compared to untransfected cells (n=6, $p<0.05$).

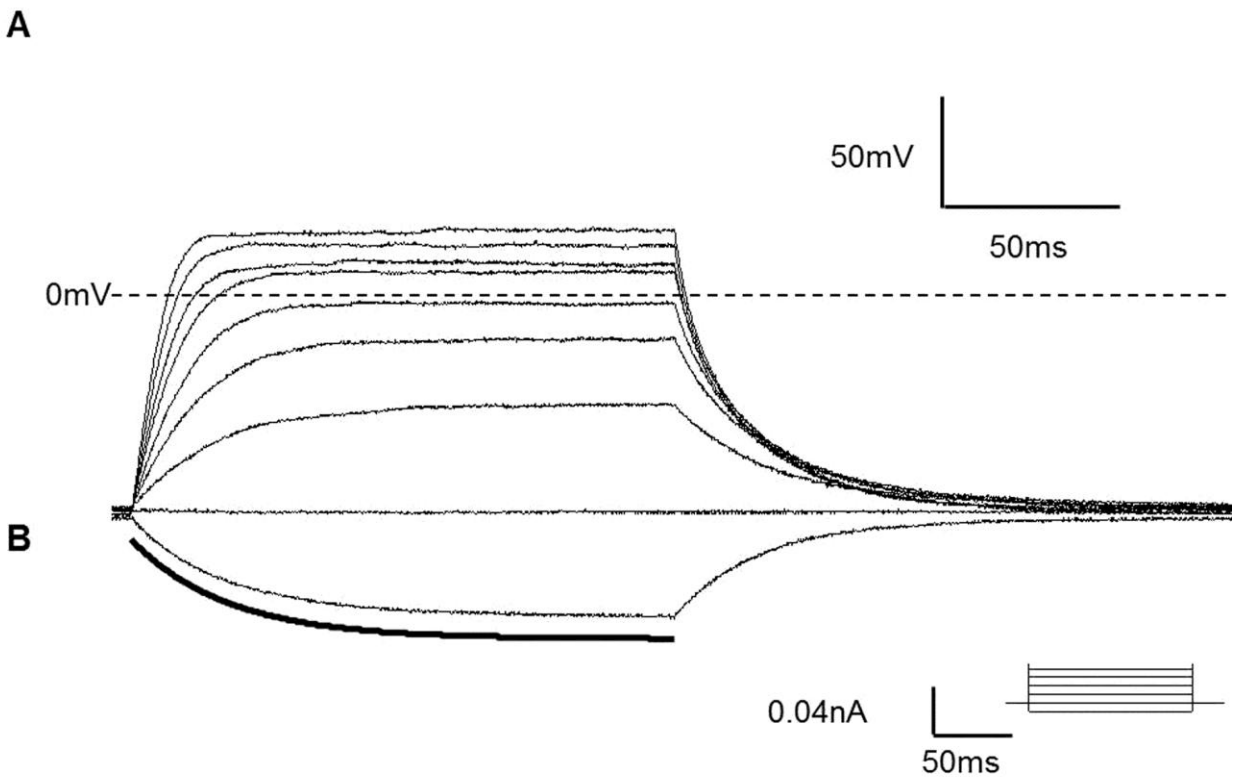

Figure 3-4 Current Clamp recordings of MASH1 transfected cells A) Whole cell current clamp recording showing to action potentials to depolarizing current pulses (n=3). B) Exponential fit of the electrotonic potential (in bold) used to calculate time constant.

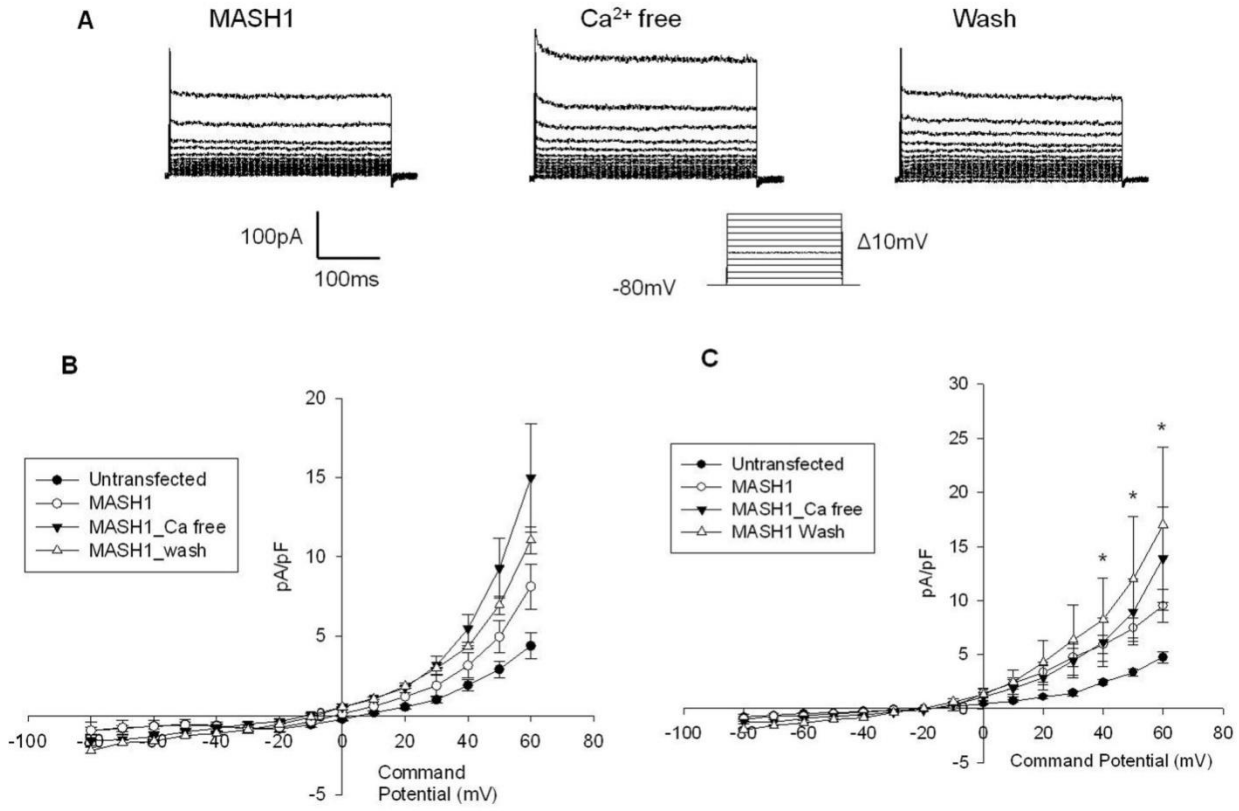

Figure 3-5 Currents of MASH1 transfected IM-PEN A) Whole cell voltage clamp recording of 1 cell treated with Ca^{2+} free solution and wash. B) IV relationship of Ca^{2+} current showing no inward current. C) IV relationship generated from the end of pulse. MASH1 (n=6) outward currents were significantly larger then untransfected (n=6) (*, $p<0.05$)

V. Discussion

IM-FEN and IM-PEN have a neuronal background and expressed many of the proteins characteristic of enteric neurons (Anitha et al., 2008). Our ultimate goal was to determine if these cell lines could be used as a model to study the effects of drugs on the electrophysiological properties of enteric neurons. The introduction outlined what is currently known about the electrophysiology of enteric neurons and was used as a guide to determine the properties of IM-FEN and IM-PEN. Our results show that both IM-FEN and IM-PEN share very similar characteristics and most likely require further maturation in order to produce fully differentiated enteric neurons.

A. Propagation

Propagation of the cell line was complicated by the transgene necessary to make these cells immortal. As a result, it was first necessary to confirm that both IM-FEN and IM-PEN underwent phenotypic neuronal differentiation using our differentiation conditions. Bright field images showed a notable difference in the morphology of IM-PEN cells before and after growth in the differentiation conditions. Immuno-reactivity with neuronal markers βIII-tubulin and PGP9.5 was positive in IM-PEN cells while S100, a glial cell marker, was negative. This data correlated well with previously published literature on IM-FEN. The majority of our studies were performed on IM-PEN with the hypothesis that, being post-natal, these cells were more mature than IM-FEN (Burns et al., 2009; Roberts et al., 2010). When these cell lines were first developed little research was conducted on the neurotransmitters that are so important in gastrointestinal signaling. We looked for two of the most abundant neurotransmitters in the enteric nervous system and were unable to find immuno-reactivity for ChAT or NOS1 under our

differentiation conditions. A 2010 publication by Anitha et al. found that BMP-2 induced differentiation to both nitrergic and catecholaminergic neurons in IM-FEN and had no effect on the expression of cholinergic neurons. In the same article, the presence of ChAT and substance P were measured by RT-PCR and no difference was observed between IM-FEN cells treated with GDNF, BMP-2, or GDNF + BMP-2 (Anitha et al., 2010). BMP-2 is part of the transforming growth factor β (TGF-β) superfamily and functions through a heterodimeric receptor which activates the Smad transcription factor signaling cascade. In enteric neurons BMP-2 was found to be important in early neural crest cell initiation, migration and proliferation (Fu et al., 2006). As we only looked for two of the multitude of possible neurotransmitters in enteric neurons it is plausible that expression of other neurotransmitters was present in IM-PEN cells however, our primary focus was on their electrophysiological properties.

B. Passive membrane properties

The postnatal RMP's shown in Table 2-1 are more depolarized than the RMP's of mature adult enteric neurons. There could be a species difference because the postnatal measurements were conducted in the rat. This is unlikely, however, considering that mature mouse, guinea pig, and human enteric neurons have approximately the same RMP. The immortalized cell lines IM-FEN and IM-PEN were generated from E13 and P2 mice respectively. If these cell lines were not fully mature, we would expect them to have depolarized RMP's. Table 2-1 of the passive membrane properties shows in the first row that the average RMP for IM-FEN, IM-PEN, and IM-PEN grown on laminin are all depolarized compared to previously published values of enteric neurons (Table 2-1 and Table 0-1). To confirm the depolarization was not an effect of the recording conditions cultured DRG neurons recorded in whole cell mode with the same solutions had RMP's of approximately -55 ± 3.4mV (n=4). A majority of the RMP's in Table

0-1 were measured from guinea pig enteric neurons. A 2010 methods paper published by Osorio et al. demonstrated a technique to perform whole cell recordings on mouse enteric neurons in situ. Although a great achievement, the authors list several drawbacks; beyond the difficulty of making the preparation and performing the electrophysiology, measurements must be made in solutions that prevent spontaneous muscle contraction. These solutions usually contain atropine to block muscarinic receptors and nicardipine to block L-type Ca^{2+} channels (Osorio et al., 2010).

Immature neurons have been found to have depolarized RMP's resulting from high concentrations of intracellular chloride (Blaesse et al., 2009). The normal RMP for mature neurons is closer to the equilibrium potential of K^+ as determined by the Nernst equation (Table 0-1). The equilibrium potential for Cl^- is more positive and depolarizes the RMP if there is a higher intracellular Cl^- concentration as opposed to K^+. This seems to be the case in IM-PEN as the RMP of the cells lies near the equilibrium potential of Cl^-. There is a shift in the expression of cation-chloride co-transporters from immature to mature neuronal states. Maintenance of the electrostatic potential could have been the result of Na^+ cations replacing the K^+ cations inside the cell. A review by Blaesse et al. depicts how the expression of NKCC1 transports Cl^- into the cell in immature hippocampal and cortical neurons. In mature neurons Cl^- is expelled through a series of KCC co-transporters thereby hyperpolarizing the cell (Blaesse et al., 2009). Mature neurons will demonstrate an inward Cl^- current to GABA treatment, whereas, no response was seen in treatment of GABA to IM-PEN (Ben-Ari et al., 2007). This is most likely because the GABA receptor, if present, was not active.

Other passive membrane properties include measurement of the input resistance (Ir), cell size, and time constant of the electrotonic potential. These properties can be dependent on

several factors such as the method used to make the measurement, the solutions used, the species and tissue, and age of the animal (Nurgali 2009). This is apparent in Table 0-1 where the RMP's are relatively similar, but, the Ir(s) are variable, ranging from 60 – 713 MΩ's. Measurements of Ir in the immortalized cell lines are consistent with those made using the whole cell patch clamp technique. A high input resistance has been noted in immature neurons of the mouse hippocampus and decreases upon expression of the K_{ir} conductance (Mongiat et al., 2009). Unfortunately there is no precedence in the literature for the size of enteric neurons and we cannot make conclusions based on size determining if IM-PEN correlates to either mature or immature enteric neurons. Furthermore, although IM-PEN cells did not fire action potentials, immature neurons of the CNS have been shown to be excitable. These cells however were harvested from adult mice and had hyperpolarized RMP (Mongiat et al., 2009). Further support of IM-PEN being immature in status comes from a recently published article in which cultured human neuronal progenitor cells (NPC) took 6 weeks to fire action potentials. Within 1 week the first neuronal marker seen was βIII-tubulin while expression of K^+ channels took 2 weeks and Na^+ channels after 1 month of differentiation. They did not publish results on the RMP's but the Ir did decrease as the cells matured and ion channels were expressed (Lepski et al., 2011). The electrophysiological measurements on IM-PEN were conducted on cells ranging from 5-10 days old. After that the cells were too fragile to make the giga-ohm seal necessary for our studies. Forming a giga-ohm seal was found to be easier on IM-PEN cells that were quickly treated with trypsin as opposed to those which remained adhered to a coverslip (see Methods). One more potential experiment would be to maintain the cells in the differentiation conditions for up to 6 weeks and determine if the electrophysiological characteristics have changed. Although culture conditions can affect cells in many ways the study by Lepski et al. used a very similar

differentiation protocol as that of the IM-PEN cells. This supports the theory that cells under our treatment conditions should have the ability to become fully mature neurons and maybe a longer incubation time is all that is necessary to produce mature neurons.

C. Ion channels

As represented in Table 0-2 several voltage gated ion channels have been identified in enteric neurons using different electrophysiological methods and diverse species. Our first goal was to quickly determine if a subset of these channels were also expressed in IM-PEN cells. Using RT-PCR we were able to detect mRNA for TRPV1, TRPA1, ClCa1, Kcnn4 ($K_{Ca}3.1$), $Na_v1.3$ and $Na_v1.9$ while $Ca_v2.2$ (N-type Ca^{2+} channel) and TASK1 ($K_{2p}3.1$) had very faint bands.

1. TRPV1

A majority of electrophysiological studies on the enteric nervous system seem to focus on AH neurons possibly because they comprise approximately 60% of the myenteric plexus (Johnson 2006). Several ion channels found in IM-PEN are also known to be expressed in AH neurons. These channels were TRPV1, TRPA1, ClCa1, and Kcnn4 ($K_{Ca}3.1$) and are involved in a multitude of diverse functions. TRPV1 was shown to co-localize and release several neurotransmitters upon activation such as CGRP, NO and SP. Immunohistochemistry of IM-PEN for TRPV1 found distinct immuno-reactivity on what appear to be intracellular vesicles rendering the channel inactive. The inability to activate a TRPV1 current was confirmed when no response was seen to the administration of 10µM capsaicin. DRG's were used as a control to confirm that 10µM capsaicin would activate TRPV1. A possible explanation for the lack of activity in IM-PEN is that previous studies were performed in adult mice (Matsumoto et al.,

2011). Since IM-PEN were harvested from post-natal day 2 mice, it is possible that TRPV1 was not yet developed in these cells and undergoes a process of developmentally regulated expression. It is also possible the TRPV1 channels are fully developed, but their sequestration in intracellular vesicles renders them inactive. Several studies have shown that during development proteins are expressed sequentially at different times of the maturation process (Burns et al., 2009). One course that has not been determined for TRPV1 in enteric neurons is the time point in development at which they are expressed and become functional. Immuno-reactivity of the EN system from neonatal and postnatal mice of TRPV1 along with electrophysiology would be necessary to answer this question.

2. Sodium channel

Expression of the Na^+ channels, $Na_v1.3$ and $Na_v1.9$, were also determined to be present in the IM-PEN cell line. Although light bands were found indicating transcription of these channels, the inward current was insensitive to TTX and NMDG (Figure 2-2) in IM-PEN. A TTX insensitive channel the current could have been the result of $Na_v1.9$. However, replacement of the Na^+ cation with non-permeant NMDG should have inhibited the current if it was due to a Na^+ conductance. The addition of NMDG did shift the outward current to the left in the IV curve nevertheless this was not significant and there was no inhibition in the maximum inward current. In combination these data indicate the inward current was not the result of Na^+.

3. Calcium channel

Identification of the Ca^{2+} channel was complicated for several reasons. Whole cell voltage clamp measures and summates all of the currents that occur at a particular potential. Therefore isolation of a specific current requires inhibition of all others. We confirmed the presence of the Ca^{2+} channel through two methods: 1) removal of Ca^{2+} from the external solution

and 2) the addition of 200uM Cd^{2+}, both of which inhibited the inward current. As seen in Table 0-2 there are at least 5 possible Ca^{2+} channels that have been identified in enteric neurons. Specific toxins, such as the conotoxins, and classes of compounds such as the dihydropyridines can be used to quickly determine the presence of an active ion channel. The N-type Ca^{2+} channel ($Ca_v2.2$) was initially sought because it comprises the largest contribution of the Ca^{2+} current in enteric neurons (Bian et al., 2004). However, mRNA for $Ca_v2.2$ was not detected in IM-PEN. In conjunction with this data, omega-conotoxin, is a specific inhibitor of neuronal type or N-type ($Ca_v2.2$) channels, did not inhibit the inward current. Inhibition by nifedipine points to expression of L-type Ca^{2+} channels ($Ca_v1.X$). There are at least 3 of these in the literature, not including their various subtypes, and the nature of $Ca2^{+}$ channels expressed in IM-PEN remains unknown. Previously published reports on enteric neurons clearly demonstrated partial inhibition of the Ca^{2+} current by nifedipine of 20-30% indicating that a portion of the total Ca^{2+} current is L-type in vivo (Table 0-2). Established protocols for measuring currents of L-type Ca^{2+} channels typically involve intracellular Cs^{2+} and external Ca^{2+} or Ba^{2+}. Barium is a better charge carrier then Ca^{2+} giving rise to larger currents through L-type Ca^{2+} channels and also minimizing Ca^{2+} dependent inhibition of the channel. In the presence of intracellular Cs^{2+}, inward currents could not be generated and this may partially reflect the ability of Cs^{2+} to permeate K^{+} channels producing an outward current. Substitution of the Ca^{2+} cation in the external solution with Ba^{2+} should have yielded larger currents in these channels. As seen in Figure 2-7 this was not the case and could be because of the small number of channels present. Another method to increase the current would have been the use of the dihydropyridine BAYK8644, which increases the open time of L-type Ca^{2+} channels.

4. Steady state activation and inactivation

The steady state activation and inactivation measurements can be used as a fingerprint to identify and distinguish ion channels. A caveat in making these measurements is that in whole cell voltage clamp all of the currents on a cells' surface are measured and summated if they are activated at a particular voltage potential. It is therefore necessary to make these measurements under conditions in which only the desired current is active. As previously mentioned, in the presence of intracellular Cs^{2+}, inward currents could not be produced. Therefore the steady state activation and inactivation curves that were measured and calculated are actually those which may contain an unknown contribution of outward current. There is most likely a contribution from other channels which would cause a shift in the steady state curves that is dependent on the unknown active channels.

5. Chloride channel

There were two reasons we thought a chloride conductance was present in IM-PEN cells. The first was that there appeared to be a maintained outward conductance when K^+ channels were blocked by Cs^{2+} and 4-AP. The second reason was that the calculated equilibrium potential of Cl^- using the Nernst equation for solutions 5 and C was -36.8mV while the actual measured reversal potential (E_{rev}) was -38mV. The most likely ion to create an outward current with these solutions was Cl^-. Had the resting conductance been K^+ dependent, the E_{rev} would have been much more negative. Further confirmation of the Cl^- current was established when 100mM Cl^- was removed from the external solution, causing a decrease in the outward current and removing the apparent tail current (Figure 2-11). The tail currents are indicative of Cl_{Ca} channels that were inhibited by niflumic acid (NA) (Figure 2-12). Measurement of this current correlates to the mRNA expression that was performed in which there is a distinct band for the ClCa1 gene.

Regulation of osmolarity is an important facet to the health and viability of any cell. As a result the majority of cells contain mechanisms to alter their internal osmolarity and prevent swelling from damaging their physiological function. It has been demonstrated that Cl^- is one of the major permeating ions which cells use to regulate their osmolarity through mechanisms of regulatory volume decrease. These channels are referred to as, VRAC, VSOAC, and, $I_{Cl,swell}$ nevertheless they all seem to be a chloride channel that is activated by a hypoosmotic external solution (Lang et al., 1998). Our data suggest that this ion channel is expressed in IM-PEN cells. Evidence for this was demonstrated by the fact that $I_{Cl,swell}$ was inhibited by DCPIB and was removed when Cl^- was replaced with gluconate. Gluconate has previously been shown to be impermeable through Cl^- channels and can be used to identify if Cl^- is the permeant ion. On the other hand, insensitivity to H_2O_2 and a linear IV curve distinguish the DCPIB sensitive channel to $I_{Cl,swell}$ present in several other cell types. The positive holding potential gave outward currents that were typically induced after 1-2 minutes of perfusion in the hypoosmotic solution in 9/11 cells however, 5 of these currents were transient in nature (Figure 2-14). There are many possible reasons for the observance of transient currents; 1) regulation of $I_{Cl,swell}$, 2) desensitization of the channel, 3) rectification of the osmolar imbalance, and 4) other inactivation mechanisms. There have been reports in the literature that this channel may be induced by stretch and/or swelling (Lang et al., 1998). Either of these mechanisms would be commonly seen in the GI, however, it is much more likely that a stretching type event would regulate ion channels in the myenteric plexus, as they are protected by several layers of tissue and do not receive much vascular innervation. As a result it is unlikely that they experience large changes in osmolar imbalance. Another common method used to induce $I_{Cl,swell}$ is through activation by reactive oxygen species (ROS). Compared to previously published data we were not able to

induce the $I_{Cl,swell}$ currents with H_2O_2 through the development of reactive oxygen species (Browe et al., 2006; Matsuda et al., 2010). There are multiple mechanisms by which H_2O_2 can induce $I_{Cl,swell}$ either through direct activation or through indirect signaling cascades (Ren et al., 2008). Several conclusions about $I_{Cl,swell}$ can be made from these data; 1) $I_{Cl,swell}$ in IM-PEN is either a stretch or osmosensor, 2) it does not require ATP and 3) $I_{Cl,swell}$ is not directly activated by H_2O_2. Many aspects of the channel have yet to be studied such as its permeability to other ions and regulation by kinases or phosphatases. The IM-PEN cell line may show an important aspect of $I_{Cl,swell}$ expression during enteric neuron development.

6. Potassium channel

As a pore blocker 4-aminopyridine is used to identify outwardly rectifying voltage sensitive K^+ channels. Since only 5/20 cells showed a K^+ current, this ion did not make a major contribution to the RMP in IM-PEN. This was further supported by the depolarized RMP's in Table 0-1 which are near the equilibrium potential for chloride. The recently published articled by Lepski et al. demonstrated that it took at least 2 weeks for K^+ channels to develop in cultured human neuronal progenitor cells (Lepski et al., 2011). The majority of electrophysiology studies on IM-PEN were conducted between 5-8 days as this was found to be the optimum time for the cells to remain in culture and remain viable for patching. As a result, it is possible that with additional time K^+ channels will develop. The positive mRNA detection of $K_{Ca}3.1$ indicated that a channel key for the distinct afterhyperpolarization seen in AH neurons was present in IM-PEN. However, functional measurement of the channel was not indicated in whole cell voltage clamp experiments.

7. Removal of Ca^{2+} increased outward current

While performing the Ca^{2+} channel measurements an increase in the amplitude of outward current at positive potentials was noted when Ca^{2+} was removed from the external solution. The current subsided back to normal when the IM-PEN cells were perfused with external solution containing 2mM Ca^{2+}. We hypothesize that this is due to a surface charge effect rather than the actual activation of an ion channel (Hille 2001). The membrane potential is defined as the potential difference between the outside and inside of the cell. The cellular membrane is typically charged as the phospholipid head groups and membrane proteins carry charge through basic and acidic amino acids to function. The sum of these membrane charges are known as the surface-charge and can be an important aspect of changes in extracellular Ca^{2+} concentration. Voltage gated ion channels contain voltage sensors which are dependent on the difference between the external and internal potentials, also known as the membrane potential. However, they are also sensitive to the surface potential which applies a small electrical field across the membrane. The external membrane surface charge can be altered most greatly by divalent ions carrying an opposing charge to that of the membrane. For example, Ca^{2+} added in the external solution may bind to negatively charged constituents on the membrane thereby increasing the effect of the electric field on the voltage sensor of an ion channel. In effect, this means that the voltage sensor senses a larger hyperpolarization than there may actually exist. If Ca^{2+} is removed the negative charge of the membrane decreases the electric field felt by the voltage sensor to closer that of the RMP. On a physiological level Ca^{2+} is more likely to remain in a high concentration on the outside of the cell and the cell itself depolarizes decreasing the electric field on the voltage sensor. These characteristics are important because it is this voltage sensor that dictates at what potential the ion channel is active. In our experiments, a possible

explanation for the increase in outward current seen at positive potentials when Ca^{2+} is removed may relate to the voltage sensor of the ion channel. If we lower the external potential and depolarize the cell it is possible that the voltage sensor is detecting a more depolarized level than it otherwise would thereby opening more channels for a longer period of time resulting in a larger current. This theory is supported by the fact that when Ca^{2+} is reintroduced to the external solution the outward current drops down to its previous level (Figure 2-8). The outward current was also decreased upon the administration of the L-type Ca^{2+} channel blocker nifedipine (1μM). This supports the theory that the absence of Ca^{2+} did not have a direct effect on the outward current and it is most likely relating to the valence of the cation. The same effect was seen in the MASH1 transfected IM-PEN cells.

Ideally, in order to test whether the valence of the cation is contributing to the outward current, we should remove Ca^{2+} and replace it with other divalent ions such as Ba^{2+} or Sr^{2+}. If the outward current is the result of the surface-charge effect there would be little change upon the replacement of one divalent cation with another. One important aspect to keep in mind is that these measurements were conducted under whole cell voltage clamp conditions. Therefore, the amplifier is clamping the cell at the desired voltage potential. If the measurements were made in current clamp we may be able to measure the shift detected by the voltage sensor between solutions with different divalent cations, thereby confirming our hypothesis.

8. Ligand gated ion channels

Ligand gated ion channels play an extremely important and diverse role in GI physiology. Detection of mRNA for the serotonin receptor $5HT_3$ along with mRNA and protein (Western blot) for the 5HT transporter (SERT) was present in IM-FEN and IM-PEN cells. These data suggested the presence of LGIC in IM-PEN cells which had higher expression levels of both

$5HT_3$ and SERT (Anitha et al., 2008). However IM-PEN cells did not express currents from LGIC's (Table 2-2) and this might be explained by the young age and lack of development of P2 neurons. A study recently determined the timeframe of neurotransmitter development which depended on BMP-4 signaling in enteric neurons. They showed that calretinin and serotonergic neurons developed first along with some NOS neurons early at E8. While GABA, TH, and TrkC developed later in development closer to E18 and CGRP neurons develop even later into post-natal stages of development (Chalazonitis et al., 2008). These data also suggest that IM-PEN would be expressing active LGIC's. As seen in Table 2-2, the addition of several different neurotransmitters failed to yield a response in IM-PEN

Our conclusion of the previous data is that perhaps either the age or differentiation conditions were insufficient for the complete development of IM-PEN cells into enteric neurons. The original study showed that when these cells were transplanted into aganglionic mice these cells did develop into functional neurons (Anitha et al., 2008). Therefore, we knew the ability to transform the cells existed in vivo but perhaps we were missing a signaling event in vitro.

D. MASH1

The transfection of MASH1 in IM-PEN did significantly change certain cell characteristics such as a decrease in cell size and a large increase in the Ir. A major hindrance in this experiment was the low transfection efficiency (1%) which made it extremely difficult to find MASH1 transfected cells. It was also assumed in the double transfection that those cells showing GFP would also contain MASH1 however we are unable to verify if this was the case. We tried to confirm the double transfection through both the electrophysiology data, which was inconclusive, and the immuno-reactivity of neurotransmitter development which was negative. In current clamp the GFP labeled cells were not excitable even when maintained at

hyperpolarized potentials (figure 3-4). An experiment to verify if the double transfection contained MASH1 treated cells would have been to immunostain the transfected cells with a MASH1 antibody and a secondary that does not excite in the same range as GFP. We could then determine if the non-transfected IM-PEN cells express MASH1 and if there was co-labeling of GFP and the MASH1 label.

It is also possible that a viral transfection would yield better transfection efficiency. The IM-PEN cells were originally transfected with BMP-2 using a chemical method however the Ascl1/MASH1 article by Vierbuchen used a viral transfection procedure (Anitha et al., 2010; Vierbuchen et al., 2010). There is also the possibility of generating a stable transfection of MASH1 in the IM-PEN cell line. Once made a stable transfection would accomplish two things; 1) it would no longer be necessary to search for GFP transfected cells and 2) the cells may express MASH1 for a longer period of time. Although we considered evaluating this experimentally, the transfection efficiency was much too low to yield a cell population that would practically generate a stably transfected cell line. Another problem was that IM-PEN appears to be a heterogeneous cell line. Selection for a stably transfected cell line could result in an alteration of the genotypic and phenotypic makeup of the IM-PEN.

VI. Conclusions

In conjunction with previously published research our data show that the IM-PEN cell line represents a collection of immature enteric neurons. Neuronal markers are clearly defined in IM-PEN; nevertheless the cells do not functionally express many of the ion channels necessary for the normal function of adult enteric neurons. There are several possible reasons for the lack of activity in these cells including; 1) the differentiation conditions 2) the culture conditions 3) the age mice at which the immortal culture was made and 4) effect of the transgene on enteric neuron development. Our differentiation and culture conditions are consistent with those used for the guinea pig and rat and suggest that these are not the problem (Mao et al., 2006). However, a recently published article showed that culture conditions can delay the differentiation of human neuronal progenitor cells (Lepski et al., 2011). Very similar culture conditions were used as those of the human neuronal progenitor cells suggesting that more time in culture would be beneficial to IM-PEN. However, the IM-PEN cells did not remain sustainable in culture for performing electrophysiology for more than 10 days. Furthermore, we were unable to make consistent patch clamp recordings from mouse enteric neurons at P2, hence the initial generation of the cell line. Enteric neurons from other species do fire action potentials at this age suggesting that they should in the mouse as well (Franklin et al., 1992). There is also no data on the effect of the transgene on development of the enteric nervous system. Although the transgene is temperature sensitive and tissues in these mice were found to be macroscopically normal the thymus of these mice was hyperplasic and eventually led to death (Jat et al., 1991). A comprehensive study on gastrointestinal movement in the H-2kb-tsA58 mouse has not been performed. As a result there is a question as to whether these mice develop a “normal” enteric

nervous system. A detailed study on contractions of the gastrointestinal system in these mice would be necessary to ascertain if they develop normal enteric neurons.

We conclude that the IM-PEN cell line is a useful cell line for studying the differentiation and maturation of enteric neurons as well as the ion channels involved in this process. The cells can be matured in vivo demonstrating that our differentiation conditions lack the appropriate signals. Although MASH1 is a major part of enteric neuron development there are several other neurotransmitters and transcription factors which are necessary for IM-PEN development. Adding these different factors in a systematic manner to IM-FEN or IM-PEN may generate the signaling mechanisms inherent to adult enteric neurons. The results of the work in this thesis have led to an understanding of the research that is most likely necessary to make the IM-FEN and IM-PEN cell lines develop neurotransmitters and generate action potentials.

VII. List of References

Ackerman MJ, Wickman KD, Clapham DE. 1994. Hypotonicity activates a native chloride current in xenopus oocytes. J Gen Physiol 103(2):153-79.

Akbarali HI, E GH, Ross GR, Kang M. 2010. Ion channel remodeling in gastrointestinal inflammation. Neurogastroenterol Motil 22(10):1045-55.

Altschul SF, Gish W, Miller W, Myers EW, Lipman DJ. 1990. Basic local alignment search tool. J Mol Biol 215(3):403-10.

Anitha M, Shahnavaz N, Qayed E, Joseph I, Gossrau G, Mwangi S, Sitaraman SV, Greene JG, Srinivasan S. 2010. BMP2 promotes differentiation of nitrergic and catecholaminergic enteric neurons through a Smad1-dependent pathway. Am J Physiol Gastrointest Liver Physiol 298(3):G375-83.

Anitha M, Joseph I, Ding X, Torre ER, Sawchuk MA, Mwangi S, Hochman S, Sitaraman SV, Anania F, Srinivasan S. 2008. Characterization of fetal and postnatal enteric neuronal cell lines with improvement in intestinal neural function. Gastroenterology 134(5):1424-35.

Baidan LV, Zholos AV, Wood JD. 1995. Modulation of calcium currents by G-proteins and adenosine receptors in myenteric neurones cultured from adult guinea-pig small intestine. Br J Pharmacol 116(2):1882-6.

Barajas-Lopez C, Peres AL, Espinosa-Luna R. 1996. Cellular mechanisms underlying adenosine actions on cholinergic transmission in enteric neurons. Am J Physiol 271(1 Pt 1):C264-75.

Bartoo AC, Sprunger LK, Schneider DA. 2005. Expression and distribution of TTX-sensitive sodium channel alpha subunits in the enteric nervous system. J Comp Neurol 486(2):117-31.

Bayliss WM and Starling EH. 1901. The movements and innervation of the small intestine. J Physiol 26(3-4):125-38.

Bayliss WM and Starling EH. 1900. The movements and the innervation of the large intestine. J Physiol 26(1-2):107-18.

Bayliss WM and Starling EH. 1899. The movements and innervation of the small intestine. J Physiol 24(2):99-143.

Ben-Ari Y, Gaiarsa JL, Tyzio R, Khazipov R. 2007. GABA: A pioneer transmitter that excites immature neurons and generates primitive oscillations. Physiol Rev 87(4):1215-84.

Beyak MJ, Ramji N, Krol KM, Kawaja MD, Vanner SJ. 2004. Two TTX-resistant na+ currents in mouse colonic dorsal root ganglia neurons and their role in colitis-induced hyperexcitability. Am J Physiol Gastrointest Liver Physiol 287(4):G845-55.

Bian X, Zhou X, Galligan JJ. 2004. R-type calcium channels in myenteric neurons of guinea pig small intestine. Am J Physiol Gastrointest Liver Physiol 287(1):G134-42.

Bian X, Ren J, DeVries M, Schnegelsberg B, Cockayne DA, Ford AP, Galligan JJ. 2003. Peristalsis is impaired in the small intestine of mice lacking the P2X3 subunit. J Physiol 551(Pt 1):309-22.

Blaesse P, Airaksinen MS, Rivera C, Kaila K. 2009. Cation-chloride cotransporters and neuronal function. Neuron 61(6):820-38.

Blaugrund E, Pham TD, Tennyson VM, Lo L, Sommer L, Anderson DJ, Gershon MD. 1996. Distinct subpopulations of enteric neuronal progenitors defined by time of development, sympathoadrenal lineage markers and mash-1-dependence. Development 122(1):309-20.

Bondurand N, Natarajan D, Barlow A, Thapar N, Pachnis V. 2006. Maintenance of mammalian enteric nervous system progenitors by SOX10 and endothelin 3 signalling. Development 133(10):2075-86.

Brookes S. 2001. Retrograde tracing of enteric neuronal pathways. Neurogastroenterol Motil 13(1):1-18.

Brookes SJ, Ewart WR, Wingate DL. 1987. Intracellular recordings from myenteric neurones in the human colon. J Physiol 390:305-18.

Brookes SJ, Meedeniya AC, Jobling P, Costa M. 1997. Orally projecting interneurones in the guinea-pig small intestine. J Physiol 505 (Pt 2)(Pt 2):473-91.

Browe DM and Baumgarten CM. 2006. EGFR kinase regulates volume-sensitive chloride current elicited by integrin stretch via PI-3K and NADPH oxidase in ventricular myocytes. J Gen Physiol 127(3):237-51.

Burns AJ, Roberts RR, Bornstein JC, Young HM. 2009. Development of the enteric nervous system and its role in intestinal motility during fetal and early postnatal stages. Semin Pediatr Surg 18(4):196-205.

Camilleri M. 2007. Alpha2delta ligand: A new, smart pill for visceral pain in patients with hypersensitive irritable bowel syndrome? Gut 56(10):1337-8.

Campbell DT. 1992. Large and small vertebrate sensory neurons express different na and K channel subtypes. Proc Natl Acad Sci U S A 89(20):9569-73.

Chalazonitis A, Pham TD, Li Z, Roman D, Guha U, Gomes W, Kan L, Kessler JA, Gershon MD. 2008. Bone morphogenetic protein regulation of enteric neuronal phenotypic diversity: Relationship to timing of cell cycle exit. J Comp Neurol 509(5):474-92.

Chen WP and Kirchgessner AL. 2002. Activation of group II mGlu receptors inhibits voltage-gated Ca2+ currents in myenteric neurons. Am J Physiol Gastrointest Liver Physiol 283(6):G1282-9.

Copel C, Osorio N, Crest M, Gola M, Delmas P, Clerc N. 2009. Activation of neurokinin 3 receptor increases na(v)1.9 current in enteric neurons. J Physiol 587(Pt 7):1461-79.

Coste B, Osorio N, Padilla F, Crest M, Delmas P. 2004. Gating and modulation of presumptive NaV1.9 channels in enteric and spinal sensory neurons. Mol Cell Neurosci 26(1):123-34.

Decher N, Lang HJ, Nilius B, Bruggemann A, Busch AE, Steinmeyer K. 2001. DCPIB is a novel selective blocker of I(cl,swell) and prevents swelling-induced shortening of guinea-pig atrial action potential duration. Br J Pharmacol 134(7):1467-79.

Ferens D, Baell J, Lessene G, Smith JE, Furness JB. 2007. Effects of modulators of ca(2+)-activated, intermediate-conductance potassium channels on motility of the rat small intestine, in vivo. Neurogastroenterol Motil 19(5):383-9.

Franklin JL, Fickbohm DJ, Willard AL. 1992. Long-term regulation of neuronal calcium currents by prolonged changes of membrane potential. J Neurosci 12(5):1726-35.

Fu M, Vohra BP, Wind D, Heuckeroth RO. 2006. BMP signaling regulates murine enteric nervous system precursor migration, neurite fasciculation, and patterning via altered Ncam1 polysialic acid addition. Dev Biol 299(1):137-50.

Furness JB, Robbins HL, Xiao J, Stebbing MJ, Nurgali K. 2004. Projections and chemistry of dogiel type II neurons in the mouse colon. Cell Tissue Res 317(1):1-12.

Furukawa K, Taylor GS, Bywater RA. 1986. An intracellular study of myenteric neurons in the mouse colon. J Neurophysiol 55(6):1395-406.

Galligan JJ. 2002. Ligand-gated ion channels in the enteric nervous system. Neurogastroenterol Motil 14(6):611-23.

Galligan JJ, North RA, Tokimasa T. 1989. Muscarinic agonists and potassium currents in guinea-pig myenteric neurones. Br J Pharmacol 96(1):193-203.

Galligan JJ, Tatsumi H, Shen KZ, Surprenant A, North RA. 1990. Cation current activated by hyperpolarization (IH) in guinea pig enteric neurons. Am J Physiol 259(6 Pt 1):G966-72.

Gershon MD. 2010. Developmental determinants of the independence and complexity of the enteric nervous system. Trends Neurosci 33(10):446-56.

Ginzinger DG. 2002. Gene quantification using real-time quantitative PCR: An emerging technology hits the mainstream. Exp Hematol 30(6):503-12.

Grider JR. 2003a. Reciprocal activity of longitudinal and circular muscle during intestinal peristaltic reflex. Am J Physiol Gastrointest Liver Physiol 284(5):G768-75.

Grider JR. 2003b. Neurotransmitters mediating the intestinal peristaltic reflex in the mouse. J Pharmacol Exp Ther 307(2):460-7.

Grider JR. 1989. Identification of neurotransmitters regulating intestinal peristaltic reflex in humans. Gastroenterology 97(6):1414-9.

Guillemot F and Joyner AL. 1993a. Dynamic expression of the murine achaete-scute homologue mash-1 in the developing nervous system. Mech Dev 42(3):171-85.

Guillemot F, Lo LC, Johnson JE, Auerbach A, Anderson DJ, Joyner AL. 1993b. Mammalian achaete-scute homolog 1 is required for the early development of olfactory and autonomic neurons. Cell 75(3):463-76.

Hamodeh SA, Rehn M, Haschke G, Diener M. 2004. Mechanism of butyrate-induced hyperpolarization of cultured rat myenteric neurones. Neurogastroenterol Motil 16(5):597-604.

Hanani M, Francke M, Hartig W, Grosche J, Reichenbach A, Pannicke T. 2000. Patch-clamp study of neurons and glial cells in isolated myenteric ganglia. Am J Physiol Gastrointest Liver Physiol 278(4):G644-51.

Hansen MB. 2003. The enteric nervous system I: Organisation and classification. Pharmacol Toxicol 92(3):105-13.

Harvey VL, Saul MW, Garner C, McDonald RL. 2010. A role for the volume regulated anion channel in volume regulation in the murine CNS cell line, CAD. Acta Physiol (Oxf) 198(2):159-68.

Haschke G, Schafer H, Diener M. 2002. Effect of butyrate on membrane potential, ionic currents and intracellular Ca2+ concentration in cultured rat myenteric neurones. Neurogastroenterol Motil 14(2):133-42.

Hille B. 2001. Ion channels of excitable membranes. Sunderland Mass.: Sinauer.

Hirning LD, Fox AP, Miller RJ. 1990. Inhibition of calcium currents in cultured myenteric neurons by neuropeptide Y: Evidence for direct receptor/channel coupling. Brain Res 532(1-2):120-30.

Hirst GD and McKirdy HC. 1975. Synaptic potentials recorded from neurones of the submucous plexus of guinea-pig small intestine. J Physiol 249(2):369-85.

Hirst GD and Spence I. 1973. Calcium action potentials in mammalian peripheral neurones. Nat New Biol 243(123):54-6.

Hirst GD, Johnson SM, van Helden DF. 1985. The calcium current in a myenteric neurone of the guinea-pig ileum. J Physiol 361:297-314.

Hirst GD, Holman ME, Spence I. 1974. Two types of neurones in the myenteric plexus of duodenum in the guinea-pig. J Physiol 236(2):303-26.

Hodgkiss JP and Lees GM. 1983. Morphological studies of electrophysiologically-identified myenteric plexus neurons of the guinea-pig ileum. Neuroscience 8(3):593-608.

Holt CE, Garlick N, Cornel E. 1990. Lipofection of cDNAs in the embryonic vertebrate central nervous system. Neuron 4(2):203-14.

Jat PS, Noble MD, Ataliotis P, Tanaka Y, Yannoutsos N, Larsen L, Kioussis D. 1991. Direct derivation of conditionally immortal cell lines from an H-2Kb-tsA58 transgenic mouse. Proc Natl Acad Sci U S A 88(12):5096-100.

Johnson L. 2006. Physiology of the gastrointestinal tract. fourth edition ed. . 1-1031 p.

Kang M, Morsy N, Jin X, Lupu F, Akbarali HI. 2004. Protein and gene expression of Ca2+ channel isoforms in murine colon: Effect of inflammation. Pflugers Arch 449(3):288-97.

Kang SH, Vanden Berghe P, Smith TK. 2003. Ca2+-activated cl- current in cultured myenteric neurons from murine proximal colon. Am J Physiol Cell Physiol 284(4):C839-47.

Knowles RG and Moncada S. 1994. Nitric oxide synthases in mammals. Biochem J 298 (Pt 2)(Pt 2):249-58.

Kozlowski R. 1999. Chloride channels physiology. Oxford: Isis Medical Media. 200 p.

Lang F, Busch GL, Ritter M, Volkl H, Waldegger S, Gulbins E, Haussinger D. 1998. Functional significance of cell volume regulatory mechanisms. Physiol Rev 78(1):247-306.

Lepski G, Maciaczyk J, Jannes CE, Maciaczyk D, Bischofberger J, Nikkhah G. 2011. Delayed functional maturation of human neuronal progenitor cells in vitro. Mol Cell Neurosci .

Lomax AE, Bertrand PP, Furness JB. 2001. Electrophysiological characteristics distinguish three classes of neuron in submucosal ganglia of the guinea-pig distal colon. Neuroscience 103(1):245-55.

Ludlow JW. 1993. Interactions between SV40 large-tumor antigen and the growth suppressor proteins pRB and p53. FASEB J 7(10):866-71.

Mao Y, Wang B, Kunze W. 2006. Characterization of myenteric sensory neurons in the mouse small intestine. Journal of Neurophysiology 96(3):998-1010.

Mathie A. 2007. Neuronal two-pore-domain potassium channels and their regulation by G protein-coupled receptors. J Physiol 578(Pt 2):377-85.

Matsuda JJ, Filali MS, Moreland JG, Miller FJ, Lamb FS. 2010. Activation of swelling-activated chloride current by tumor necrosis factor-alpha requires ClC-3-dependent endosomal reactive oxygen production. J Biol Chem 285(30):22864-73.

Matsumoto K, Hosoya T, Tashima K, Namiki T, Murayama T, Horie S. 2011. Distribution of transient receptor potential vanilloid 1 channel-expressing nerve fibers in mouse rectal and colonic enteric nervous system: Relationship to peptidergic and nitrergic neurons. Neuroscience 172:518-34.

Matsuyama H, Nguyen TV, Hunne B, Thacker M, Needham K, McHugh D, Furness JB. 2008. Evidence that TASK1 channels contribute to the background current in AH/type II neurons of the guinea-pig intestine. Neuroscience 155(3):738-50.

Mongiat LA, Esposito MS, Lombardi G, Schinder AF. 2009. Reliable activation of immature neurons in the adult hippocampus. PLoS One 4(4):e5320.

Mueller MH, Xue B, Glatzle J, Hahn J, Grundy D, Kreis ME. 2009. Extrinsic afferent nerve sensitivity and enteric neurotransmission in murine jejunum in vitro. Am J Physiol Gastrointest Liver Physiol 297(4):G655-62.

Murakami M, Ohta T, Otsuguro KI, Ito S. 2007. Involvement of prostaglandin E(2) derived from enteric glial cells in the action of bradykinin in cultured rat myenteric neurons. Neuroscience 145(2):642-53.

Mustafa AK, Gadalla MM, Snyder SH. 2009. Signaling by gasotransmitters. Sci Signal 2(68):re2.

Narahashi T, Moore JW, Scott WR. 1964. Tetrodotoxin blockage of sodium conductance increase in lobster giant axons. J Gen Physiol 47:965-74.

Needham K, Bron R, Hunne B, Nguyen TV, Turner K, Nash M, Furness JB. 2010. Identification of subunits of voltage-gated calcium channels and actions of pregabalin on intrinsic primary afferent neurons in the guinea-pig ileum. Neurogastroenterol Motil 22(10):e301-8.

Neylon CB, Fowler CJ, Furness JB. 2006. Regulation of the slow afterhyperpolarization in enteric neurons by protein kinase A. Auton Neurosci 126-127:258-63.

Neylon CB, Nurgali K, Hunne B, Robbins HL, Moore S, Chen MX, Furness JB. 2004. Intermediate-conductance calcium-activated potassium channels in enteric neurones of the

mouse: Pharmacological, molecular and immunochemical evidence for their role in mediating the slow afterhyperpolarization. J Neurochem 90(6):1414-22.

Noble M, Groves AK, Ataliotis P, Ikram Z, Jat PS. 1995. The H-2KbtsA58 transgenic mouse: A new tool for the rapid generation of novel cell lines. Transgenic Res 4(4):215-25.

North RA. 1973. The calcium-dependent slow after-hyperpolarization in myenteric plexus neurones with tetrodotoxin-resistant action potentials. Br J Pharmacol 49(4):709-11.

Nurgali K. 2009. Plasticity and ambiguity of the electrophysiological phenotypes of enteric neurons. Neurogastroenterol Motil 21(9):903-13.

Nurgali K, Stebbing MJ, Furness JB. 2004. Correlation of electrophysiological and morphological characteristics of enteric neurons in the mouse colon. J Comp Neurol 468(1):112-24.

Oda Y. 1999. Choline acetyltransferase: The structure, distribution and pathologic changes in the central nervous system. Pathol Int 49(11):921-37.

Okada Y. 1997. Volume expansion-sensing outward-rectifier cl- channel: Fresh start to the molecular identity and volume sensor. Am J Physiol 273(3 Pt 1):C755-89.

Osorio N and Delmas P. 2010. Patch clamp recording from enteric neurons in situ. Nat Protoc 6(1):15-27.

Penuelas A, Tashima K, Tsuchiya S, Matsumoto K, Nakamura T, Horie S, Yano S. 2007. Contractile effect of TRPA1 receptor agonists in the isolated mouse intestine. Eur J Pharmacol 576(1-3):143-50.

Ratcliffe EM. 2010. Molecular development of the extrinsic sensory innervation of the gastrointestinal tract. Auton Neurosci .

Ren J, Bian X, DeVries M, Schnegelsberg B, Cockayne DA, Ford AP, Galligan JJ. 2003. P2X2 subunits contribute to fast synaptic excitation in myenteric neurons of the mouse small intestine. J Physiol 552(Pt 3):809-21.

Ren Z, Raucci FJ,Jr, Browe DM, Baumgarten CM. 2008. Regulation of swelling-activated cl(-) current by angiotensin II signalling and NADPH oxidase in rabbit ventricle. Cardiovasc Res 77(1):73-80.

Ritter JM, Garner MM, Chilton JA, Jacobson ER, Kiupel M. 2009. Gastric neuroendocrine carcinomas in bearded dragons (pogona vitticeps). Vet Pathol 46(6):1109-16.

Roberts RR, Ellis M, Gwynne RM, Bergner AJ, Lewis MD, Beckett EA, Bornstein JC, Young HM. 2010. The first intestinal motility patterns in fetal mice are not mediated by neurons or interstitial cells of cajal. J Physiol 588(Pt 7):1153-69.

Roussa E, Wittschen P, Wolff NA, Torchalski B, Gruber AD, Thevenod F. 2010. Cellular distribution and subcellular localization of mCLCA1/2 in murine gastrointestinal epithelia. J Histochem Cytochem 58(7):653-68.

Rugiero F, Gola M, Kunze WA, Reynaud JC, Furness JB, Clerc N. 2002. Analysis of whole-cell currents by patch clamp of guinea-pig myenteric neurones in intact ganglia. J Physiol 538(Pt 2):447-63.

Rugiero F, Mistry M, Sage D, Black JA, Waxman SG, Crest M, Clerc N, Delmas P, Gola M. 2003. Selective expression of a persistent tetrodotoxin-resistant na+ current and NaV1.9 subunit in myenteric sensory neurons. J Neurosci 23(7):2715-25.

Sage D, Salin P, Alcaraz G, Castets F, Giraud P, Crest M, Mazet B, Clerc N. 2007. Na(v)1.7 and na(v)1.3 are the only tetrodotoxin-sensitive sodium channels expressed by the adult guinea pig enteric nervous system. J Comp Neurol 504(4):363-78.

Seidman KJ, Barsuk JH, Johnson RF, Weyhenmeyer JA. 1996. Differentiation of NG108-15 neuroblastoma cells by serum starvation or dimethyl sulfoxide results in marked differences in angiotensin II receptor subtype expression. J Neurochem 66(3):1011-8.

Sitmo M, Rehn M, Diener M. 2007. Stimulation of voltage-dependent Ca2+ channels by NO at rat myenteric neurons. Am J Physiol Gastrointest Liver Physiol 293(4):G886-93.

Spencer NJ, Kerrin A, Zagorodnyuk VP, Hennig GW, Muto M, Brookes SJ, McDonnell O. 2008. Identification of functional intramuscular rectal mechanoreceptors in aganglionic rectal smooth muscle from piebald lethal mice. Am J Physiol Gastrointest Liver Physiol 294(4):G855-67.

Starodub AM and Wood JD. 2000a. A-type potassium current in myenteric neurons from guinea-pig small intestine. Neuroscience 99(2):389-96.

Starodub AM and Wood JD. 2000b. Histamine suppresses A-type potassium current in myenteric neurons from guinea pig small intestine. J Pharmacol Exp Ther 294(2):555-61.

Storr M. 2007. TRPV1 in colitis: Is it a good or a bad receptor?--a viewpoint. Neurogastroenterol Motil 19(8):625-9.

Takehara T, Teramura T, Onodera Y, Kishigami S, Matsumoto K, Saeki K, Fukuda K, Hosoi Y. 2009. Potential existence of stem cells with multiple differentiation abilities to three different germ lineages in mouse neurospheres. Stem Cells Dev 18(10):1433-40.

van Nassauw L and Timmermans JP. 2010. Detailed knowledge of cellular expression of G protein-coupled receptors in the human enteric nervous system is essential for understanding their diverse actions. Neurogastroenterol Motil 22(9):959-64.

Vierbuchen T, Ostermeier A, Pang ZP, Kokubu Y, Sudhof TC, Wernig M. 2010. Direct conversion of fibroblasts to functional neurons by defined factors. Nature 463(7284):1035-41.

Vogalis F, Harvey JR, Furness JB. 2003. PKA-mediated inhibition of a novel K+ channel underlies the slow after-hyperpolarization in enteric AH neurons. J Physiol 548(Pt 3):801-14.

Vogalis F, Furness JB, Kunze WA. 2001. Afterhyperpolarization current in myenteric neurons of the guinea pig duodenum. J Neurophysiol 85(5):1941-51.

Vogalis F, Harvey JR, Lohman RJ, Furness JB. 2002a. Action potential afterdepolarization mediated by a Ca2+-activated cation conductance in myenteric AH neurons. Neuroscience 115(2):375-93.

Vogalis F, Harvey JR, Neylon CB, Furness JB. 2002b. Regulation of K+ channels underlying the slow afterhyperpolarization in enteric afterhyperpolarization-generating myenteric neurons: Role of calcium and phosphorylation. Clin Exp Pharmacol Physiol 29(10):935-43.

Wade PR and Wood JD. 1988. Electrical behavior of myenteric neurons in guinea pig distal colon. Am J Physiol 254(4 Pt 1):G522-30.

Whitehead RH and Robinson PS. 2009. Establishment of conditionally immortalized epithelial cell lines from the intestinal tissue of adult normal and transgenic mice. Am J Physiol Gastrointest Liver Physiol 296(3):G455-60.

Xiao J, Nguyen TV, Ngui K, Strijbos PJ, Selmer IS, Neylon CB, Furness JB. 2004. Molecular and functional analysis of hyperpolarisation-activated nucleotide-gated (HCN) channels in the enteric nervous system. Neuroscience 129(3):603-14.

Zholos AV, Baidan LV, Starodub AM, Wood JD. 1999. Potassium channels of myenteric neurons in guinea-pig small intestine. Neuroscience 89(2):603-18.

VIII. Vita

Edward Gregory Hawkins was born on the east coast of the United States in Baltimore, Maryland on March 13, 1978. He grew up in Los Angeles, California graduating from Bonita High School in 1996. He then attended the University of California at San Diego, La Jolla, California, and graduated in 2000 with a Bachelor's degree in Animal Physiology and Neuroscience. After graduation he worked as a research technician for several years in the laboratory of Dr. Benjamin Cravatt at The Scripps Research Institute in the cannabinoid field. In 2005, Gregory furthered his academic career when he was accepted into the Pharmacology and Toxicology program at Virginia Commonwealth University. He began his studies and research in electrophysiology and enteric neurons in the laboratory of Dr. Hamid I. Akbarali. His thesis is on the characterization of an enteric neuron cell line developed from the transgenic immorto-mouse. Gregory has presented abstracts at several scientific conferences winning several travel awards and presentation awards. Some of these include the graduate student poster competition in neuropharmacology in 2009 at Experimental Biology and the graduate student poster competition for the division for integrative systems and translational and clinical pharmacology at Experimental biology in 2010. He also served as the chairman of the Virginia Academy of Sciences, medical sciences division, 2007. He is involved with the VCU program in enteric and neuromuscular sciences (VPENS) and is a contributor to Faculty 1000, a post-publication review website.

Publications

Hawkins, E.G., Akbarali, H.I., Review of voltage gated ion channels in the myenteric plexus (in preparation).

Hawkins, E.G., Dewey, W.L., Srinivasan, S., Akbarali, H.I., Electrophysiological characteristics of enteric neurons from the immortomouse (submitted).

Akbarali, H.I., Hawkins, E.G., Ross, G.R., Kang, M., Ion channel remodeling in gastrointestinal inflammation. *Neurogastroenterol Motil* 22(10), 1045-1055 (2010).

Cravatt, B.F., Saghatelian A., **Hawkins E.G.,** Clement A.B., Bracey M. H., Lichtman A. H. Functional disassociation of the central and peripheral fatty acid amide signaling systems. Proc Natl Acad Sci USA 101, 10821-10826 (2004).

Ortega-Gutierrez, S., **Hawkins, E.G.,** Viso, A., Lopez-Rodriguez, M.L. & Cravatt, B.F. Comparison of anandamide transport in FAAH wild-type and knockout neurons: evidence for contributions by both FAAH and the CB1 receptor to anandamide uptake. *Biochemistry* 43, 8184-8190 (2004).

Saghatelian, A., Trauger S.A., Want E.J., **Hawkins E.G.,** Siuzdak G., Cravatt B.F. Assignment of endogenous substrates to enzymes by global metabolite profiling. *Biochemistry* 43, 14332-14339 (2004).

Clement, A.B., **Hawkins, E.G.,** Lichtman, A.H. & Cravatt, B.F. Increased seizure susceptibility and proconvulsant activity of anandamide in mice lacking fatty acid amide hydrolase. *J Neurosci* 23, 3916-3923 (2003).

Lichtman, A.H., **Hawkins, E.G.,** Griffin, G. & Cravatt, B.F. Pharmacological activity of fatty acid amides is regulated, but not mediated, by fatty acid amide hydrolase in vivo. *J Pharmacol Exp Ther*. 302, 73-79 (2002).